RSC Advances

REVIEW

View Article Online
View Journal | View Issue

Cite this: *RSC Adv.*, 2023, **13**, 19981

Advanced progress on the significant influences of multi-dimensional nanofillers on the tribological performance of coatings

Ruili Wang,[a] Yahui Xiong,*[bc] Kang Yang,*[b] Taiping Zhang,[d] Feizhi Zhang,[b] Bangying Xiong,[bc] Yongxing Hao,*[d] Honglei Zhang,[bc] Yang Chen[bc] and Jun Tang[bc]

Received 9th March 2023
Accepted 8th June 2023

DOI: 10.1039/d3ra01550e

rsc.li/rsc-advances

Over the past two decades, nanofillers have attracted significant interest due to their proven chemical, mechanical, and tribological performances. However, despite the significant progress realized in the application of nanofiller-reinforced coatings in various prominent fields, such as aerospace, automobiles and biomedicine, the fundamental effects of nanofillers on the tribological properties of coatings and their underlying mechanisms have rarely been explored by subdividing them into different sizes ranging from zero-dimensional (0D) to three-dimensional (3D) architectures. Herein, we present a systematic review of the latest advances on multi-dimensional nanofillers for enhancing the friction reduction and wear resistance of metal/ceramic/polymer matrix composite coatings. Finally, we conclude with an outlook for future investigations on multi-dimensional nanofillers in tribology, providing possible solutions for the key challenges in their commercial applications.

1. Introduction

Presently, the significant increase in energy consumption in modern industry has attracted increasing attention; however, its reduction is still a considerable challenge.[1–3] According to numerous reports, friction is responsible for approximately one-third of the energy consumed in automobiles.[4,5] It is believed that even just a 20% reduction in wear substantially lowers the economic costs in terms of energy usage and environmental impact.[6–8] Hence, controlling friction and wear has attracted great scientific interest and is technically valuable for reducing the consumption of energy and promoting industrial development.

The application of surface coatings has been increasingly regarded as an effective method to optimize the tribological performance of materials.[9–11] In this case, the two fundamental prerequisites for the design of surface coatings are low friction and high wear resistance.[12,13] However, under increasingly severe working conditions, traditional coatings fail to meet the ever-increasing requirements for their tribology performance.[14,15] In this regard, an improvement in the friction and wear of coatings can be achieved by incorporating functional additives or other components. Among the various additives, nanofillers have attracted particular interest due to their attractive tribological potential based on their excellent corrosion resistance, unique mechanical behaviors, and high thermal conductivities.[16–18] According to their macro/microscale structures, nanofillers can be classified into zero-dimensional (0D), one-dimensional (1D), two-dimensional (2D) and three-dimensional (3D) architectures.[19,20] As shown in Fig. 1, 0D-nanofillers mainly include nanoparticles and nanospheres, where all their dimensions are maintained at the nanoscale.[21] 1D-nanofillers refer to nanofibers, nanorods and nanotubes, which have nanoscale diameters but high aspect ratios.[22,23] The family of 2D-nanofillers is comprised of various nanosheets and their corresponding multilayer structures, where their ultrathin sheet-like structures have a thickness ranging from a few to dozens of nanometers.[24,25] Alternatively, 3D-nanofillers include pure 3D nanomaterials or hybrids mainly composed of one or more 0D, 1D, and 2D basic structural units.[26,27] For example, when nanodiamonds are ~5 nm in size, they are classified as 0D;[28] in contrast, their pure 3D structures have a size of ~12 nm and above.[29] In addition, it has been shown that three-dimensional nanostructures composed of graphene oxide nanolayers and C60 have excellent lubricity at a wide strain level of 0–62%.[30,31]

As a nanomaterial, 0D-fillers have been demonstrated to be suitable for a wide range of tribological applications in ceramic, metal and polymer coatings owing to their nearly spherical nanostructure, high thermal conductivity, and low thermal

[a]*Faculty of Engineering, Huanghe Science and Technology University, Zhengzhou 450000, China*

[b]*Department of Mechanical Engineering, Anyang Institute of Technology, Avenue West of Yellow River, Anyang 455000, China. E-mail: angongyangkang@163.com; yahui1228@foxmail.com; Fax: +86-372-2986271; Tel: +86-372-2986271*

[c]*School of Mechanical Engineering, Sichuan University of Science & Engineering, 180 Xueyuan Street, Huixing Road, Zigong 643000, China*

[d]*School of Materials Science and Engineering, North China University of Water Resources and Electric Power, Zhengzhou, Henan 450045, China. E-mail: haoyongxing@ncwu.edu.cn*

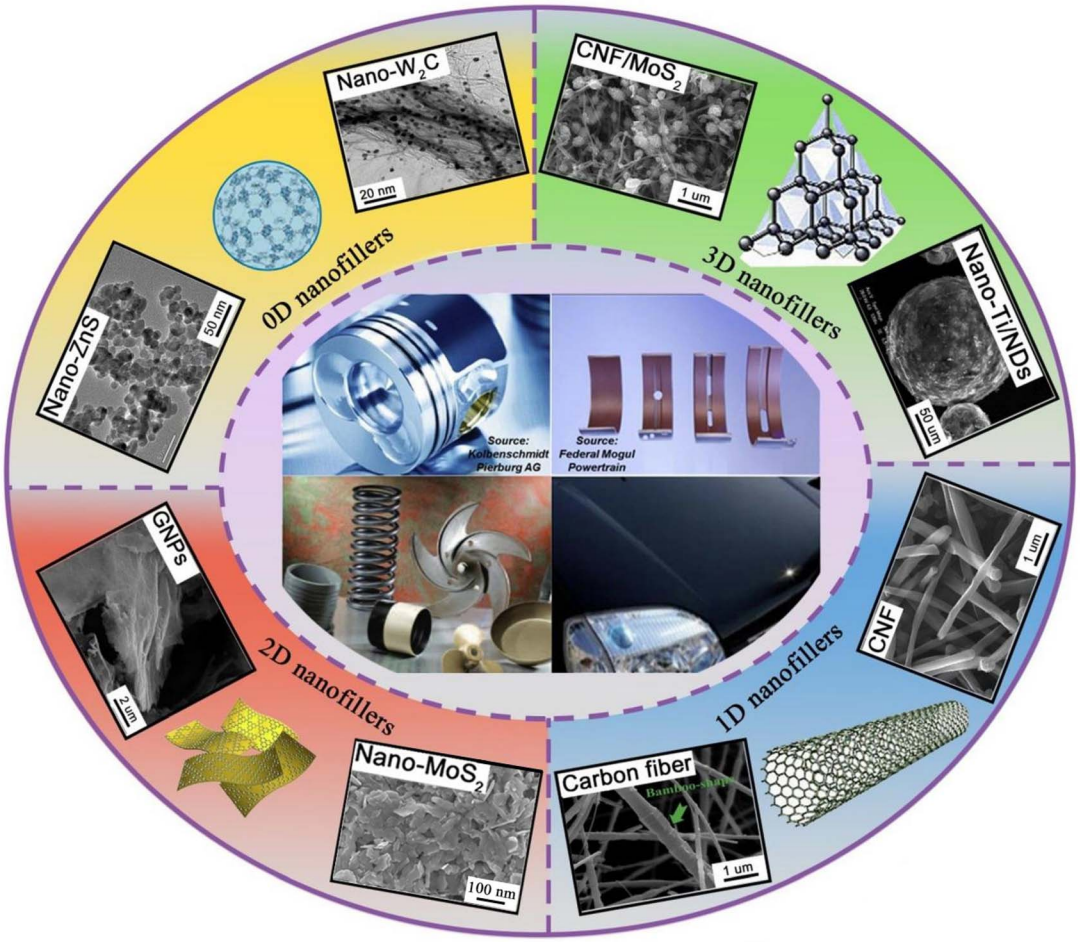

Fig. 1 Typical nanofillers for coating applications such as 0D nanofillers (nano-ZnS and nano-W_2C particles[52,53]), 1D nanofillers (carbon nanofiber (CNF)[54,55]), 2D nanofillers (MoS_2 (ref. 56) and graphene nanoplates (GNPs)[57]), 3D nanofillers (CNF/MoS_2 hybrid[55] and Ti/ND power[58]).

expansion coefficient.[32–34] However, attention has gradually shifted from 0D nanofillers to candidates in other dimensions with the introduction of multi-dimensional nanomaterials.

Similar to 0D-nanofillers, 1D- and 2D-fillers have stimulated extraordinary interest in tribology. 1D-nanofillers with high aspect ratios and unique layered 2D-nanofillers are considered ideal materials for achieving excellent lubricity.[2,35–37] The enhancement of the tribological behaviors of nanofiller-reinforced coatings mainly depends on their inherent characteristics, such as their micro/nanoscale structure, dispersion state, and bonding strength of the resulting composite.[38] The nano-rolling effect of 1D-nanofillers has been proven to be an effective strategy for reducing the friction and wear of coatings. Multilayer 2D-nanomaterials are combined through weak van der Waals forces, which can result in a relatively low shear strength,[39–41] endowing 2D-filler nanosystems with excellent self-lubricating performances.

In contrast to 0D, 1D and 2D nanofillers, 3D-nanofillers are defined as pure 3D nanomaterials or hybrid mainly composed of one or more 0D, 1D, and 2D structural units.[42,43] The use of well-designed 3D structures presents a feasible strategy for enhancing the tribological behaviors of surface coatings, enabling the applications of their composites in many important fields, such as electricity, medical science, and superlubricity.

As rapidly developing nanotechnology globally, nanofillers have attracting interest in the design of solid lubrication coatings due to their unique structures and excellent physical/chemical properties. Compared with micro-scale additives, nano-additives have the advantages of smaller particle size and larger specific surface area. Furthermore, they are not only capable of improving the interface compatibility between additives and solid matrices, but also easily enter the tribo-interface during the friction process, providing excellent lubrication effects.[44] Recently, the widespread use of nanofillers in coatings has promoted the design of friction interface optimization strategies, playing an important role in improving the friction performance and reducing the energy consumption. Numerous studies have shown that multi-dimensional nanofillers can serve as the solid lubrication components of the coatings[45–48] to form friction films during the friction process. This helps to reduce friction and wear. To date, the studies on coatings have mainly focused on their synthesis and potential applications,[49–51] whereas the tribological functions of

nanofillers in coatings have not been reviewed fully. In particular, insight into the crucial roles of multi-dimensional nanomaterials in different coating substrates has not been provided thus far. In this review, we focus on the tribological performance of coatings in three key areas. It is divided into the following five parts. After a brief introduction on the macro/microstructures and properties of nanofillers, the tribological behaviors and wear mechanisms of 0D-nanofillers as effective additives for ceramic, metal, and polymer coatings are described in Section 2. Additionally, the recent progress in the development of 1D and 2D nanofillers for coating tribology is elaborated in Section 3 and 4, respectively. In section 5, we explore the increasing efforts on 3D-nanofillers to realize superior anti-wear and friction-reduction behaviors. Finally, the important conclusions and outlooks of nanofillers in crucial tribological fields are discussed in Section 6.

2. Zero-dimensional nanofillers

0D-nanofillers, including various particles with a size ranging from 1 nm to 100 nm,[59,60] have attracted significant attention due to their demonstrated tribological potential. Recent studies on coatings have accelerated the application of 0D-nanofillers in various matrices, such as metals, ceramics, and polymers. Generally, most nanofillers have well-organized structures (atomic and mesoscopic). This endows them with considerable size effects and outstanding mechanical properties,[26] making them very attractive for tribological and electromechanical applications. Over the past ten years, nanofillers have proven to be ideal candidates for improving the lubrication behaviors of coatings.[61,62] In the following sections, we review and discuss the friction reduction and anti-wear abilities of 0D nanofillers in metal, ceramic, and polymer coatings. Table 1 presents a summary of the latest data on the tribological properties of 0D nano-filler-reinforced coatings.

2.1. Metal-based coatings

Traditional coatings have been extensively applied in mechanical devices, such as pumps, compressors and turbines, to control friction and wear. However, under extreme conditions, they exhibit a poor performance under friction and wear owing to the presence of structural defects. Alternatively, metal-based coatings (MBCs) such as Ni, Fe, and MgAl-based coatings,[63–65] which are fabricated *via* the incorporation of various particles or fibers in the coating, generally possess superior properties, such as high hardness and good wear-resistance compared to that of unreinforced coatings. Among the various reinforcements, nanomaterials have attracted particular attention due to their favorable attributes, such as unique structure, high thermal conductivity, low thermal expansion coefficient, and good self-lubrication performance.[66–69]

Numerous studies have established that reinforcements with a smaller size in composite coatings resulted in more remarkable enhancement functions.[70] According to the study

Table 1 Friction and wear behaviors of 0D-nanofillers in coatings[a]

			Tribological results	
Matrix	Reinforcement	Tested conditions	COF	Wear
Fe–Al coatings	Nano-Al_2O_3 (ref. 116)	440C tool steel (ball-on-disk, 6 m min^{-1}, 10 N, RT)	0.53	Wear rate: 0.1811×10^{-3} mm^3 N m^{-1}
Ni–P coatings	Nano-TiN[75]	Cylinder liner (piston ring-cylinder liner, 0.44 mm min^{-1}, 5 Hz, 140 N, RT)	~0.080	Wear loss: 0.5 mg
Cu–P coatings	Nano-SiC[81]	Al_2O_3 ball (ball-on-disk, 1.0 cm s^{-1}, 1 N, 1500 cycles)	NM	Wear loss: 0.15 mg per 1000 cycles
Ni–Cu coatings	Nano-Al_2O_3 (ref. 72)	Chromium-coated steel (pin-on-disk, 0.02 m s^{-1}, 5 N, RT)	0.55	Wear rate: 4.20×10^{-4} mm^3 N m^{-1}
CrN coatings	Nano-Ag[89]	Rockwell-type diamond (reciprocating multi-pass scratching, 0.7 mm s^{-1}, 1 N, 100 cycles, RT)	0.04–0.06	Wear scar depth: 0.19 μm per 100 cycles
Ultra-fine ceramic coatings	Nano-Ni[90]	Chromium-plated GCr15 steel (block-on-wheel, 0.45 m s^{-1}, 50 N, 120 s)	0.35–0.42	Wear loss: 0.6–1.1 mg
Ceramic coating	GO-Al_2O_3 (ref. 117)	Si_3N_4 ball (ball-on-disc, 20 mm s^{-1}, 20 N, 15 min)	~0.45	Wear rate: $\sim 0.7 \times 10^{-4}$ mm^3 N m^{-1}
PMMA coatings	Nano-SiO_2 (ref. 107)	Silicon nitride ball (pin-on-plate, 2 mm, 1 Hz; 5, 10 and 15 mN; 22 °C)	0.27–0.4	NM
PEEK-based coatings	IF-WS_2 (ref. 110)	Stainless steel balls (ball-on-flat, 1800 mm min^{-1}, 1 N)	0.15	NM
PTFE coatings	BMG[114]	GCr15 bearing steel ball (4.2 mm, 2 Hz; 1 N, RT)	0.086	Wear volume: 2.31×10^6 μm^3

[a] RT = room temperature; NM = not mentioned.

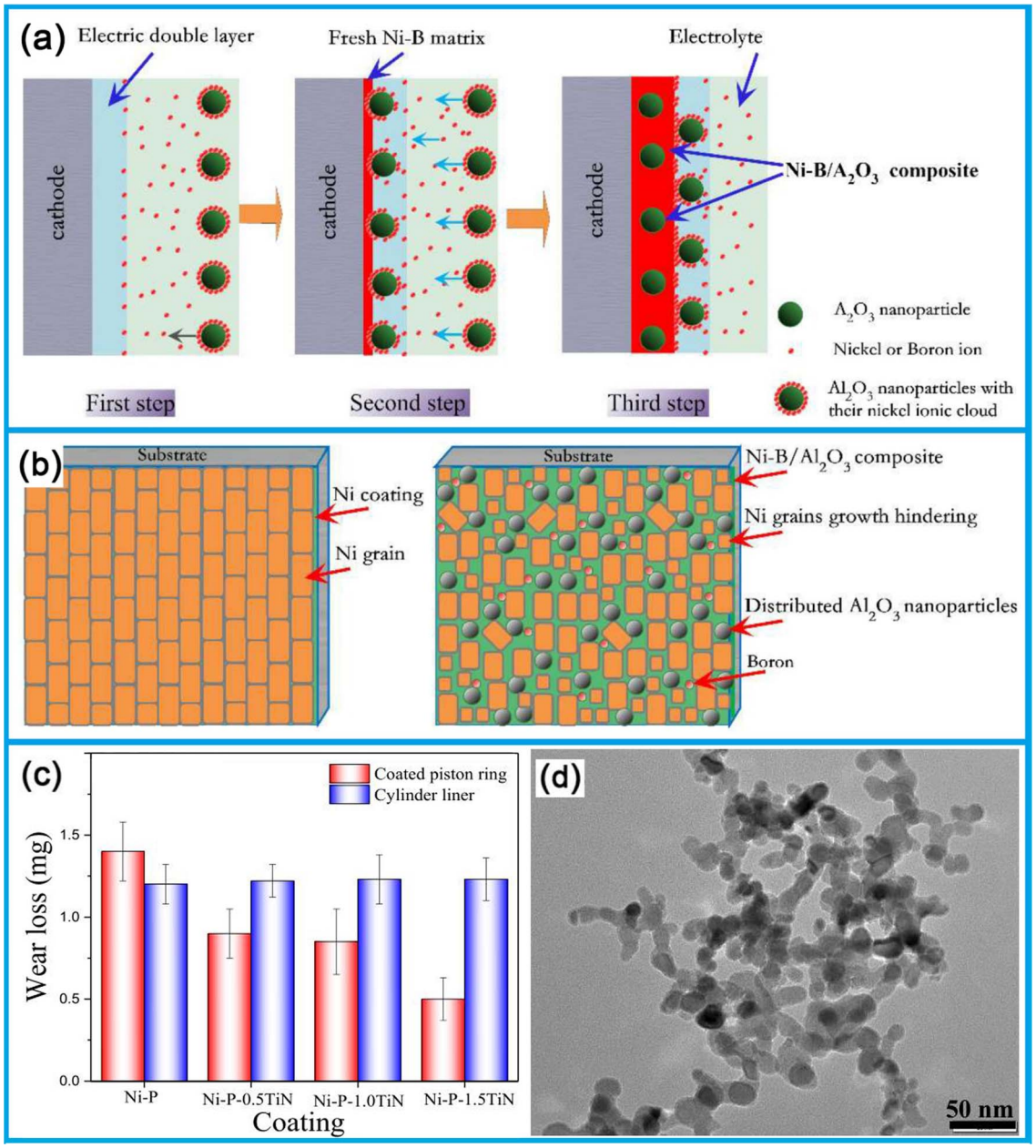

Fig. 2 Schematic of the typical electro-co-deposition process (a) and refinement mechanism (b) of Ni–B/Al_2O_3 coating. Reproduced from ref. 73 with permission from Elsevier, Copyright 2018. (c) Influence of TiN nanoparticle concentration on wear loss, and TEM image (d) of nano-TiN powder. Reproduced from ref. 75 with permission from Elsevier, Copyright 2019.

by Zhang *et al.*,[71] the hardness and wear resistance of an Sm_2O_3/Ni-base coating increased as the filler size decreased from the micrometer to nanometer level. Al_2O_3 at a concentration of 20 g L^{-1} in an Ni–Cu alloy coating was demonstrated to be effective for inhibiting crystal growth, endowing the deposited compact structures on the Ni–Cu alloy coating with compact structures.[72] The crystallite size of the coating decreased from 91 nm to 16 nm, enabling the composite coating to achieve an extremely high level of wear resistance, which was ~3.75 times that of the pure Ni coating. The friction coefficient and wear rate are specified in detail in Table 1. The role of Al_2O_3 nanoparticles in the tribological properties of Ni–B nanocoating was studied by Li *et al.*[73] Fig. 2a depicts the electro-co-deposition of nano-Al_2O_3 in a metallic matrix in detail. Microscopic analysis and friction tests revealed that the addition of Al_2O_3 particles to the Ni–B coating significantly improved its hardness and wear resistance. This was attributed to the nano-Al_2O_3 dispersed in the Ni–B coating, which increased the number of nuclei available for the nucleation of Ni–B metal crystals, resulting in an Ni–B composite with a smaller grain size than the pure Ni coating (Fig. 2b). These compact structures and enhanced mechanical properties enabled the effective optimization of the friction and wear behavior of the coating.

Based on aforementioned reports, nanoscale fillers can effectively fix the matrix grain boundaries in the coating, increasing the restriction on grain boundary movements and achieving grain refinements.[74] The refined grain sizes and the limitation of dislocation motions provide effective methods to improve the mechanical and tribological properties of coatings.[75–77] In the case of MBCs, 0D-particles with excellent mechanical properties have been increasingly regarded as the most promising candidates for tribological enhancement.[78,79] Although plenty of research has been conducted on MBCs reinforced by nanofillers, it is still a challenge to synthesize MBCs with well dispersed nanofillers due to the high surface energy of 0D-fillers.[80,81]

An appropriate concentration is a critical prerequisite for achieving a uniform dispersion of 0D-nanofillers in coatings. In the case of nano-Al_2O_3-reinforced Ni–P coatings,[77] the microhardness increased from 850 to 1016 HV with an increase in the concentration of Al_2O_3 particles from 0.5 to 2.0 g L^{-1}. Additionally, the wear resistance increased proportionately. These enhancements in the microhardness and anti-wear properties of the nanocoatings were attributed to the dispersion hardening effects of the nanoparticles. Thereafter, Ghavidel *et al.*[82] further reported the effect of nano-SiC concentration on the tribological behavior of Ni–P coatings. The plating solution containing 1 g L^{-1} SiC nanoparticles endowed the Ni–P coating with a maximum hardness of 795 HV and the corresponding tribological optimization. However, this tendency was weakened with an increase in the concentration to 2 g L^{-1}. The origin of this weakening effect was the uneven distribution of high concentration 0D-additives on the coating surface. Hence, a deterioration in the friction and wear behaviors of the nanocoatings was detected.

The study of the synergistic effect of coatings and nanolubricants is also of great significance for practical applications. However, most of the data are obtained from laboratory-made test substrates, and this type of conclusion is apparently not sufficient to guide practical use. Thus, to enhance the tribological performance of a piston ring-cylinder liner pair in engines, Xu *et al.*[75] prepared Ni–P–TiN-coated piston rings *via* the electroless plating technique. They investigated the tribological properties of coated friction pairs on a multifunctional piston ring-cylinder liner tribometer and evaluated the effect of the concentration of additive. The specimens were cut from the real piston ring-cylinder liner pairs and the chosen test conditions were sliding distance of 80 mm; sliding time of 3 h; normal load of 140 N; reciprocating frequency of 5 Hz and sliding wear was carried out at room temperature. Given that the tested matrix came from real components, the experimental results could be regarded as data generated by the actual working environment of the part. Fig. 2c shows the variation in the wear loss of the coated piston rings with different concentrations of TiN nanoparticles and cylinder liners under oil lubrication. It can be seen that the wear loss of the Ni–P–1.5TiN coating decreased by ~64% compared with that of the Ni–P coating. Fig. 2d shows the transmission electron microscopy image of nano-TiN powder. It can be seen clearly that the mean size of the TiN nanoparticles was about 20 nm, and there was a little aggregation. Although the hard TiN nanoparticles could lead to local pits on the frictional surface, the hardness of the coating was improved with the addition of TiN. A smoother surface with light furrows was formed in the case of the Ni–P–1.5TiN coating, where its better anti-wear performances could be ascribed to the moderate abrasive wear. Table 1 provides its specific friction coefficient and wear loss. This was attributed to the good combination of TiN and the Ni–P coating and the excellent lubricating effect of nano-TiN.

Fe-based amorphous nanocrystal coatings have attracted significant attention due to their unique wear and corrosion resistance. Particle reinforcement is the main method to improve the wear resistance of coatings. Shan *et al.*[64] investigated the effect of TiC content on the wear resistance of Fe-based amorphous nanocrystalline coatings. The addition of TiC reduced the microhardness of the coating compared to the coating without TiC. With an increase in the content of TiC, the microhardness of the coating increased first, and then decreased. When the content of TiC was 10%, the friction coefficient and wear volume of the coating were the lowest, indicating the best wear resistance. When the TiC content exceeded 10%, aggregation occurred, which weakened its combination with the matrix and made it easy for it to fall off in the process of friction and wear, resulting in a decrease in the wear resistance.

2.2. Ceramic-based coatings

Ceramics have been increasingly recognized as promising candidates as coatings and for other tribological applications owing to their low density, high thermal stability, and good corrosion resistance.[83] The incorporation of 0D-nanofillers in ceramic films is expected to endow ceramic-based coatings (CBCs) with excellent overall properties, such as a high elastic modulus, good wear resistance, and excellent thermal conductivity.[84–86]

One of the fascinating features of these composites is the possibility to tailor their functionality by selecting the appropriate type, concentration and size of nanofillers. In general, metal nanoparticles have made outstanding contributions to the tribological optimization of ceramic coatings.[87–90] Reasonable lattice parameter matching of the ceramic/metal interface endows the nanofiller and matrix with excellent interfacial bonding strength, which is greatly beneficial in the nanofiller repair of micro-defects in coatings and optimizing the mechanical and tribological behaviors of composite systems. In this case, the content of nanofillers plays a leading role in the strengthening mechanism. The mechanical and tribological properties of nano-coatings such as CrN/Ag, ZrN/Ag, TiN/Ag and TiN/Cu with different Ag or Cu contents were determined using nanoindentation and wear tests, respectively.[87,88] The friction coefficient decreased as the Ag or Cu content increased, but this was accompanied by a decrease in the hardness and wear resistance of the coatings. The CrN–Ag composite coatings with various nano-Ag atomic ratios (0, 3, 12 and 22 at%) exhibited different tribological behaviors.[89] The microscratch tests revealed that the coating with the highest Ag content (22 at%)

exhibited the best tribological performance. As shown in Table 1, after 100 cycles of reciprocating at 0.7 mm s^{-1} and applying a normal force of 1 N, 22 at% Ag enabled the coating to achieve the low friction level ranging from 0.04 to 0.06, owing to the lubricating properties of Ag and the easily formed tribofilm across the friction interface. It should be noted that similar to MBCs, the agglomeration tendency of 0D-nanofillers with high concentrations is an issue. Although nano-Ni endowed the ceramic coatings with attractive tribological behaviors,[90] as demonstrated in Table 1, the friction and wear of the surface coating containing 10 wt% nano-Ni particles decreased by 16.6% and 45.4%, respectively, compared to that of the pure ceramic coating. Unfortunately, when the nano-Ni concentration exceeded 10 wt%, agglomerated nanoparticles were observed to fall off the coating surface, resulting in poor surface quality and deteriorated wear resistance.

Meanwhile, many studies have been conducted to explore the tribological potential of nanofillers at extreme temperatures.[91,92] When the test temperature was 400 °C, the synergistic combination of high temperature and contact load applied to these areas led to densification of the coating; subsequently, TiC nanoparticles of different sizes were observed on the coating surface. These particles formed microscopic spherical protrusions and carried most of the contact load, providing significant protection against wear. In the case of nanofiller-reinforced CBCs, outstanding thermal conductivity is increasingly regarded as the key for resisting the local accumulation of frictional heat.[93] A yttria-stabilized zirconia (YSZ) ceramic matrix coating was prepared using mixed solution precursor plasma spraying (SPPS).[91] After the SPPS process, a significant microporous structure was observed given that the nano-YSZ was uniformly distributed in the coating. These pores could release the mismatch of the thermal expansion coefficient of the nanofiller with respect to its matrix, which is an efficient strategy for enhancing the thermal conductivity of composites. Hence, the YSZ ceramic coatings exhibited superior thermal stability and tribological properties when the temperatures increase up to 700 °C.

An interesting investigation on the tribological behaviors of TiC particle-reinforced WC-Co coatings was performed.[92] It was observed that during dry sliding at 400 °C, a mass of nano-TiC particles was extruded from the coating, preventing direct collision of the matching tribo-pairs and carrying most of the contact load, resulting in a significant enhancement in the friction performances of the WC-Co/TiC coatings. However, the improvement in anti-wear behavior was observably restricted because densified TiC-clusters were formed with related inter-lamellar delamination of the coating.

In the case of nano-coatings, friction-induced deformation manifests as substrate fatigue, nanofiller pull-out, coating cracking, and delamination.[94,95] These processes not only accompany the evolution of the coating micromorphology, but also result in tribo-chemical reactions and the formation of oxide layers. These tribo-chemical layers provide a layer of protection on the surface, thus resulting in a high level of anti-wear behavior.

It is very interesting that the tribochemical reactivity strongly depends on the material combination. Förg *et al.*[96] comparatively explored the sliding tribological properties of various ceramic coatings (Al_2O_3, YSZ and TiO_2 coating) against an SiC ball. In the case of the Al_2O_3 coating, tribochemical wear was the most intense, which led to the formation of tribo-chemical layers. Although these layers appeared to be quite stable, the lubrication become worse as the tribochemical interaction intensified, resulting in relatively high friction coefficients and wear rates. Compared to Al_2O_3, the YSZ coating showed less chemical interaction with the SiC ball, and therefore reduced wear. Among the coatings, the lowest wear but highest friction was achieved with the TiO_2 coating. The proposed tribological mechanism was that the inadequate tribochemical reactivity due to the combination of SiC and TiO_2 hindered the formation of a surface layer, deteriorating the friction. Distinctly, the tribochemical effects played a decisive role in the friction and wear behaviors. In the case of possible materials for combination with SiC, YSZ coatings may be the most promising due to their moderate tribochemical interaction.

Meanwhile, with respect to CBCs, crucial explorations demonstrated the attractive potential of 0D-nanofillers in optimizing their fracture toughness which is a prerequisite for high wear-resisting behavior.[97] Ultra-fine ceramic coatings containing nano-Ni particles were prepared;[90] subsequently, it was discovered that the incorporation of nano-Ni obstructed the propagation of crack and enhanced the fracture toughness. This nanocoating with increased fracture toughness ensured superior tribological performances compared with that of conventional coatings. Nevertheless, the roles of toughening mechanisms in the tribological behaviors of interfacial coatings are still unknown to researchers due to the complex nature of wear.

Considering the particular interest in the mechanical and tribological behaviors of CBCs, the model of dependence between surface stress and crack propagation has been proven to be effective for describing the effects of 0D-nanofillers on crack propagation,[98] which can be expressed as Formulas (1)–(3), as follows:

$$E_{SM} = A^{-1}\left(\frac{v_s}{v}\right)^2 KT\left[\frac{E_S}{RT}(1-3w)+\frac{3}{2}\ln\frac{3}{4}(1+w)\right] \quad (1)$$

$$E_{SE} = E_{SM}\left(1-\frac{3}{4}\frac{\alpha}{\beta^{2/3}}N_t^{-1/3}\right) \quad (2)$$

$$G_l = \int_0^l \frac{E\varepsilon^2}{2(1-\nu')}\,dx \quad (3)$$

where E_{SM}: surface energy (mJ m^{-2}), v: the molar volume at any temperature, v_s: the melting point molar volume (cm^3 mol^{-1}), A^{-1}: the area occupied by one atom (cm^2 per atom), T: absolute temperature (K), K: the Boltzmann constant, E_S: sublimation energy, R: the gas constant, w: a constant, which is equal to 0.287 for all metallic elements, E_{SE}: surface energy of a nanoparticle, α and β: packing parameters, N_t: the total number of atoms in the nanoparticles, G_l: the energy release rate, E: the

elastic modulus of the coating, l: the coating thickness, ν': Poisson's ratio, and ε: the strain.

According to the mentioned-above equations, it can be concluded that the surface energy and surface tension are proportional to the dimension of 0D-nanofillers. With respect to the smaller sizes, 0D-nanofillers possess a smaller surface energy and surface tension, resulting in better interfacial bonding strength between the nanofiller and coating substrate. During wear, the voids in ceramic coatings concentrate the stress and become the source of cracks. 0D-nanofillers with small sizes anchored in the voids provide an effective way to induce crack deflection and crack bridging, which are crucial to improve the anti-wear behavior of CBCs.

An important study was performed on YSZ ceramic coatings reinforced using nano-Ag_2MoO_4 and nano-Ag particles.[99] Fig. 3a presents a schematic diagram of the route for the synthesis of YSZ-Ag-Ag_2MoO_4 coatings. According to this figure, microcracks and pores were observed in the lamellar-structure YSZ-coatings. These inherent defects favored the storage of composite lubricants. As observed in the SEM image of the fractured surface of the YSZ-Ag-Ag_2MoO_4 coating (Fig. 3b), octahedron-like particles were present in the coating. Element analysis indicated that the

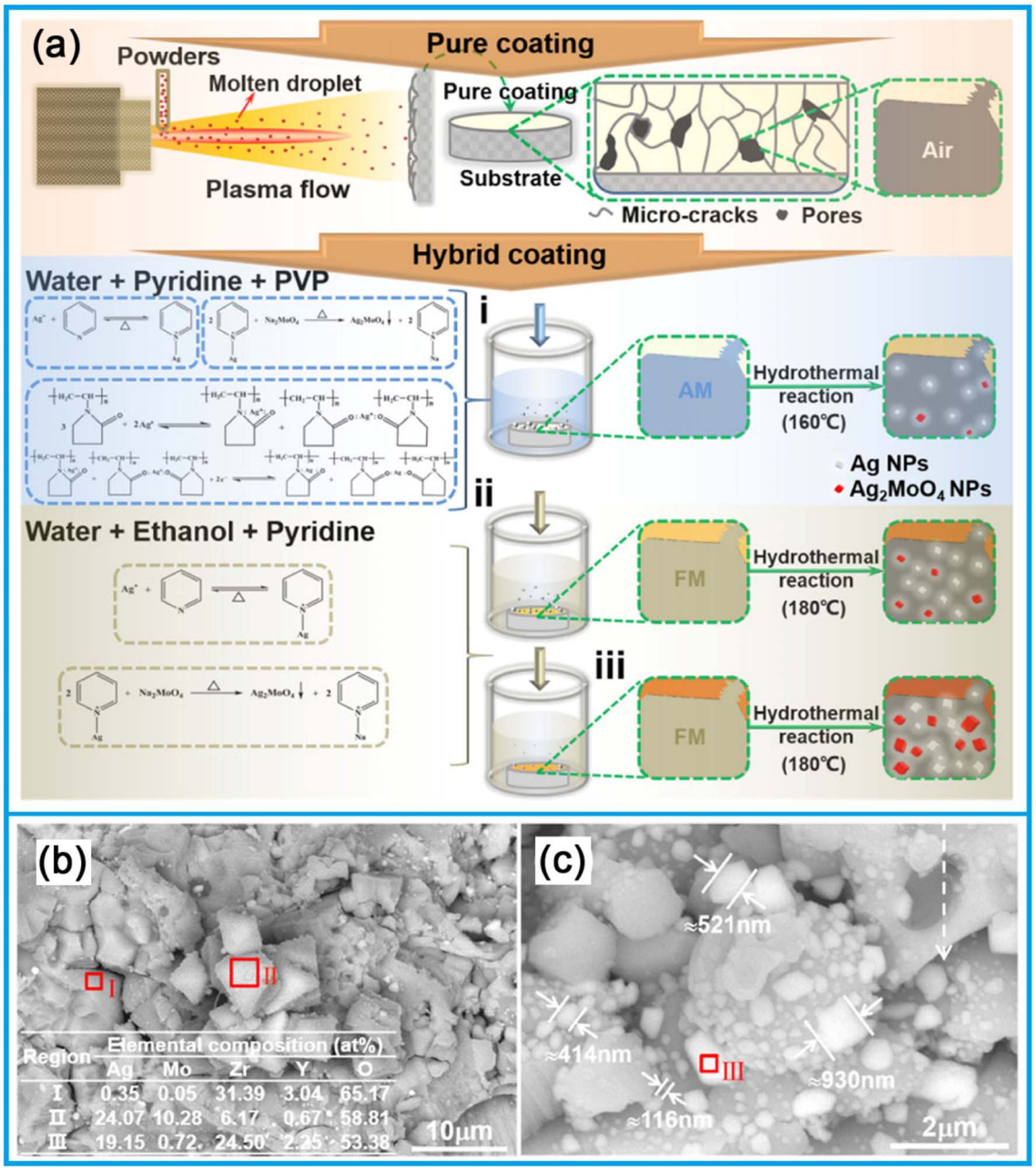

Fig. 3 (a) Schematic diagram of the route for the synthesis of YSZ-Ag-Ag_2MoO_4 coatings. (b) and (c) SEM images of the fractured surfaces of YSZ-Ag-Ag_2MoO_4 coatings, coupled with element analysis of the selected regions inside the hybrid coatings. Reproduced from ref. 99 with permission from Elsevier, Copyright 2021.

octahedron-like particles in Region II corresponded to Ag_2MoO_4 and the nanoparticles in Region III were mainly Ag, as can be in Fig. 3b and c, respectively. Thus, Ag and Ag_2MoO_4 nanoparticles were ingeniously anchored in the defects (cracks and pores) to modify the mechanical and tribological properties of the YSZ coatings. Compared with the YSZ coatings, the YSZ-Ag-Ag_2MoO_4 coatings exhibited a lower friction coefficient (~0.15) at 800 °C and the average wear rate of the hybrid coatings (6.81×10^{-6} mm^3 N m^{-1}) was greatly reduced by about 91.77%.

2.3. Polymer-based coatings

Owing to their low cost and low density, polymer coatings are advantageous for the design of lightweight tribological applications such as automobile parts and electronic devices. However, their application potential in tribology is limited by their poor hardness, adhesion strength, and thermal conductivity.[100] As a result of these concerns, research has concentrated on 0D-polymer coatings, which exhibit superior antifriction, wear resistance, thermal conductivity, and mechanical properties.[101–103] For example, the large specific surface area of 0D-nanoparticles endows them with strong interface interactions with their polymer matrixes. By incorporating nanoparticles into polymer coatings, it is possible to improve their load-bearing characteristics and adhesion strength, resulting in composite coatings with improved frictional properties.[104]

When the size of the filler is reduced to the sub-micron- or nano-scale, the wear behaviors of composites may exhibit significant differences from that of microparticle-filled systems.[105] One of the low friction and wear mechanisms of 0D-fillers is their smaller contact area in comparison to microparticles, which plays a notable role in the reduction of the abrasiveness of hard particles. Additionally, once these nanofillers become freely movable in the friction interface, they serve as distance holders and nanobearings, resulting in an increase in the load-bearing capacity and optimization of the friction coefficient of the coating.[106] Consequently, 0D-nanofillers contribute significantly more to an improvement in tribological behavior than large particles. Based on the systematic evaluations on the performances of PEEK coatings containing micro-/nano-SiC under friction and wear, Kadiyala *et al.*[104] proposed that nano-SiC coatings possessed higher binding strength and better bearing capacity compared to micro-SiC systems. These advantages were conducive to improving the tribological abilities of the as-prepared coatings.

A further investigation on the tribological behaviors of nano-silica-reinforced polymer coating was performed[50] and the abrasion and friction behaviors of the coatings with different nano-silica weight fractions are presented in Fig. 4a and b, respectively. According to these figures, the addition of nano-silica resulted in considerable improvements in the tribological performances of the coatings. Especially at high concentrations, it was observed that the friction coefficients of the composite coatings decreased by 18% compared to that of the pure polymer coatings. The wear debris-induced lubrication accounted for the enhanced friction and wear properties, given that the surface contacts between the frictional pairs were effectively prevented.

Distinctly, the concentration of 0D-nanofillers plays an important role in the improvement of the tribological performances of polymer coatings. An in-depth study on the tribological characteristics of poly-methylmethacrylate/silica (PMMA/SiO_2) coatings was conducted by Lin *et al.*[107] The experimental results are presented in Table 1, which indicated that with an increase in the weight ratio of nanofillers from 0 to 0.3 wt%, the wear-resistance ability of the coating significantly improved at the cost of an increase in the friction coefficient from 0.27 to 0.4. This unsatisfactory coefficient of friction for the coating was mainly ascribed to the deterioration of its surface roughness at a high concentration of 0D-nanofiller.

Remarkably, the observed tendency of agglomeration occurs at excessive particle concentrations,[108] resulting in undesirable friction and wear behaviors of the coating. According to recent studies on nanofillers, it has been proposed that appropriate concentrations are of great importance to improve the tribological potential of coatings. The use of nano-TiO_2-sol provided an effective method for the uniform distribution of particles in Cu–Sn–polytetrafluoroethylene (Cu–Sn-PTFE) coatings.[109] Particularly, 40 ml L^{-1} TiO_2-sol in the coating resulted in the minimum and most stable friction coefficient, as illustrated in Fig. 4c. However, the friction coefficient sharply increased when the concentration of TiO_2-sol exceeded 40 ml L^{-1}, resulting in an observable deterioration in the tribological behaviors of the coatings.

Considering the high strength and outstanding thermal stability of PEEK, is increasingly regarded as an ideal candidate for tribological applications, which attracted significant interest by Hou *et al.*[110] Tentatively, inorganic fullerene-like tungsten disulfide (IF-WS_2) nanoparticles were incorporated in PEEK coatings to enhance their tribological behaviors. It was observed that the lowest friction coefficient of 0.15 was achieved at 2.5 wt% IF-WS_2, as shown in Table 1. When the concentration of IF-WS_2 exceeded 5 wt%, the friction coefficient of the nanocoating gradually deteriorated. This was mainly attributed to the agglomeration of the IF-WS_2 particles at high concentrations, resulting in a reduction in the lubricating capability of the nanofillers.

Besides the aforementioned concentration effects, the adhesion values of the coatings and substrates are also increasingly regarded as dominant factors affecting the friction and wear behaviors. Choudhury *et al.*[111] fabricated a polytetrafluoroethylene (PTFE) coating on a steel surface, where polydopamine/Ag-nanoparticles (PDA/AgNPs) were applied as the interlayers of the PTFE coatings with respect to their substrates. This peculiar construction of PDA/AgNPs/PTFE hybrid coatings was shown to be an effective solution to address the issue of inadequate adhesion of the coatings to stainless steel. PDA/AgNPs endowed the PTFE film with a longer wear life in comparison with the pristine PTFE, where a 3.6-times increase in durability was achieved by adding only 2.0 wt% of AgNPs. This worthwhile improvement was mainly attributed to the improved adhesion strength, fibrillar PTFE network, and a formation of a transfer film.

Numerous works have demonstrated that the characteristics of transfer films play dominant roles in determining the

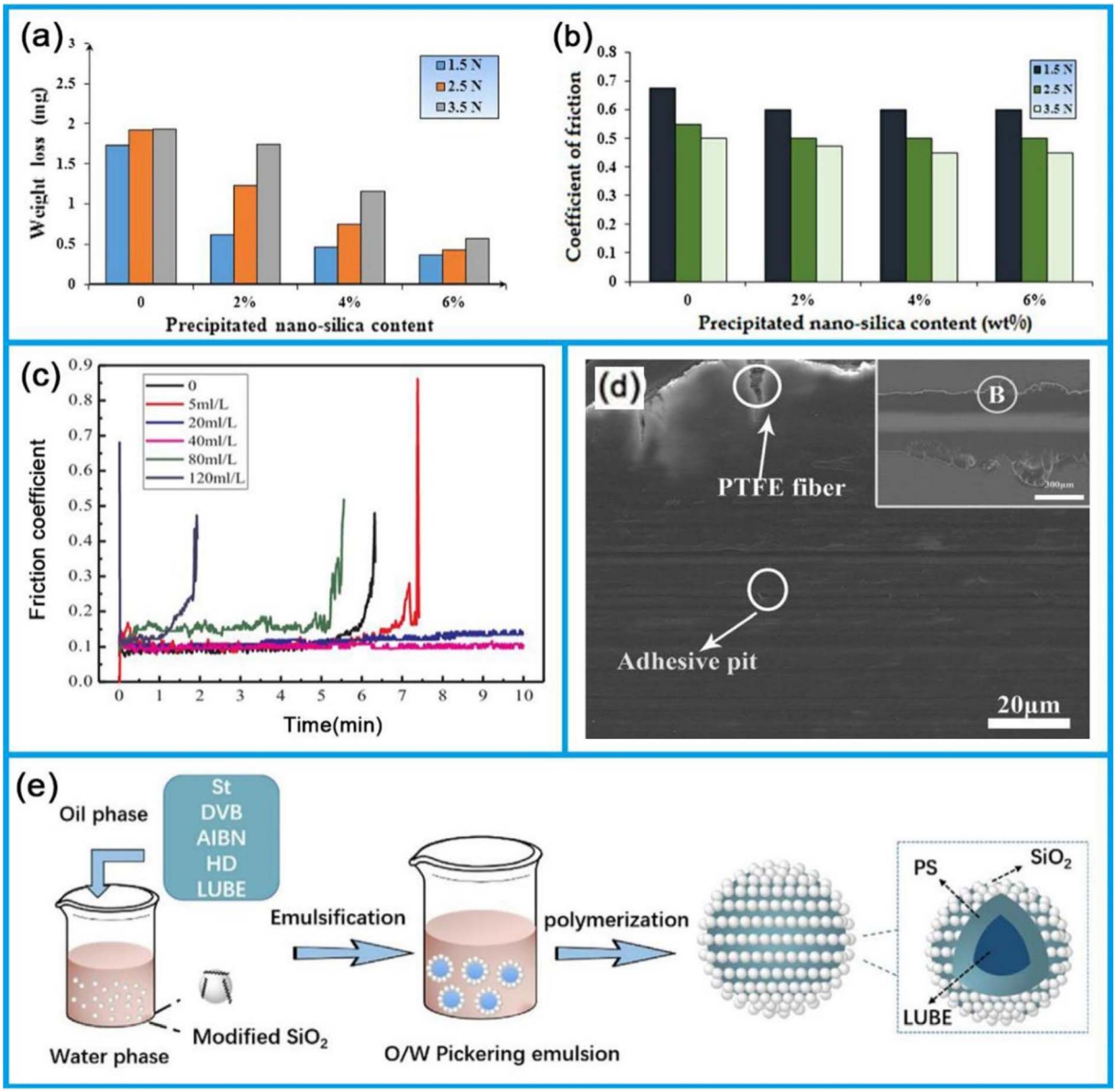

Fig. 4 Weight loss (a) and friction coefficient (b) of varying nano-silica contents at different loads. Reproduced from ref. 50 with permission from Elsevier, Copyright 2018. (c) COF-time curves of the coatings with different TiO_2-sol concentrations. Reproduced from ref. 109 with permission from Elsevier, Copyright 2019. (d) SEM morphology of BMG/PTFE. Reproduced from ref. 114 with permission from Elsevier, copyright 2018. (e) Illustration of the formation for PS/SiO_2 hybrid microcapsule. Reproduced from ref. 115 with permission from Elsevier, Copyright 2018.

tribological properties of PBCs.[112] In the case of pristine polymer/transfer film systems, the poor adhesion of the transfer film to the surface of the friction surface resulted in degraded wear and friction behaviors. Thus, 0D-nanofillers provide a feasible strategy to improve the adhesion strength of transfer films, thus endowing coatings with improved tribological behaviors.[113] Under the test conditions with a frequency of 2 Hz and sliding displacement amplitude of 4.2 mm, a composite lubrication film with high adhesion was formed on the frictional pair of PTFE coating reinforced with graphite nanoparticles.[114] The presence of the lubricating film reduced the mechanical damage caused by wear of the contact interface, reducing the coefficient of friction by ~26%. As shown in Fig. 4d, the addition of ball-milled graphite did not change the wear mechanism of the composites, but it reduced the friction at the contact interface caused by the adhesion of mechanical damage wear.

Thereafter, polystyrene/nano-SiO_2 (PS/SiO_2) microcapsules encapsulating lubricating oil were fabricated using the Pickering polymerization technique,[115] and then the tribological behaviors of the microcapsules explored as epoxy (EP) coating additives. Fig. 4e shows the process for the preparation of the microcapsules in detail. As can be seen, nano-SiO_2 was uniformly coated on the surface of the polystyrene microcapsules, playing an important role in the improvement in the thermal stability and lubrication behaviors of microcapsules.

Thermogravimetric analysis (TGA) showed that the microcapsules displayed outstanding thermal stability with a decomposition temperature of 250 °C (see Fig. 4d), significantly improving their potential for high-temperature tribological applications. In the case of the microcapsule/coating systems, the PS/SiO_2 hybrid shell microcapsules endowed the coatings with prominent self-lubricating properties. The released lubricant oil and SiO_2 particles from the broken microcapsules formed a transfer film to effectively suppress the surface fatigue wear, hence providing an effective approach to optimize the friction and wear behaviors of coatings.

0D nanofillers have good organizational structures and unique performances, playing an important role in optimizing the microstructure and load-bearing capacity of coatings. The smaller the size of the reinforcing materials in composite coatings, the more significant the enhancement in function. The addition of nanofillers can inhibit crystal growth in metal-based coatings and deposit dense structures on the alloy coating, thereby improving the microhardness of the nanocomposite coating. The introduction of 0D nanofillers in ceramic coatings can generate frictional chemical reactions and form the corresponding oxide layers. These frictional chemical layers provide a protective layer on the surface, but the activity of frictional chemical reactions largely depends on the combination of materials. A reasonable ratio of nanofiller endows coatings with good interfacial bonding strength, which can optimize their mechanical and tribological properties. In the case of polymer coatings, the addition of nanofiller induces excellent wear resistance, thermal conductivity, and mechanical properties. It can form a highly cohesive composite lubrication film on the friction pair, thus reducing the wear and mechanical damage of the contact interfaces.

In addition, for microcapsule/coating systems, nanofiller hybrid shell microcapsules endow the coating with a significant self-lubricating performance. The lubricating oil is released after the fragmentation of the microcapsules to form a transition film with the nanoparticles, effectively suppressing the fatigue wear, and thus obtaining a composite coating with improved friction and wear performance.

3. One-dimensional nanofillers

1D-nanofillers have been demonstrated to be suitable for wide range of tribological applications in ceramics, metals and polymers.[118–120] Similar to 0D nanofillers, significant research has been also conducted on 1D nano-coatings owing to their attractive tribological potential, and the recent results are presented in Table 2. In this section, we introduce the methods, behaviors, and wear mechanisms for 1D-nanofillers as effective additives in various coatings to enhance their tribological performance.

3.1. Metal-based coatings

MBCs have been extensively studied for controlling friction and wear. In recent reports on nano-coatings, the high thermal conductivity and excellent mechanical performance of 1D-nanofillers have been increasingly recognized, which are of great importance for the improvement of the friction and wear behaviors of coatings.[120,121] Unlike 0D-nanofillers, 1D-nanofillers possess a high aspect ratio, and this well-organized structure endows them with immense potential in the field of tribology.

As one type of nanofillers, 1D nanofillers exhibit nano-rolling effects similar to 0D nanofillers, and thus separate the rubbing surfaces to reduce the tribo-contacting of two surfaces, which is of great significance for widespread tribological applications.[68,69,122] This rolling effect provides an effective method to reinforce the lubrication function and mechanical strength of

Table 2 Anti-wear and friction-reducing effects of 1D-nanofillers in coatings[a]

			Tribological results	
Substrate	Reinforcement	Tested conditions	COF	Wear
Cu coatings	CNTs[131]	GCr15 bearing steel ball (ball-on-disk, 200 rpm, 6–10 N, RT)	~0.2	Wear rate: 1–2.5 × 10^{-8} mm^3 N m^{-1}
Ni-based coatings	CNTs[126]	GCr15 sliding disk (pin-on-disk, 200 rpm, 8 N, RT)	0.35	Wear loss: 12.5–38 mm^3
Ni-based coatings	Nanotubular titanates[124]	Spherical steel ball (ball-on-disk, 0.1 m s^{-1}, 0.2 N, RT)	~0.10	Wear rate: ~2.4 × 10^{-3} mm^3 N m^{-1}
SiC coating	SiC nanowire[141]	SiC balls (ball-on-disk, 0.1 m s^{-1}, 2 N, 600 °C)	0.41	Wear rate: 2.38 × 10^{-4} mm^3 N m^{-1}
SiO_2 coatings	CNTs[154]	Steel ball (pin-on-disc, 0.1 m s^{-1}, 1 N, RT)	0.40	Wear rate: 1 × 10^{-3} mm^3 N m^{-1}
UHMWPE coatings	CNTs[158]	Silicon nitride ball (ball-on-disk; 1000, 2000 and 2500 rpm; 4 N, 25 °C)	~0.16	Wear life: > ~250 000 cycles
UHMWPE coatings	CNTs[168]	440C stainless steel ball (ball-on-disk, 0.5 m s^{-1}, 9 N, 25 °C)	~0.09	Wear life: > ~25 000 cycles

[a] RT = room temperature.

substrates.[122–125] In one study, the direct growth of carbon nanotubes (CNTs) from an Ni-based coating on a copper substrate was reported[126] using the hydrothermal method. After the tests employing a rotating speed of 200 rpm and normal force of 8 N, the volume loss on copper substrate was 3.5-times that of the Ni-CNTs/Cu composite; furthermore, a relatively low coefficient of friction was observed in the Ni-CNT coating compared to the copper matrix. The anti-friction mechanism was explained by the following analysis.

High microhardness was achieved in the Ni-CNT coating after heat treatment at 500 °C. Furthermore, high-strengthened CNTs were *in situ* grown in the Ni-CNT coating, which firmly bridged and wrapped the Ni–P and Ni nanoparticles in the Ni-based coatings. Consequently, good load-transferring ability was achieved during wear, which led to decreased plastic deformation and adhesive wear.[127] Because the contact area between the pin samples and disk counter-body was reduced in these cases, sliding wear only occurred on limited contact surfaces, which resulted in a decrease in friction coefficient.

Table 2 presents the friction and wear data of CNTs in detail, which enhanced the tribological properties of coatings. The enhancement in the tribological performances was mainly attributed to the excellent load-bearing ability and self-lubricant effects of the CNTs, as well as the good metallurgical bonding of the CNTs incorporated in the Ni-based coating.

To confirm the enhancement of the tribological coatings by CNT, Karslioglu *et al.*[123] studied the friction and wear behaviors of Ni–Co/multiwalled carbon nanotube (MWCNT) coatings. Owing to the prominent load-bearing effect of MWCNTs, the composite coatings exhibited better microhardness and wear resistance compared to the Ni–Co alloy coatings. However, the surface hardness and the anti-wear behavior were improved at the cost of the surface roughness, resulting in higher friction coefficients for the Ni–Co/MWCNT coatings than that of the unreinforced coatings.

Tubular nanostructures not only endow 1D-nanofillers with the unique rolling effect, but also provide a feasible strategy for achieving ideal structural and mechanical (such as stiffness and strength) improvements, resulting in enhanced wear-resistance. For example, Ni coatings reinforced with regularly shaped nanotubular titanates were fabricated by Low *et al.*[124] The suggested cross-linked and mesh-like tubular interlocked structures caused the added hard second phase element to have a large surface area, which exhibited high resistance to angular abrasive during friction sliding, thus improving the wear resistance of the coating. This structure also led to a reduction in the contact pressure between two bodies, effectively preventing the nanotube titanate from pulling out and/or breaking. Hence, the nanocomposite coatings exhibited an ~22% reduction in friction and ~29% enhancement in wear resistance compared with the Ni coatings containing nano-TiO_2 particles. As shown in Table 2, the friction coefficient and wear rate were ~0.10 and ~2.4×10^{-3} mm^3 N m^{-1}, respectively.

The dispersive state and morphology of the nanofillers, as well as their interfacial bonding strength with substrates have been increasingly regarded as dominant factors affecting the tribological behaviors of MBCs. The homogeneous distribution of filler was responsible for the microstructure evolution of the coatings, which inhibited the growth of the coating grains and resulted in a dense structure, resulting in an improved hardness of the coating.[128,129] According to the report by Ahmad *et al.*,[130] the relationship between the wear rate and hardness can be described by the following equations:

$$V = a\frac{F^{9/8}}{K_{IC}{}^{1/2}H^{5/8}}\left(\frac{E}{H}\right)^{4/5} \quad L = a\frac{(\sigma_s A_c)^{9/8}}{K_{IC}{}^{1/2}H^{5/8}}\left(\frac{E}{H}\right)^{4/5} L \quad (4)$$

$$W = \frac{V}{FL} = a\frac{F^{1/8}}{K_{IC}{}^{1/2}H^{5/8}}\left(\frac{E}{H}\right)^{4/5} = a\frac{(\sigma_s A_c)^{1/8}}{K_{IC}{}^{1/2}H^{5/8}}\left(\frac{E}{H}\right)^{4/5} \quad (5)$$

where F: applied load in N, σ_s: contact stress in MPa, A_c: contact area in mm^2, K_{IC}: fracture toughness in MPa, H: Vicker's hardness of wear surface in GPa and a: constant independent of material type. According to Formulas (4) and (5), the wear rate of the nanocomposite is inversely proportional to the hardness. Thus, the enhancement in hardness has great significance in optimizing the tribological performances of coatings.

Friction and wear tests were carried out on Ni-CNT coatings.[129] It was observed that acid functionalization contributed to the uniform dispersion of CNTs in the Ni-based coatings. This dispersion state was of great importance to reduce the porosity of the coating. Accordingly, the Ni-CNT coatings exhibited excellent mechanical properties. The measured hardness increased with an increase in the volume fraction of CNTs, consequently having a positive impact on the wear resistance of the coating. The Ni-based coatings containing functionalized CNTs exhibited a significant reduction in wear rate compared with the pure Ni coating in the friction tests.

An important factor for achieving well-dispersed 1D-nanofillers in the coating is the homogenous distribution of fillers in the initial mixtures. Zhou *et al.*[131] proposed the use of a colloidal solution containing uniformly dispersed CNTs for the preparation of CNT/Cu coatings. The negatively charged metal ions in solution were considered to be the main factor for inhibiting the agglomeration of CNTs. Accordingly, CNTs remained stable and were homogeneously dispersed in the aqueous solution of $[Cu^{II}EDTA]^{2-}$ complexes, as confirmed in Fig. 5a. Meanwhile, in the case of the CNT/Cu systems, Fig. 5b indicates that the well-distributed CNTs enabled the as-prepared coating to achieve an attractive compact structure, which greatly facilitated the improvement in the friction and wear behaviors of the coatings. Simultaneously, it can be observed in Fig. 5c that the wear track of the composite coating was very smooth, which was reduced to 250 μm. Compared with a large width of 450 μm for the pure copper coating, the friction and wear performance of the composite coating with moderate carbon nanotube content was greatly improved.

Table 2 indicates that the composite coating possessed a relatively low friction coefficient (~0.2) and high wear resistance, which were 35–50% and 6–20 times that of the pure Cu coating, respectively. The improvement in tribological properties was mainly associated with the formation of a tribofilm containing CNTs. Fig. 5d exhibits the Raman spectroscopy overlaid on the optical microscopy image of the composite

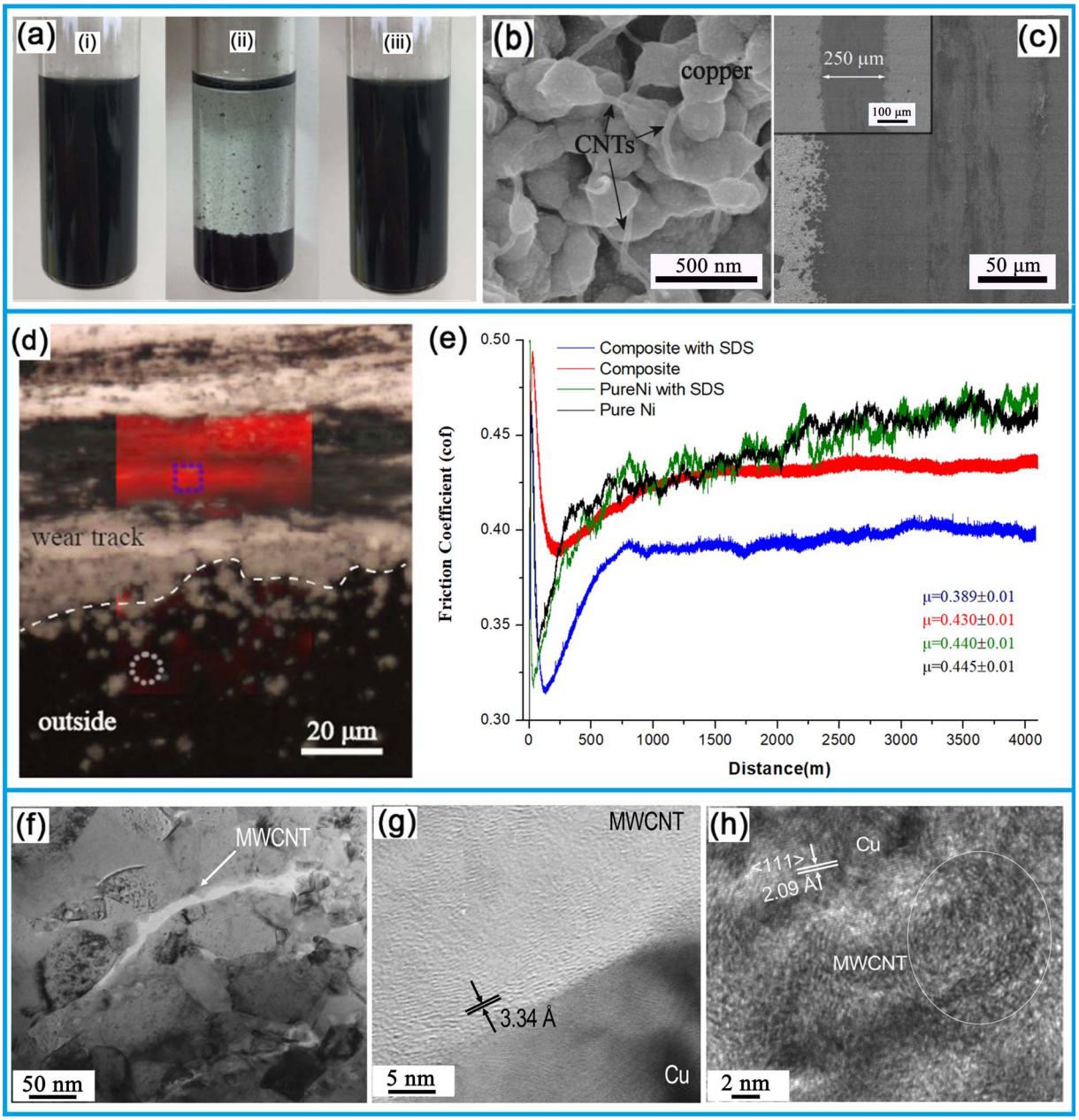

Fig. 5 (a) Photographs of 0.12 g L^{-1} CNT aqueous dispersion without copper salt (i) and with 10 mmol L^{-1} $CuSO_4$ (ii) or 10 mmol L^{-1} $[Cu^{II}EDTA]^{2-}$ complexes (iii). (b) Surface feature of coatings with CNTs, surface morphology (c) of wear track, and (d) Raman spectroscopy overlaid on the optical microscopy image of 0.12-CNT/Cu composite coating. Reproduced from ref. 131 with permission from Elsevier, Copyright 2018. (e) Variation in the dry sliding COF as a function of sliding distance of the coatings. Reproduced from ref. 134 with permission from Elsevier, Copyright 2018. (f) TEM image of kinetic-sprayed MWCNT/Cu coating and (g) and (h) HREM images of MWCNT. Reproduced from ref. 135 with permission from Elsevier, Copyright 2015.

coating. The presence of preferential regions with an obvious increase in relative intensity inside the wear track revealed the formation of a carbon-rich tribolayer.

Given the well-developed techniques for the synthesis of 1D-nanocoatings, many works demonstrated the potential of 1D-nanofillers to significantly improve the mechanical and tribological behaviors of MBCs.[120,132,133] Chronopoulou *et al.*[134] produced MWCNT-Al_2O_3/Ni coatings *via* the pulse plating technique. It was detected that the presence of sodium dodecyl sulfate (SDS) promoted the well-proportioned dispersion of the hybrid MWCNT-Al_2O_3 particles on the coating surface. The compactness of the deposited coating was determined by the pulse frequency, and applying a high pulse frequency resulted in a more uniform and less porous structure compared to the coating produced at a low pulse current frequency. More importantly, the combined action of homogeneously dispersed nanofillers and the dense structures endowed the MWCNT-Al_2O_3/Ni coatings with more excellent tribological behaviors

than the pure Ni coating. Fig. 5e shows the variation in the friction coefficient value as a function of the sliding distance for the coatings. The tribological experiments demonstrated that the composite coating produced in the presence of SDS exhibited the lowest friction coefficient compared to the pure coating and composites produced in the absence of additives.

Thereafter, Kang *et al.*[135] systematically studied the effects of kinetic spraying and high velocity oxygen fuel (HVOF) processes on the tribological behaviors of MWCNT-reinforced Cu-coatings. According to the experimental results, the friction and wear properties of the composite coatings were associated with the microstructural features and MWCNT state. The close physical contact of the embedded MWCNTs with regard to their substrate coating can be observed in Fig. 5f and the high-resolution electron microscopy (HREM) image is shown in Fig. 5g, indicating that MWCNTs preserved their original structure after kinetic spraying. By contrast, the structural integrity of MWCNTs was destroyed during the HVOF process, where curled MWCNTs were detected, as shown in Fig. 5h. This structural destruction played a negative role in the self-lubricant effects of MWCNTs. Hence, according to the wear and friction results, the kinetic-sprayed MWCNT/Cu coatings were superior to that of the thermal-sprayed coatings.

3.2. Ceramic-based coatings

Similar to MBCs, extensive investigations have been conducted on CBCs over several decades owing to their attractive tribological potential. Based on recent reports, the inherent defects (such as pores and cracks) in ceramic coatings lead to brittle behavior and low cohesive strength with their substrates;[136] thus, acting as major bottlenecks in the widespread application of ceramic coatings. In 1D nanofiller systems, the simple addition of nanofiller is an efficient approach to improve the fracture toughness and anti-wear properties of CBCs.[137,138]

The multiple-scale wear exploration of a plasma-sprayed Al_2O_3-CNT nanocoating was performed.[139] CNTs endowed the Al_2O_3 coating with enhanced macro-wear resistance by more than about 49 times. This improvement was primarily ascribed to the increase in fracture toughness, load-bearing capacity, and self-lubricating effects of CNTs. According to the wear models, the relationship between load-bearing capacity and fracture toughness could be appropriately predicted using the following equations:

$$W_v = \frac{1}{2}\cos\theta d_n^2 l \quad (6)$$

$$k = W_v H/p \quad (7)$$

$$a = \frac{-\ln\left(W_v H^b\right)}{\ln k} \quad (8)$$

$$P_{cr} = \frac{4.5}{1+10f}\frac{\left(kpW_v^{-\frac{b+1}{b}}\right)^{\frac{b}{a}}}{\sqrt{\pi a_0}} \quad (9)$$

where W_v: wear volume, d_n: normal displacement of vertical depth, l: scratch length, p: applied pressure, H: hardness of composite, k: wear constant, a: fracture toughness exponent, b: hardness exponent, f: coefficient of friction, P_{cr}: critical contact pressure, and a_0: wear debris size.

According to the above-mentioned formulas, high fracture toughness and great critical pressure are required to initiate cracking. 1D-nanofillers induced the densification of the coating, which produced a bridging effect to endow CBCs with reinforced fracture toughness. Consequently, significant improvements in load-bearing capacity and wear resistance were observed. It was report that the addition of 0.5 wt% graphene nanoplatelets (GNPs) and 1 wt% CNTs to an Al_2O_3 coating resulted in a reduction of 93.25% in wear volume loss and 90.94% in wear rate.[140] The proposed explanation for the enhancements was the strong interfaces of Al_2O_3 with the reinforcements, as well as toughening offered by the GNPs and CNTs.

A dense SiC nanowire-reinforced SiC (SiCNW–SiC) coating on a carbon/carbon (C/C) composite was synthesized.[141] Further, the typical SEM morphology of the synthesized SiCNWs on C/C substrate is shown in Fig. 6a, where the SiCNW nanowires show a random distribution to form a porous network microstructure. Fig. 6b and c present the fracture morphology of the coatings reinforced by SiCNWs. Some SiCNWs with debonding and pullout feature were observed, while the rest of the nanowires were embedded in the coating. This indicated the reliable interfacial adhesion of the nanowires with their coating matrix. The strong bonding was expected to effectively transfer stress from the matrix to the nanowires, and then promoted the SiCNWs to absorb the fracture energy, consequently providing a feasible solution for the improvement in fracture toughness and tribological behaviors. After friction testing at a sliding speed of 0.1 m s^{-1} and an applied load of 2 N at 600 °C, the friction coefficients and wear rates of the SiCNW-SiC coatings were significantly reduced compared with that of the SiC coating, with the corresponding values of ~0.41 and ~2.38×10^{-4} mm^3 N m^{-1}, respectively. Fig. 6c shows the worn surface of the SiCNW-SiC coating at 600 °C. Many micron-sized fine debris were observed on the worn surface. This debris consisted of Si and O elements and should be silica. These fine fragments were scattered over the wear track, which created the rolling friction on the contact surface, thus reducing the adhesive wear. In addition, many tongue-shaped tribo-islands were observed, suggesting that mild plastic deformation of the SiCNW-SiC coating occurred under frictional stress. The specific wear rate of the coatings was calculated using the following equation:

$$\omega = \frac{2\pi r A}{FL} \quad (10)$$

where F is the applied load, L is the sliding distance, r is the disk wear track radius, and A is the cross-sectional area of the wear track on the coating. A was measured by measuring using a microscope.

After the addition of SiC nanowires, the fracture toughness of the SiC coating was improved evidently, which is an

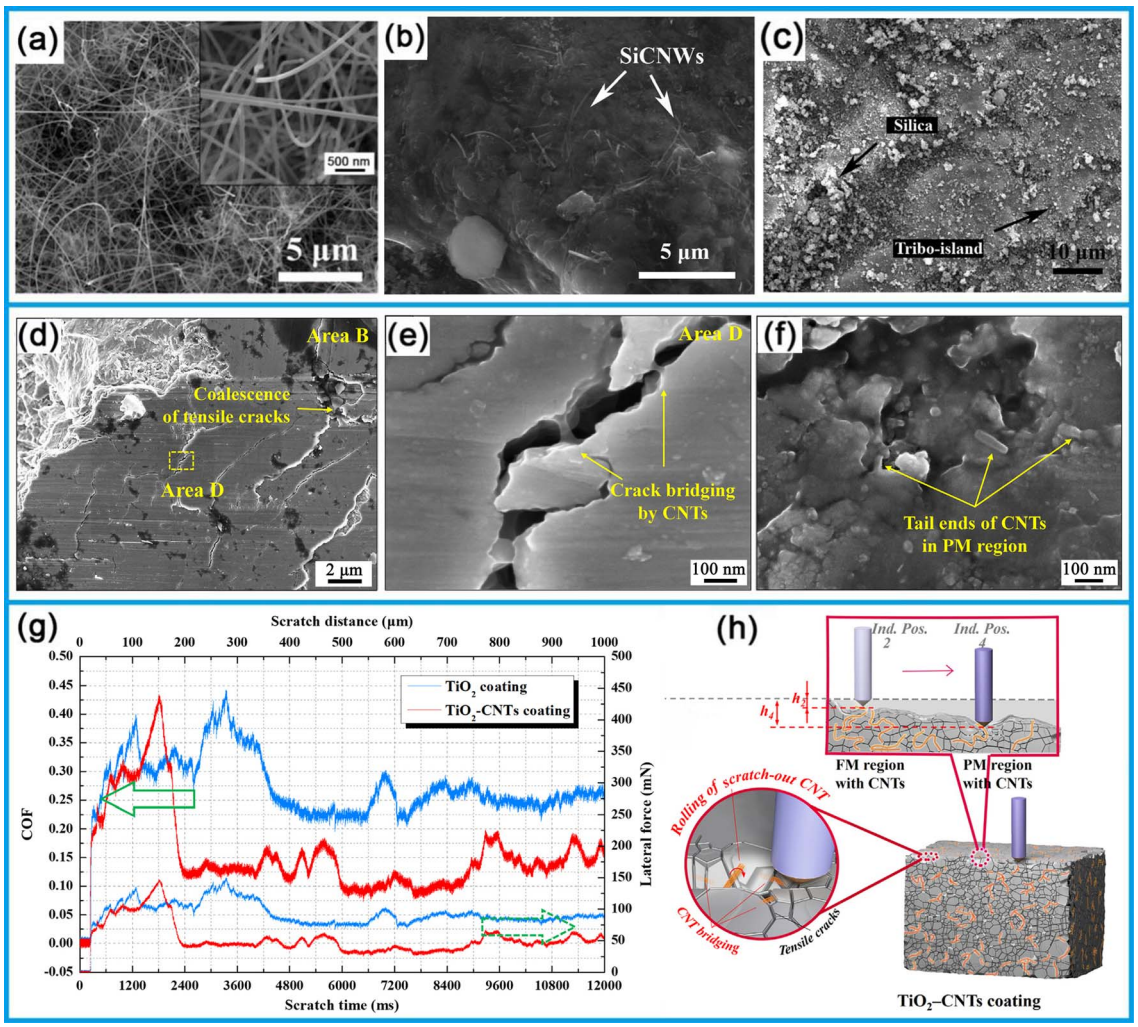

Fig. 6 SEM images of SiCNWs on a matrix surface (a), and fracture (b). Worn surface (c) generated on SiCNW-SiC at 600 °C. Reproduced from ref. 141 with permission from Elsevier, Copyright 2013. (d) Image of scratch track on TiO_2-CNT coating at high-magnification. (e) Enlarged view of area D in (d). (f) Scratched surface on the partially molten (PM) region. (g) Relation curves of COF and lateral force with an increase in scratch time and distance of coatings. (h) Wear mechanism during scratch tests. Reproduced from ref. 143 with permission from Elsevier, Copyright 2020.

advantage in wear resistance. The wear rate of the SiCNW-SiC coating was lower than that of the SiC coating without SiC nanowires. Therefore, it was feasible to calculate the fracture toughness of the coating to investigate its tribological properties. The hardness and elastic modulus of the as-prepared coating were measured using a nano-indenter (Agilent Nano-indenter G200) with a diamond Berkovich indenter on the polished cross-section of the coating. The fracture toughness (K_c) of the SiCNW-SiC coating was evaluated on the polished surface of the coating by the indention method using a micro-indenter (Nanovea, MHT-M) with Vickers indenter. A load of 1 N was used to generate cracks in the coatings for the calculation of the fracture toughness using the following equation:[142]

$$K_c = 0.016\left(\frac{E}{H}\right)^{1/2}\frac{P}{c^{3/2}} \quad (11)$$

where P is the applied load, E is the elastic modulus, H is the hardness, and c is the radial length (measured from center of indent).

Comparative exploration of the tribological properties of TiO_2-CNT and TiO_2 coatings was carried out using constant load scratch tests.[143] Then, the ability of TiO_2 and TiO_2-CNT coatings for resisting scratch damage was compared using the micro-scratch method. Eqn (12) can be used as a wear model for evaluating the scratching and anti-scratch performance (W_R) of ceramic coatings,[144] as follows:

$$W_R \propto \frac{H_v^{1/2}K_{IC}^{2}}{F_n^{3/2}L} \quad (12)$$

where H_V and K_{IC} are the micro-hardness and fracture toughness of the coating, respectively, F_n is the normal load, L is the sliding distance, and $\propto$ is the proportional relationship. According to this equation, the TiO_2-CNT coating with enhanced hardness and fracture toughness has better scratch resistance, thus indicating a higher cohesive strength.

Thermally sprayed ceramic nanostructured coatings commonly have inherent defects, such as pores, unmelted particles, and weakly bonded splats. Hence, during the scratch

test, these defects, as potential sources of cracks, initiated small cracks perpendicular to the scratch direction and gradually spread to the surface, then forming through cracks, which eventually led to the partial brittle peeling-off of the coating.[145] Also, the cracks could coalesce with the neighboring tensile cracks and intrinsic flaws of the coating, hence producing larger cracks, followed by the release of fractured fragment or debris from the coating. Fig. 6d displays a dramatic decrease in the amount of scratch and debris on the grooves of the scratched surface compared with that of its counterpart without CNTs. This was attributed to the presence of CNTs, which effectively inhibited the initiation and expansion of cracks, playing a dominant role in reinforcing the cohesive strength of the coating. These CNTs effectively prevented the lamellar peeling caused by the crack interconnection, as observed in Fig. 6e and f. The CNT bridging under the coating surface increased the cohesive strength of the coating, thereby enhancing the scratch resistance of the coating. This was crucial to realize high wear resistance. Hence, the friction forces and frictional coefficients of the TiO_2-CNT coating were remarkably reduced under the same test conditions compared to the coating without CNTs (see Fig. 6g). Fig. 6h shows a scheme of the strengthening mechanisms of CNTs. As shown in Fig. 6h, the scratched-out CNTs in the wear surface were directly contacted with the applied indenters, producing a rolling effect and lowering the friction resistance, thus achieving a reduction in the friction coefficient.

To improve the tribological performance of carbon/carbon (C/C) composites at high temperature, an SiC coating with the added Ni (SiC–Ni coating) was prepared by pack cementation.[146] The SiC–Ni coating was mainly composed of SiC and $NiSi_2$, and the adhesion between the coating and substrate was reliable.

The friction coefficient of the SiC–Ni coating was about 0.35 at 25 °C, and the predominant wear mechanisms were micro-cutting and plastic deforming. At 600 °C, the oxidation rates of SiC and $NiSi_2$ were not fast enough to form adequate oxide films, which can work as lubricant.[147] This means that the tribo-pairs worked under dry sliding, which resulted in severe adhesion between the SiC asperities on the contact surfaces.

As the temperature increased to 800 °C, Ni reacted with Si to form $NiSi_2$, which filled the voids among SiC particles to obstruct the high diffusion path of oxygen. Thus, micro-cutting dominated the friction process in the initial stages, and significant debris was generated on the worn surface. Subsequently, the debris reattached to the wear track and could be oxidized to form SiO_2 and NiO. The worn surface of the SiC–Ni coating got smooth owing to the formation of a continuous glaze layer. These oxides, especially NiO, which had low hardness and could act as lubricants, sticking to the asperities on coating easily, decreased the friction and promoted the formation of a tribofilm.[148] Moreover, the $NiSi_2$ was located at the boundary of the SiC particles, which was softer than SiC. $NiSi_2$ was beneficial to release the stress and prevented brittle facture of the coating.

The dominant prerequisites for acquiring distinguished mechanical and tribological behaviors are homogeneous dispersion of nanofillers and ideal filler/matrix bonding.[128,146] Similar to 0D-fillers, the natural agglomeration tendency of 1D-nanofillers remains an obstacle in their tribological application as efficient lubricants.[129,149] Thus, researchers have investigated various strategies to effectively disperse nanofillers in CBCs.[150–152]

To reduce the agglomeration of 1D-nanofillers, chemical vapor deposition (CVD) was applied to prepare a homogeneous dispersion of CNTs in an Al_2O_3 coating.[153] The addition of 1.5 wt% CNTs presented approximately 24% increase in the fracture toughness of the composite coating. Friction and wear tests were carried out on the Al_2O_3 coating reinforced with CNTs. They indicated that after the 60 min at a rotation speed of 250 rpm and normal load of 50 N, an improvement of ~27% in the wear resistance was achieved by the Al_2O_3-CNT coating compared to that of the Al_2O_3 coatings.

Besides CVD, the sol–gel route has also been proven to be a suitable technique to fabricate SiO_2 coatings with well-dispersed CNTs on the surface of WE54 magnesium alloys.[154] Pin-on-disc wear experiments were performed on the SiO_2-CNT coatings under the chosen speed of 0.1 m s^{-1} and sliding distance of 60 m. The results demonstrated that the friction coefficients of the coatings were slightly changed with the addition of CNTs, but the wear volume of the coated magnesium alloy was reduced by 80% compared to bare WE54. The detailed friction coefficient and wear rate are presented in Table 2, corresponding to ~0.40 and 1×10^{-3} mm^3 N m^{-1}, respectively. The crack bridging and pull-out of the CNTs were responsible for the toughening of the SiO_2-CNT ceramic coatings, consequently providing an effective way to improve the wear resistance of coatings.

Numerous studies have also proven that the interfacial interaction of nanofillers with the substrates has a great influence on the tribological properties of CBCs.[155,156] Jambagi *et al.*[157] investigated the crucial roles of CNTs in the phase transformation and tribological behaviors of ceramic coatings. The homogeneous dispersion of CNTs was important for the heat transfer during the plasma spraying process, resulting in a high proportion of stable phase for the coatings. Meanwhile, the stable phase layers were tightly engulfed in the entire CNT surface, playing a significant role in protecting them from thermal degradation. This interaction endowed the CBCs with reliable mechanical properties, which are crucial to realizing excellent anti-wear behavior. The results of the scratch tests proved that the scratch resistance of the CNT-reinforced coatings increased by ~36–176% as compared to that of the unreinforced coatings. This enhancement was attributed to the well-proportioned dispersion of the CNTs in the coatings, strong wettability of the CNT/ceramic interfaces, and the toughening mechanism of CNTs.

3.3. Polymer-based coatings

The excellent tribological potential of well-dispersed 1D-nanofillers in polymer coatings has been increasingly recognized.[100,158,159] Similar to MBCs and CBCs, numerous studies have been carried out to develop unique tribological properties in polymer coatings reinforced by nanofillers.[160–162]

Systematic investigations on the tribological performances of MWCNT/EP coatings were conducted,[163] where poly(2-butylaniline) (PBA) was used as a dispersant to obtain well-distributed MWCNTs in the tetrahydrofuran (THF) solution (Fig. 7a). The SEM morphologies of MWCNTs and MWCNTs/PBA in THF solution are presented in Fig. 7b and c, respectively. It can be observed in Fig. 7b that the untreated MWCNTs in THF tended to aggregate and intertwine with each other, while the MWCNTs mixed with PBA dispersant exhibited a relatively sparse distribution, as can be observed in Fig. 7c. Subsequently, according to the TEM image in Fig. 7d, many PBA particles were observed to be adsorbed on the surface of the MWCNTs due to their unique structures, as noted in Fig. 7e, which was conducive to the formation of π–π interaction between them and PBA. This interaction improved the dispersion and compatibility of the MWCNTs with the EP matrix, resulting in observable optimizations in the tribological properties of the MWCNT/EP coatings. Fig. 7f demonstrates that the composite coatings exhibited better wear-resisting abilities than that of the blank EP coatings, where 5%-MWCNTs

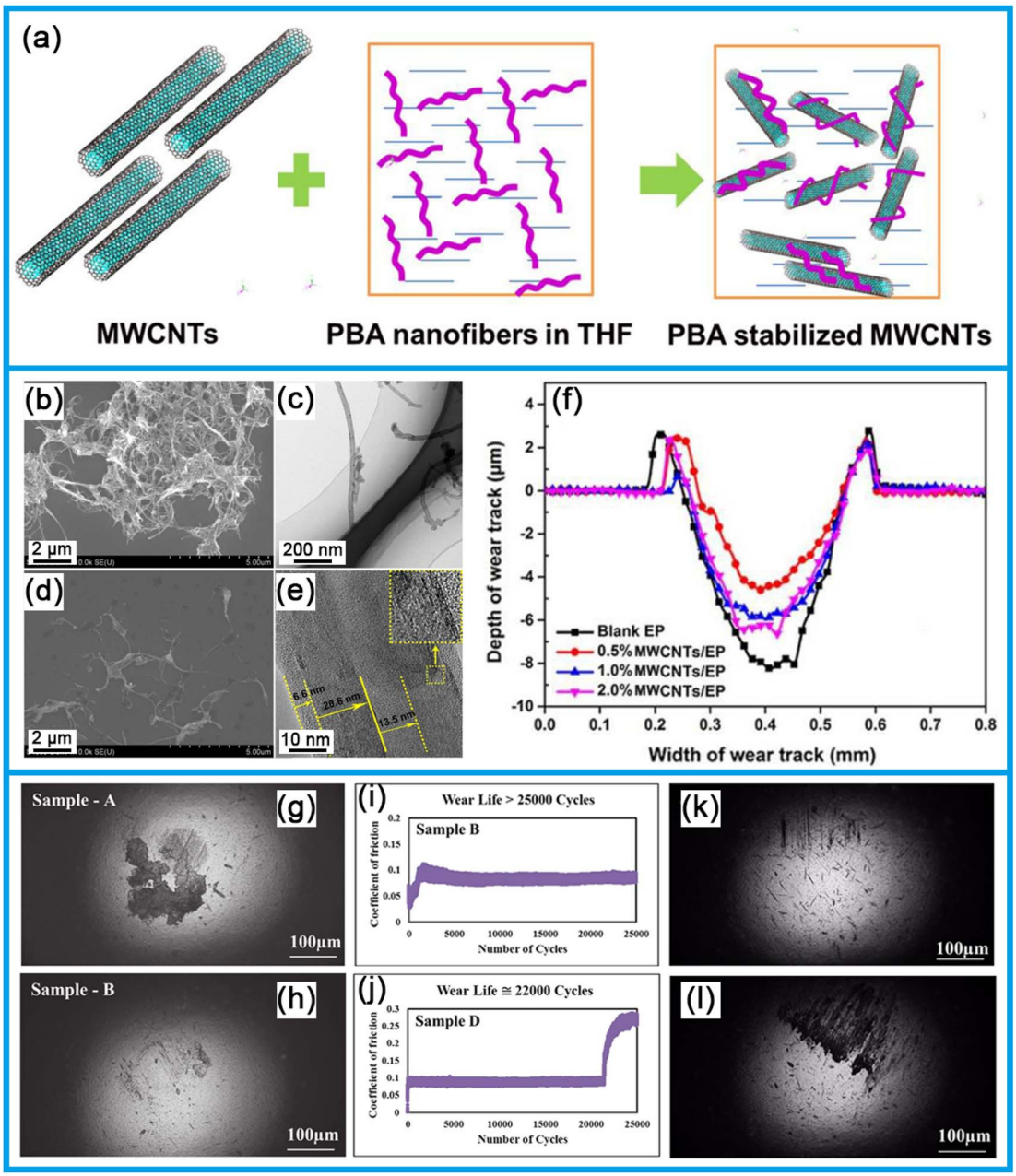

Fig. 7 (a) Dispersion of MWCNTs in THF *via* PBA dispersant. SEM morphologies of MWCNTs (b) and MWCNTs/PBA (c). TEM image of MWCNTs/PBA (d) and HRTEM morphology of CNTs (e). (f) Effect of MWCNT content on wear depth in epoxy. Reproduced from ref. 163 with permission from Elsevier, Copyright 2018. Typical morphologies of the balls sliding against samples A (g) and B (h) and (i and j) typical graph of friction coefficients, respectively. Wear-scar images of the balls sliding against sample B (k) and D (l). Reproduced from ref. 168 with permission from Elsevier, Copyright 2016.

rendered the EP coating with the smallest wear depth. The MWCNTs played an important role in inducing this improvement in the EP matrix, facilitating the formation of a transfer film on the worn surface, and consequently reducing the wear of the coatings.

Unlike CBCs, it remains a challenge to fabricate polymer coatings with excellent carrying capacity because of the inadequate strength of polymers. Based on recent research on 1D-PBCs, nanofillers present an effective strategy for the improving mechanical properties of coatings, thus playing an crucial role in exploiting the full tribological potential of polymer coatings.[164–166]

The successful preparation of a polyacrylamide-carbon nanotube (PAM-CNT) copolymer coating was realized[167] using ultraviolet radiation-initiated polymerization. The friction coefficient significantly decreased with an increase in CNT additive. Obviously, the PAM-CNT film exhibited better load-bearing ability and wear-resisting property than that of neat PAM. The additional load-bearing capacity from the CNTs accounted for these advantages. Thereafter, the tribological characteristics of a UHMWPE film reinforced by single-walled carbon nanotubes (SWCNTs) were investigated.[158] An increase in the resistance to scratch and penetration was proven with the incorporation of 2 wt% SWCNTs, which was attributed to the enhancement in the hardness and elastic modulus of the composite film. The service life of the UHMWPE/SWCNT film significantly increased (>10 million cycles) under a load of 4 N and speed of 2500 rpm. In comparison, the pristine UHMWPE film failed after 150 000 cycles at a rotational speed of less than 2500 rpm.

Further, the friction and wear behaviors of CNT-reinforced decahydronaphthalene/ultra-high molecular weight polyethylene (decalin/UHMWPE) coatings were reported.[168] Based on the different contents (wt%) of UHMWPE and CNTs, the as-prepared coatings were named as sample A (3-UHMWPE and 0.1 CNTs), sample B (3-UHMWPE and 0.2-CNTs), sample C (5-UHMWPE and 0.1 CNTs) and sample D (5-UHMWPE and 0.2-CNTs). After the ball-on-disc wear tests, microscopic images of the counter-face balls sliding against samples A and B were recorded, as displayed in Fig. 7g and h, respectively. Among the concentrations of CNTs, 0.2 wt% CNTs provided effective bridging and anchoring to prevent the pull-out of the polymer. Therefore, less amount of transfer film was observed on the counter-face ball compared to the 0.1 wt% CNT-reinforced composite coatings. According to the results in Table 2 for the 0.2 wt% CNTs, sample B possessed a longer wear life (survived for 25 000 cycles) compared to that of sample D, as also indicated in Fig. 7i and j, respectively. This behavior was mainly attributed to the CNTs and offered an effective way for inhibiting polymer pull-out at a concentration of 5 wt% of UHMWPE. Hence, more polymer transfer occurred in sample D compared to sample B, as demonstrated in Fig. 7k and l, respectively.

The formation of a stable transfer film is one of the wear mechanisms of PBCs. This film is responsible for suppressing frictional pair collisions, which is critical in realizing tribological behavior. In the case of 1D-polymeric coatings, a homogeneous distribution of 1D-nanofillers primarily contributes to an improvement in the adhesion between transfer films and their corresponding counterparts.[169,170] Song *et al.*[170] fabricated a polyurethane (PU) coating reinforced by hexamethylene diisocyanate-modified TiO_2 nanotubes (TiNTs-HDI). Friction tests were carried out to investigate the crucial roles of TiNTs-HDI in the tribological performances of the PU coatings. Compared with the PU coating filled with TiO_2 nanotubes, TiNTs-HDI/PU exhibited a lower friction coefficient and longer service life. The proposed wear mechanism was the uniform transfer of the film formed on the coating and good separation at the friction interface. Specially, the presence of TiNTs-HDI strengthened the bonding of the transfer film with regard to the PU coating filled with TiO_2 nanotubes, thus endowing the TiNT-HDI/PU coating with a reduction in friction and wear.

It is remarkable that the interfacial bonding strength of the nanofillers with their matrices also has an important influence on the friction reduction and wear-resisting functions of PBCs. The tribological behaviors of UHMWPE coatings were well-reinforced using plasma-treated SWCNTs.[158] According to the experimental results, plasma treatment resulted in the generation of oxygen-containing functionalized groups on the surface of SWCNTs, thus improving the adhesion abilities of the SWCNTs with the polymer matrix. The increased adhesion strength accounted for the inhibited peeling-off or delamination of the coatings, endowing the SWCNTs/UHMWPE with better friction and wear behaviors.

4. Two-dimensional nanofillers

The outstanding friction and wear behaviors of 2D-nanofillers have been increasingly recognized. Their unique layered structure, high thermal conductivity, and extraordinary physical and chemical abilities make them promising candidates for reinforcing tribological coatings.[171,172] With regard to 2D-nanofiller-reinforced tribo-systems, the excellent self-lubrication performance of 2D-materials is believed to be closely related to the weak interlayer interaction and ease of sliding between neighboring atomic layers.[40,173–175] In this section, the friction-reduction and wear-resistance properties of composite coatings reinforced with 2D-nanofillers are discussed, and some of the results are presented in Table 3.

4.1. Metal-based coatings

Recently, numerous reports indicated that 2D-nanofillers have excellent potential to improve the friction and wear properties of MBCs. The mechanical strength of 2D-nanofillers is remarkable due to their strong in-plane chemical bonding. For example, ultrathin graphene is one of the strongest materials, with an intrinsic strength of 130 GPa[176] and toughness of 4.0 ± 0.6 MPa $\sqrt{m}$.[177] The super-high strength and stability of graphene make it an ideal candidate for the preparation of MBCs with desirable anti-wear performances. The mean frictional coefficients and wear rates of graphene-reinforced Ni coatings were reduced by more than 60% and an order of magnitude, respectively, compared with the pure Ni coatings.[178] The excellent mechanical properties and unique lamellar

Table 3 Improvements in tribological properties of 2D-nanofiller-reinforced coatings[a]

			Tribological results	
Matrix	Reinforcement	Tested conditions	COF	Wear
Nickel coatings	GO[190]	Bearing steel ball (ball-on-disk, 40 rpm, 1 N, RT)	0.30	NM
Cobalt coatings	Graphene[221]	AISI52100 steel pin (pin-on-disc, 0.1 m s^{-1}; 5, 10, and 15 N; RT)	0.46–0.60	Wear volume: 0.02–0.11 mm^3
MoS_2 coatings	GO[222]	AISI52100 steel bearing ball (ball-on-disc, 6.28 mm s^{-1}, 1 N, 25 °C, N_2 atmosphere)	0.086	Wear volume: 0.10×10^4 μm^3
Ceramic coatings	Graphene[198]	Steel ball (ball-on-disc, 5 cm s^{-1}, 5 N, RT)	0.42	Wear rate: 3.62×10^{-6} mm^3 N m^{-1}
Ceramic coatings	Graphene[223]	Si_3N_4 ball (ball-on-plate, 0.2 m s; 20 N, 200 °C)	~0.375	Wear rate: 1.0×10^{-3} mm^3 N m^{-1}
Epoxy coatings	$NbSe_2$ nanosheets[213]	GCr15 steel ball (ball-on-disk, 0.033 m s^{-1}; 10, 15, 20, 25 and 30 N; RT)	~0.062	Wear rate: 1.48×10^{-7} mm^3 N m^{-1}
Phenolic	g-C_3N_4 nanosheets[214]	Ring (ring-on-block, 2.5 m s^{-1}, 320 N)	~0.125	Wear rate: ~2.20×10^{-8} mm^3 N m^{-1}
PI coatings	Graphene[219]	100Cr6 steel ball (ball-on-disk, 5 Hz, 1000 μm; 10 N; 100 °C)	0.66	Wear volume: ~0.60×10^{-3} mm^3

[a] RT = room temperature and NM = not mentioned.

structure endow graphene with outstanding self-lubricating effects, and thus it tends to form lubrication films. The high load-bearing capacity of the films, which were extruded to the contact surface, provided stable lubrication for the MBC. Meanwhile, although the introduction of graphene deteriorated the surface roughness of silver coatings,[179] its excellent self-lubrication played a positive role in improving their wear resistance. All the nano-coatings exhibited lower friction coefficient and higher anti-wear behaviors compared with that of the pure Ag deposited layers because of the improved load-bearing and self-lubricating effects.

Although 2D-nanofiller-reinforced composites typically possess excellent tribological properties, the insufficient interfacial bonding strength and poor dispersion of nanofillers remain an obstacle in the extensive coating applications of 2D-nanomaterials.[67,180] In the case of Ni/graphene@pDA composite coatings,[181] poly-dopamine (pDA) not only distinctly improved the dispersion of graphene in the Ni-based coatings, but also played a key role in enhancing the adhesion between graphene and its substrate. The well-distributed graphene endowed the coating with optimized load-bearing capacity and excellent lubrication systems. According to the friction test results, the friction coefficients and wear loss of composite coatings were much lower and more stable than the pure Ni coatings.

The method of ultrasonication combined with wet milling was proposed to up-regulate the adhesion rate of graphene on the surface of Ni60 powder.[182] Fig. 8a presents the specific route for the preparation of the Ni60-coating. The suggested route endowed the graphene-reinforced Ni60 coatings with observable improvements in mechanical properties. Fig. 8b and c show the back-scattered scanning (BSC) and secondary electron image (SEI) morphologies of the Ni60/graphene coatings, respectively. These figures demonstrate that the addition of graphene facilitated the refinement and homogenization of the coating structure, thereby enhancing the hardness of the coatings (Fig. 8d). Meanwhile, the TEM image is shown in Fig. 8e and selected area electron diffraction (SAED) pattern corresponding to area D in Fig. 8f. It was deduced from these figures that original graphene in the coating was partially converted to fullerene-like structures. The excellent synergistic effect of graphene and these structures effectively improved the tribological properties of the coatings. After 30 min tests under a load of 5 N and frequency of 5 Hz, Fig. 8g reveals that the friction coefficient of the composite coating was reduced by ~41.8% compared with that of the pristine Ni60 coating.

The existence of tribolayers on the wear interface can serve to well-improve the friction and wear performances. Generally, tribolayers are monolayer or multilayer structures. Monolayer tribolayers are academically defined as a tribofilm or lubricating film, which plays a key role in providing a low shear force and improving the wear-resistance of coatings.[68,69,183–185] Based on the previous work by our group,[186] a large number of advanced interfacial microchannels were successfully prepared on a Ti-based sample surface to form a beneficial tribolayer during the friction process, improving the tribology behavior. The beneficial addition of MgAl-graphene-Al_2O_3 resulted in outstanding friction reduction and improvement in wear resistance, which was attributed to the formation of a tribolayer consisting of Ti-alloy, MgAl–Al_2O_3 and graphene layers. The interlamination separation of graphene and Al_2O_3 rolling caused a significant improvement in the deformation of MgAl, which led to the self-regulation and self-repairing actions of the

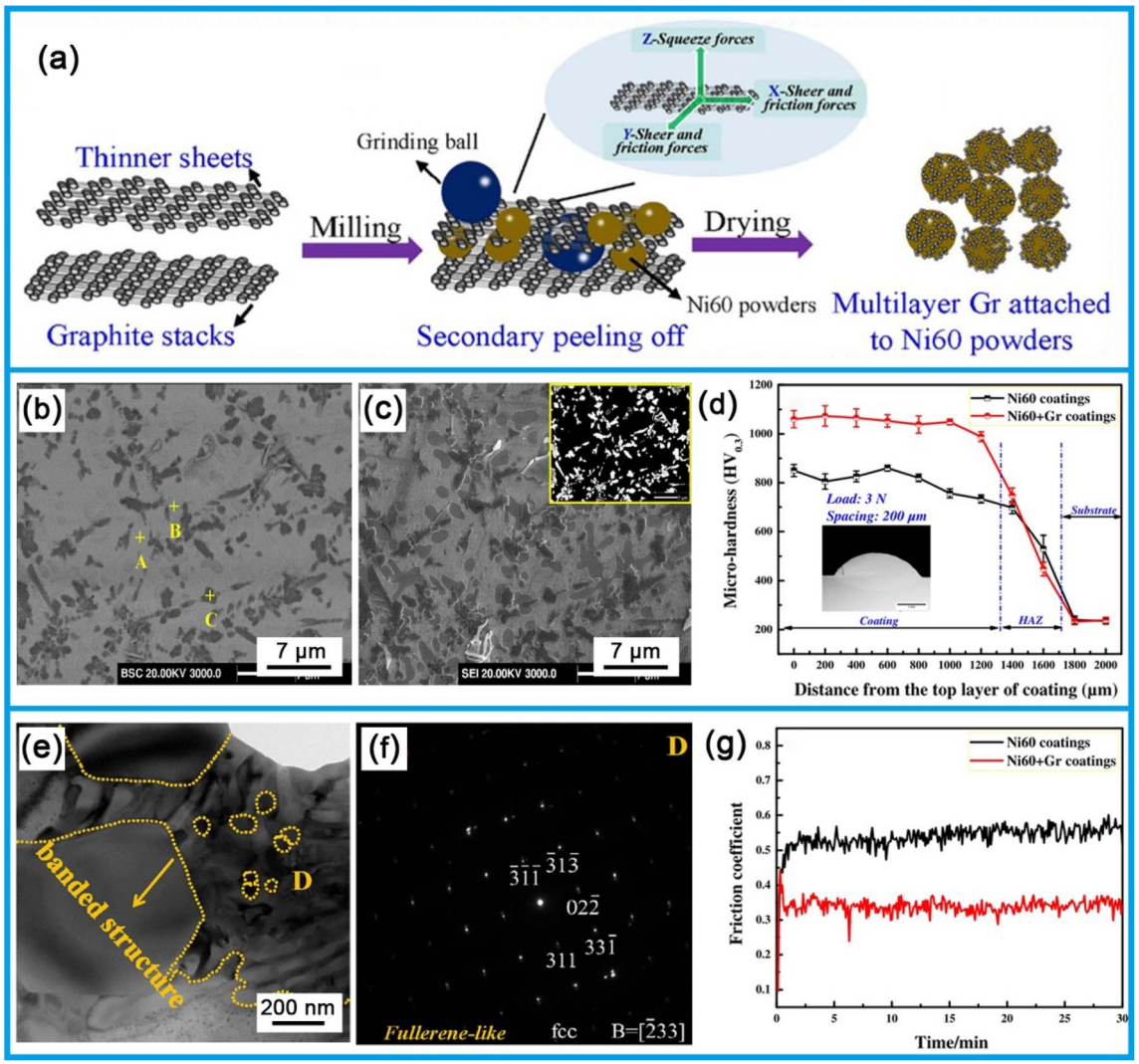

Fig. 8 (a) Schematic of *in situ*-synthesized Gr attached to Ni60 powder. BSC (b) and SEI (c) morphologies of Ni60 + Gr coatings. (d) Micro-hardness curve of laser cladding coatings. (e) High-magnification TEM image, (f) SAED pattern of area D in (e) and (g) typical curve graph of friction coefficients. Reproduced from ref. 182 with permission from Elsevier, Copyright 2019.

friction interface, finally promoting the excellent tribological behaviors. It should be noted that recently, Xu *et al.*[68] reported that an *in situ* tribolayer was form on a ball mainly composed of highly ordered graphene-like nanosheets, which was produced by sliding-induced degradation of onion-like carbon nanospheres. Combined with the retained nanospherical carbon structure in the topmost subsurface of the tribolayer, the well-constructed nanosphere-/amorphization-coupled interface was capable of offering excellent lubricity under high contact stress.

Unlike graphene, graphene oxide (GO) is a distorted structure of sp^2-carbon nanosheets. Due to the presence of oxygen functionalities, numerous sp^3-carbons are infused in its honeycomb lattice structures.[187] The nanostructure of highly hydrophilic oxygen-rich functional groups (hydroxide, carboxyl, carbonyl, *etc.*) on the surface of GO endows it with superior adhesion to the metal matrix, making it an attractive candidate as a solid lubricant. In both Ni-based coatings[188] and Co-based coatings,[189] GO showed excellent friction-reducing and anti-wear effects. According to the proposed lubrication mechanism, the presence of GO refined the coating structures, improved their mechanical properties regarding hardness and toughness, and promoted the formation of a tribofilm at the contact interface, thus avoiding the direct contact of the tribo-pairs.

To develop new types of GO-coatings, the ultrasonic-assisted electrodeposition process was applied to fabricate Ni/GO composite coatings.[190] An improved morphology, desirable microstructures and excellent tribological behaviors were observed in the composite coatings when the concentration of GO increased from 0.1 g L^{-1} to 0.3 g L^{-1}. The grain refinement and improved surface of the Ni/GO coatings were mainly responsible for these enhancements. The well-dispersed GO increased the nucleation rates of the Ni/GO coatings during electrodeposition, resulting in a denser crystal microstructure

than that of the pristine Ni-coating. Moreover, the weak interlaminar bonding of GO enabled the composite coating to form a specific lubricating film during sliding wear. Hence, the hardness and tribological performances of the Ni/GO coatings were appreciably improved. Table 3 suggests that the friction coefficients of the composites were reduced by ~33.3% compared to that of the empty Ni-coatings. Exactly, this excellent tribological performance was obtained under the condition of good lubrication environment. However, the actual working environment of the parts is harsh. In terms of Ni-coatings, composite coatings with boron nitride (BN) exhibited good wear resistance and durability even without lubrication. An in-depth study of these coatings, which do not have a strong dependence on the lubrication environment, is of great practical significance for the development of tribology. The friction behavior and compatibility between a coated piston skirt and an aluminum or cast iron bore mating surface were evaluated[191] using aluminum piston skirts with nickel/ceramic composite coatings. Among the nickel/ceramic composite-coated piston skirts, Ni-P-BN showed consistent low wear on either cast iron or the aluminum bores. The tin-plated piston skirt generated low wear depths on cast iron or 390 Al bore surfaces.

2D-MXenes (2D transition metal carbides, nitrides, and carbonitrides) were discovered in 2011, and since then have gained popularity in the field of tribology.[40] MXenes, even in trace amounts, significantly improved the friction-reducing and anti-wear properties of MBCs. Mai *et al.*[192] described the friction and wear properties of Ti_3C_2/Cu nano-coatings. The incorporation of Ti_3C_2 nanosheets significantly influenced the surface morphologies of the coatings, which were used to determine the tribological properties of the as-prepared coatings. The friction and wear tests revealed that the composite coating had a 46% friction reduction and a 19-times decrease in wear rate than the Ti_3C_2-free counterparts. This enhancement in friction and wear performance was attributed primarily to the compacted Ti_3C_2-rich tribolayer formed on the worn surface, which reduced the direct collisions between the frictional pairs and provided an easily sheared interface.

MXene-reinforced Co-coatings dramatically enhanced the mechanical properties of 35CrMo substrates (*e.g.*, hardness and toughness), thus improving the anti-wear ability of MBCs containing 10 wt% Ti_3SiC_2 MXene by approximately 6.20 times.[193] This was attributed to the excellent dispersion and compatibility of Ti_3SiC_2 in the Co-based coating, enabling an increase in hardness and toughness and reduction in plastic deformation and surface micro-cracks. An investigation ultimately confirmed the attractive potential of MXenes in tribological coatings, promoting the application of MBCs in the metallurgical industry.

4.2. Ceramic-based coatings

As a common solid lubricant, a large number of tribological reports on graphene have demonstrated that graphene is also an effective reinforcement for CBCs.[194–196] Bai *et al.*[197] reported the tribological behaviors of graphene-reinforced TiO_2 ceramic films and indicated that the single-layer TiO_2 ceramic films with 0.025 wt% graphene demonstrated the best tribological property at 100 °C. When the substrate was tightly bonded to the ceramic film, the elasticity of the TiO_2 ceramic film increased the contact area between the friction ball and the ceramic film, reducing the friction. Simultaneously, due to the strong C–C bond between graphene and TiO_2, under the synergistic effect of load and temperature, graphene easily fell off from the ceramic film during the friction process. Some of the fallen graphene nanosheets were separated to the surface of the ceramic membrane and filled the place where the ceramic film was worn, making the surface of ceramic film smoother, further reducing the friction coefficients. The mechanical property of the TiO_2 ceramic was reinforced with the introduction of GNPs, which could make the TiO_2 ceramic more tolerant to surface damage during wear. These improvements were primarily associated with the graphene-induced grain refinements and unique lubrication. Liu *et al.*[198] further explored the effect of graphene on the friction and wear behaviors of ceramic coatings. After the wear test at a linear speed of 5 cm s^{-1} under a normal load of 5 N, an extremely low friction coefficient of almost 0.42 and wear rate of approximately 3.62×10^{-6} mm^3 N m^{-1} were observed, as shown in Table 3. It was believed that the noteworthy increase in the microhardness from 400 HV for the uncoated matrix to 1250 HV for the composite coatings played dominant roles in acquiring excellent tribological property.[199]

It is remarkable that the introduction of 2D-nanofillers is not only of great significance for enhancing the hardness of coatings, but also proven to be a feasible method to improve their fracture toughness. Excellent toughness is crucial in obtaining reliable wear-resistance in coatings.[200–202] Ranjan *et al.*[203] successfully fabricated graphene nanoplatelets (GNPs) to reinforce a TiN-coating on Ti alloys. 2 wt%-GNPs endowed the coatings with an improvement of 19% in hardness and 300% in fracture toughness. The remarkable enhancement in the mechanical property resulted in the superior tribological behavior of GNPs/TiN to that of the TiN coating. Furthermore, explorations on the tribological behaviors of 1 wt%-GNP-reinforced alumina coatings were performed.[204] The sliding wear tests revealed two-orders of magnitude reduction in the specific wear rate (from ~10^5 to ~10^7 mm^3 N m^{-1}) of the composite coatings compared to the unreinforced alumina coating (Fig. 9a). Fig. 9b and c provide the SEM images of alumina and alumina + GNP coatings and optical morphology of the coating after wear. As shown, severe wear was detected in the pure-Al coating with brittle fracture characteristics (Fig. $9b_1$). In contrast, the wear track on the Al + GNP coating exhibited slight plastic deformation, as observed in Fig. $9b_2$. Meanwhile, the material transfer of the alumina coating to the wear track of the Al coating is shown in Fig. $9c_1$, which was considered to be due to inadequate mechanical property of the pure Al-coating. The proposed explanation for the outstanding wear of the Al + GNP coating ensured that GNP showed an effective pathway to improve the fracture toughness and load-bearing capacity of the coatings.

Molecular dynamics (MD) simulations revealed the strong relationship between the fracture toughness of the composite coatings and the dimensions, volume fraction, and layer count

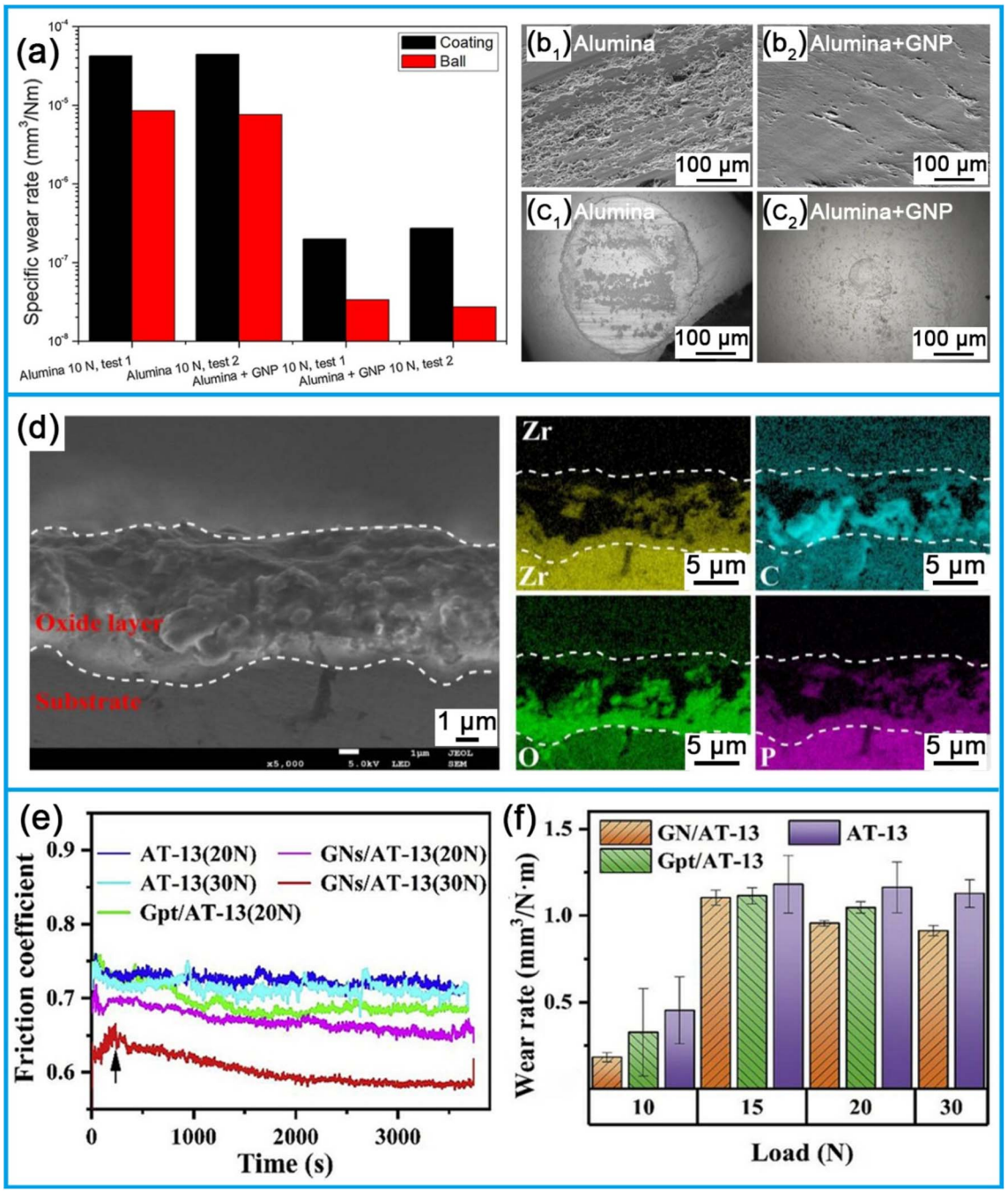

Fig. 9 (a) Specific wear rates of alumina and alumina + GNP composite coatings. (b_1) and (b_2) SEM images of wear tracks in the coatings. (c_1) and (c_2) optical images of wear spots of the contact area. Reproduced from ref. 204 with permission from Elsevier, Copyright 2018. (d) Main element distributions in the cross-section of ZrO_2/GO coating. Reproduced from ref. 207 with permission from Elsevier, Copyright 2020. (e) COF curves of the coatings with an increase in wear time. (f) Histogram of wear rates of the coatings. Reproduced from ref. 211 with permission from Elsevier, Copyright 2020.

of 2D-fillers.[205] In the case of fewer layers, the graphene sheets exhibited attractive bridging toughening effects for ceramic coatings. Meanwhile, the fracture toughness of the SiC/graphene lamellar composite gradually increased as the graphene size and volume fraction increased. However, high contents of graphene resulted in lamellar composites with poor friction and wear properties.[206] Appropriate concentrations and dimensions of 2D-nanofillers are considered to account for the increased toughness and interest in their application in coatings.

The crucial effects of different GO-concentrations on the tribological behaviors of ZrO_2 coatings were systematically studied.[207] The wear damage gradually decreased with an increase in GO concentration, indicating the ideal lubrication

by GO. Among the various GO contents, the wear volume and friction coefficient of the composites containing 0.05 g L^{-1} GO were reduced by ~97.3% and ~43.0%, respectively, compared to the pure ZrO_2 coating. However, as the GO concentration increased up to 0.1 g L^{-1}, irregular holes were confirmed in the black cross-section regions of the ZrO_2/GO coatings, which can be observed from the energy dispersive spectrometer (EDS) map in Fig. 9d. Further, it was demonstrated that 0.1 g L^{-1} GO resulted in more surface cracks and pores in the coating compared to the above-mentioned concentrations, endowing the coating with deteriorating friction and wear properties.

In the case of 2D-nanofiller/ceramic systems, investigations revealed that the formation of a nanofiller-containing tribofilm was critical in achieving an observable reduction in the friction and wear of the coatings.[140,208] According to the report by Bian *et al.*,[209] the wear volume and friction coefficient of chemically bonded phosphate ceramic coatings were significantly reduced due to the introduction of graphene nanoplatelets (GNPs). According to the proposed wear mechanism, the graphene was extruded and adhered to the surface of the coating to form a lubrication film. The tribological properties of the composite coating were investigated on a ball-on-disc configuration. It was found that the worn surface of the coating with GNPs was smoother than that without GNPs. Besides, a smooth contact surface possesses a larger surface to carry a normal load, leading to smaller internal stress. Also, the internal stress of the contact surface was reduced, which helped to reduce the friction coefficients because the interface shear strength is proportional to the contact pressure. Another reason for the low wear volume is that the GNPs were extruded from the substrate and adhered to the worn surface, thus forming an adhered lubricating tribofilm. Also, the friction coefficient was reduced because of the lubricating effect of the adhered lubricating tribofilm. Due to the weak GNPs at the interlaminar interface, the graphene sheets separated from each other. The high strength of graphene made it difficult for cracks to penetrate. Some cracks would be blocked by the GNPs and some would change the pathway, which resulted in the absorption of stress and fracture energy. Therefore, with the addition of GNPs, the mechanical properties of the material were significantly improved.

Analogously, Li *et al.*[210] investigated the tribological properties of coatings composed of zirconia/graphene nanosheets (ZrO_2/GNs). With the addition of GNs, the composite coating demonstrated a significant increase in wear resistance. Compared to the pure ZrO_2 coatings, the wear rate of the ZrO_2/GN coatings was reduced to 1.17×10^{-6} mm^3 N m^{-1}, a nearly 50% reduction. This significant improvement in wear resistance was primarily due to the formation of a GN-rich transfer layer on the wear track of ZrO_2/GN coatings. This layer protected the ZrO_2/GN coating from severe wear caused by brittle microfracture, thereby significantly improving the tribological properties of the composites.

Further evaluation of the friction and wear properties of a graphene nanosheets/Al_2O_3 + 13 wt% TiO_2 (GNs/AT-13) coating was conducted by Feng *et al.*[211] The tests were conducted on a ball-on-disk tester and the specific friction coefficient and wear rate were recorded, as shown in Fig. 9e and f. As shown in Fig. 9e, the mean friction coefficient of the GN/AT-13 coating was approximately 0.61 under a load of 30 N, resulting in an almost 13% reduction compared to the Al_2O_3 + 13 wt% TiO_2 (AT-13) coating. Besides, Fig. 9f also reveals that the GN/AT-13 coatings exhibited excellent anti-wear behaviors, in particular at 30 N, the wear rate was 19% lower than that of the AT-13 coating. A graphene-containing transfer layer was well-observed on the wear scar. This tribofilm provided an effective method to improve the lubrication abilities of the coatings.

4.3. Polymer-based coatings

2D-nanofillers have attracted particular attention because of their unique mechanical behavior, excellent thermal conductivity, and low surface energy. In addition to the exploration of MBCs and CBCs, extensive studies have demonstrated the extraordinary potential of nanofillers in polymer coatings for tribological applications.[212]

Similar to ceramic coatings, one of the key parameters controlling the friction and wear of polymer coatings is the formation of a transfer film.[213,214] This film greatly dominates the anti-wear enhancement and friction reduction of coatings under fluid lubrication failure. Chen *et al.*[213] presented an effective method to incorporate niobium diselenide ($NbSe_2$) nanosheets in the epoxy (EP) coatings to improve their tribological properties. It was observed that the frictional coefficients, ranging from ~0.337 to ~0.062 of the composite coatings, were sharply reduced by about 80% with an increase in the content of nano-$NbSe_2$ from 0 to 20 wt%, as shown in Fig. 10a. Meanwhile, 10 wt% $NbSe_2$ endowed the coatings with an observable reduction of 70% in wear rate compared to the pristine EP coating, and the details are listed in Table 3. These remarkable enhancements in friction and wear were primarily attributed to the transfer film containing $NbSe_2$, which was formed on the surface of the composite ball. Fig. 10b and c show the microcosmic morphologies of the worn surface of pure-EP and EP-10 (almost 10 wt% $NbSe_2$), respectively. As shown in these figures, the formation of a transfer film provided feasible way to prevent the direct contact of the friction pairs, resulting in the wear morphology becoming smoother and flatter, as shown in Fig. 10c, compared with that of pure EP-10 (see Fig. 10a and b), respectively. EP-10 effectively avoided the fatigue peeling of the friction surface of the substrate and promoted the formation of a good lubricating environment (shown in Fig. 10c).

Subsequently, the influence of the concentration of graphitic carbon nitride (g-C_3N_4) nanosheets on the tribological properties of phenolic coatings was evaluated.[214] The microstructure and morphology of the as-prepared g-C_3N_4 nanosheets and bulk g-C_3N_4 samples were characterized using TEM. As shown in Fig. 10d and e, the g-C_3N_4 nanosheets obviously displayed a crinkly feature. The TEM image of the bulk g-C_3N_4, as shown in Fig. 10e, showed mainly dense and stacked sheets. Understanding the underlying structure of the g-C_3N_4 nanosheets was critical to exploring the concentration effect. Among the various g-C_3N_4 contents from 0 to 2 wt%, 1 wt% g-C_3N_4 nanosheets

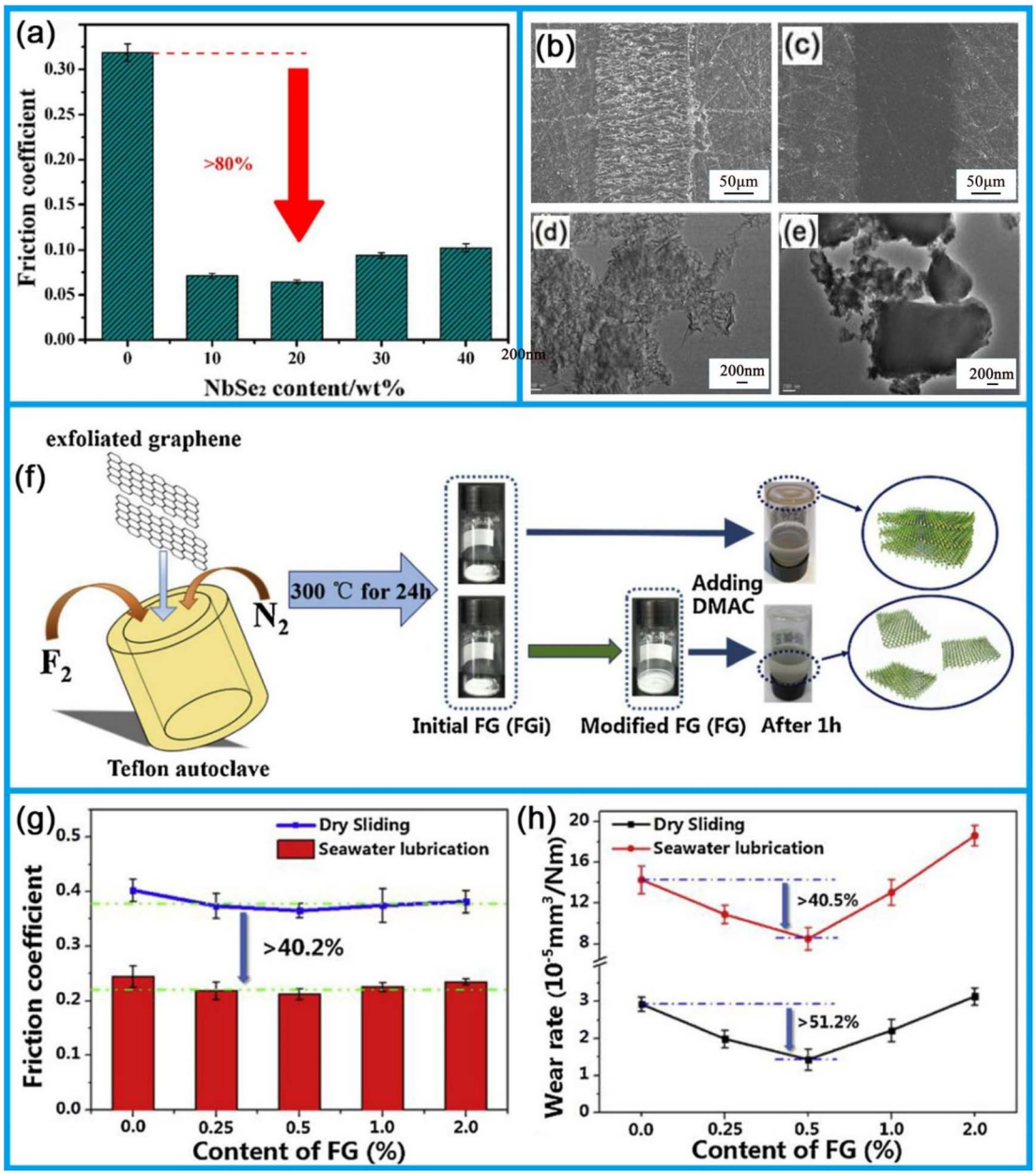

Fig. 10 (a) Effect of the content of $NbSe_2$ nanosheets in epoxy on the friction coefficient. SEM images of worn surfaces of (b) pure-EP and (c) EP-10. Reproduced from ref. 213 with permission from Elsevier, Copyright 2016. TEM images of bulk g-C_3N_4 (d) and g-C_3N_4 nanosheets (e). Reproduced from ref. 214 with permission from Elsevier, Copyright 2019. (f) Typical preparation of FG. Tribological properties of PI/FG nanofilms: (g) friction coefficient and (h) wear rate. Reproduced from ref. 216 with permission from Elsevier, Copyright 2019.

endowed the coating with the optimal friction and wear behaviors. The phenolic coating was filled with 1 wt% g-C_3N_4 nanosheets, and at an applied load of 320 N and sliding speed of 2.5 m s^{-1}, the results presented the lowest friction coefficient of ~0.125 and smallest wear rate of ~2.20 × 10^{-8} mm^3 N m^{-1}, as shown in Table 3, compared to the pure phenolic coating. Two dominant factors in improvement of friction-reducing and anti-wear actions were the formation of a uniform tribofilm and strong interface adhesion of the tribofilms compared with their frictional counterparts.

Furthermore, it was reported that the friction and wear behaviors of PBCs strongly depend on the working conditions. The tribological abilities of fluorinated graphene-reinforced polyimide (PI/FG) composite coatings under dry sliding wear and water-lubrication systems were evaluated.[215] The experimental results revealed that compared to the tribological behaviors under dry sliding, reduced friction coefficients and improved wear rate in the under-water-lubricated system was observed. The water-absorbing properties of the PI/FG coatings played a dominant role in deteriorating the anti-wear function under water lubrication.

Analogous explorations on the tribological performances of FG serving as a PI coating additive were also conducted by Zhou *et al.*[216] Fig. 10f schematically presents the typical process for the

preparation of FG. For seawater lubrication, the presence of a water film reduced the direct contact between the frictional pairs, resulting in a 40.2% decrease in friction coefficient compared with that of dry sliding wear (see Fig. 10g). However, Fig. 10h indicates that the measured wear rates of the as-prepared samples under dry wear were superior to seawater lubrication. The wear mechanism was that the FG layer covered the surfaces of the composite balls and formed a dense transfer film under dry wear, and thus helpful in attaining the desired tribological performances. Similarly, several studies have reported that 2D MXenes promoted the formation of transfer tribolayers, which were also crucial for improving the friction and wear properties.[217,218] Yin *et al.*[217] demonstrated the splendid friction-reducing and wear resistant behaviors in the case of MXene/nanodiamond coating sliding against a PTFE ball. This was due to the formation of multilayer tribolayer, *i.e.*, PTFE layer-MXene/nanodiamond multilayer-PTFE layer. The MXene-induced shear slip, combined with the rolling effect of the nanodiamond significantly reduced the friction and wear. Simultaneously, the porous structure of PTFE enables nanomaterials to easily enter the tribolayer to realize good lubrication.

Besides the above-mentioned lubrication condition, the service temperature is also considered an important influencing factor on the friction and wear performances of coatings. The tribological exploration of PI coatings filled with 1 wt%-graphene was carried out at various temperatures ranging from RT to 200 °C.[219] The addition of graphene endowed the coatings with reduced friction and improved wear-resistance at the investigated temperatures. Among the service temperatures, the graphene/PI coating exhibited the best anti-wear ability at 100 °C, which was mainly attributed to the formation of a transfer film between the chosen tribo-pairs. The detailed friction and wear data are recorded in Table 3. However, the strength of transfer films and their adhesion function were sharply reduced as the temperature increased to 200 °C, leading to a marked deterioration in the wear rate.

The crucial roles of thermal stability in the friction and wear behaviors of coatings have been increasingly recognized. With respect to higher thermal stability, a nanocoating exhibited better wear-resistance abilities at high temperatures. Li *et al.*[220] systematically explored the friction and wear properties of PI coatings reinforced with ionic liquid-modified FG nanosheets (ILs-FG). In the polymer matrix coatings, the well-dispersed ILs-FG endowed the coatings with an outstanding enhancement in thermal stability. These improvements contributed to resisting the damage caused by heat accumulation. Therefore, it was detected that the wear rate of ILs-FG/PI decreased by about 71% compared to the PI coating. The improved thermal properties, stable dispersion and expected lubrication helped ILs-FG exhibit excellent tribological performances.

5. Three-dimensional nanofillers

3D-nanofillers are mainly composed of one or more basal structural units, which are 0D, 1D, or 2D nanomaterials. Therefore, 3D-nanofillers inherit the many advantages of their components, for instance, diverse morphologies, complementary performances, and unique friction characteristics (*e.g.*, 3D-nanofillers consist of 1D and 2D nanofillers, exhibiting the 1D-rolling effect and 2D-low shearing, respectively), which are directly responsible for the lubrication functions.[212,224–226] Advanced nanohybrids have attracted particular attention due to their demonstrated tribological potential in coatings. In this section, the efforts to develop composite coatings reinforced by 3D nanofillers for anti-wear enhancement and friction reduction are summarized and Table 4 presents some of the recent progress on 3D-nanofillers enhancing the tribological behaviors of coatings.

Table 4 Friction reduction and wear-resisting enhancement of 3D-nanofillers for coatings[a]

			Tribological results	
Matrix	Reinforcement	Tested conditions	COF	Wear
Ni coatings	Nanodiamond[231]	Ruby balls (pin-on-disk, 200 rpm, 1 N, 25 °C)	0.20	NM
Ni60 coatings	WS_2-nano Ni[238]	AISI E52100 ring (pin-on-ring, 2 m s^{-1}, 20 N)	~0.36	NM
WC-Co substrates	CrN-AlN[241]	Sapphire ball (ball-on-disc, 157 mm s^{-1}, 1.5 N, 900 °C)	0.45–0.5	Wear volume: 0.043 mm^3
Ceramic coatings	GO-Al_2O_3 (ref. 117)	Si_3N_4 ball (ball-on-disc, 20 mm s^{-1}, 20 N)	~0.45	Wear rate: ~0.7×10^{-4} mm^3 N m^{-1}
PTFE coatings	PTFE@PMMA[248]	GCr15 steel ball (ball-on-disk, 8.4 mm s^{-1}, 3 N, 25 °C)	0.069	Wear rate: 1.04×10^{-6} mm^3 N m^{-1}
EP coatings	C-BN[246]	Si_3N_4 ball (ball-on-plan, 5 mm, 5 HZ; 5 N)	~0.58	Wear rate: 5.60×10^{-4} mm^3 N m^{-1}
EP coatings	CNTs/GO/MoS_2 (ref. 251)	440c stainless steel ball (ball-on-disk, 200 rpm, 300 rpm, 400 rpm, 500 rpm, 3–6 N, RT)	0.042	Wear rate: 3.44×10^{-5} mm^3 N m^{-1}
EP coatings	Ti_3C_2/graphene[253]	Si_3N_4 ball (ball-on-plate; 2 Hz, 4 mm; 5 N, RT)	0.51	Wear rate: 1.20×10^{-4} mm^3 N m^{-1}

[a] RT = room temperature and NM = not mentioned.

5.1. Metal-based coatings

According to Archard's law, wear loss is inversely proportional to the surface hardness of materials.[227] In this case, well-designed 3D-nanofillers have been increasingly regarded as promising candidates for improving the surface hardness and load-carrying capacity of the nanocoatings.[228–230] 3D nanodiamonds endowed an Ni-coating with a rougher surface topography and smaller crystalline size comparison to pure Ni.[231] An increase in the concentration of nanodiamonds to 5×10^{-2} (g dm^{-3}) led to coarsening of the particles, forming surface structures with a size in the range of ~0.4–0.7 μm. This nanostructure exhibited an increase in surface microhardness, enabling the coating to achieve an improvement in friction and wear behaviors. The details of the friction coefficient and wear rate are displayed in Table 4. After the tests at a normal load of 1 N and rotational speed of 200 rpm, a lower friction coefficient and improved wear-resistance were observed for the nanodiamond-containing coatings compared with the bare Ni-coating.

Nano-TiN particles were successfully grafted on GO due to the contribution of PDA.[232] The as-prepared composite nanostructures presented a feasible strategy to solve the poor dispersion of TiN nanoparticles in Ni-based coatings. The processes for the preparation of coatings filled with TiN and GO are shown in Fig. 11a, where the samples with/without interfacial PDA grafting are abbreviated as "G-coating" and "nG-coating", respectively. The cross-sectional morphologies and microstructures in Fig. 11b and c indicate that the G-coating possessed more compact structures than that of nG-coating, respectively. It was believed that the well-proportioned dispersion of nano-TiN/GO in the G-coating played a crucial role in the

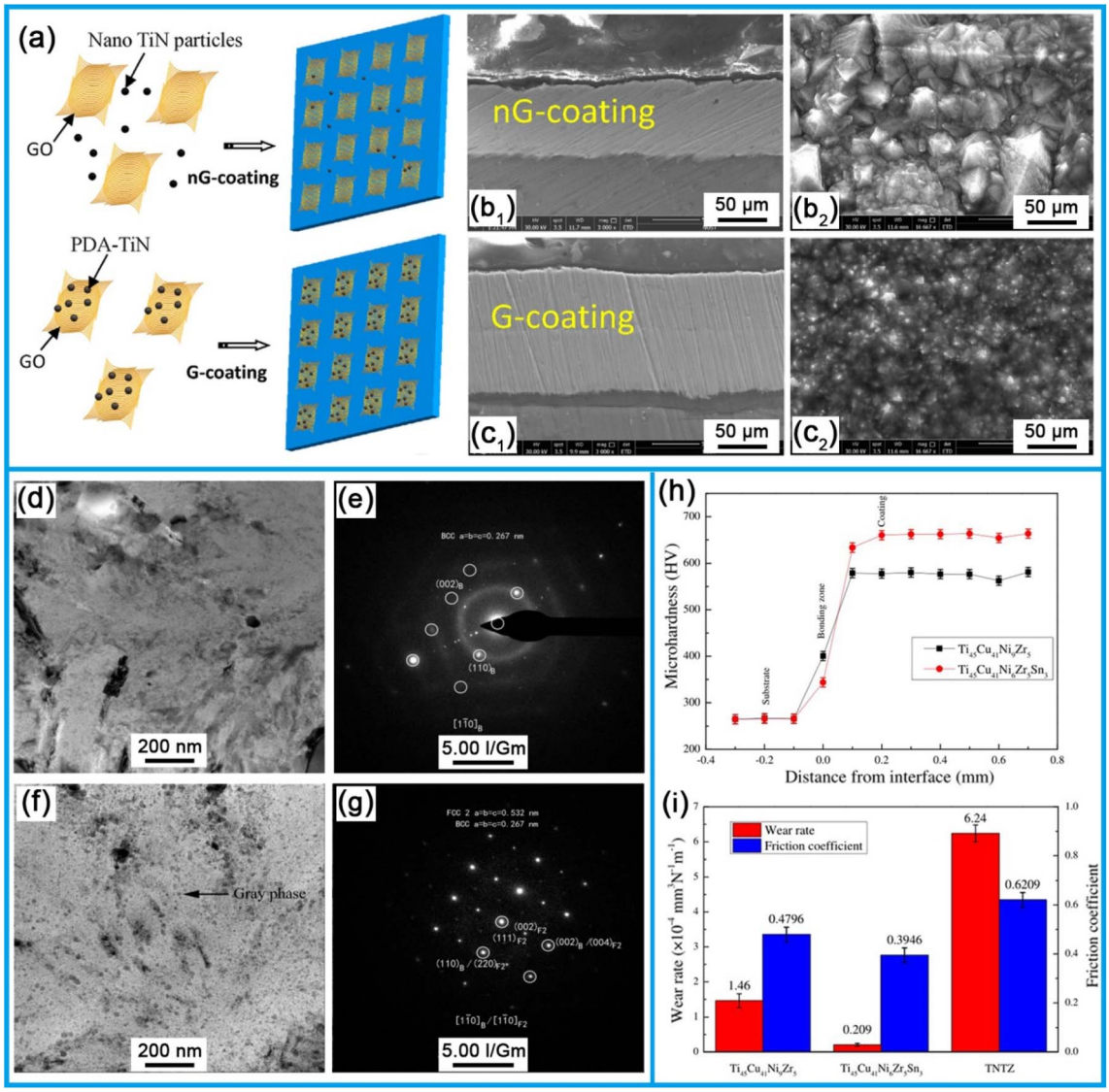

Fig. 11 (a) Schematic showing the preparation of nG-coating and G-coating. Cross-sectional morphologies (b_1 and c_1) and microstructures (b_2 and c_2) of the coatings, respectively. Reproduced from ref. 232 with permission from Elsevier, Copyright 2020. (d and f) TEM images of microstructures and (e and g) selected area electron diffraction patterns of $Ti_{45}Cu_{41}Ni_6Zr_5Sn_3$ coating. (h) Hardness along the coating thickness. (i) Wear rate and friction coefficient of the coatings. Reproduced from ref. 234 with permission from Elsevier, Copyright 2016.

grain refinement of the coating, thus endowing the Ni-based coating with significant improvements in hardness and wear resistance.

Although nanofiller-induced hardening is of great importance for increasing the wear-resisting performance, the hardness of MBCs increases at the expense of ductility and toughness.[120] Thus, a reasonable balance of hardness and toughness directly contributes to the enhancement of the tribological properties of coatings. In the case of Ni–Co/SiC coatings,[233] gradient changes in the grain size and particle content resulted in the formation of functional 3D-nanostructures, providing a feasible strategy for simultaneously improving the hardness and toughness of gradient coatings, which is crucial to realizing outstanding anti-wear behavior. $Ti_{45}Cu_{41}Ni_9Zr_5$ and $Ti_{45}Cu_{41}Ni_6Zr_5Sn_3$ metallic nanocoatings on Ti–30Nb–5Ta–7Zr (TNTZ) alloys were synthesized using laser cladding.[234] After the wear tests at a load of 20 N and speed of 300 rpm, superior friction and wear behavior was observed for the $Ti_{45}Cu_{41}Ni_6Zr_5Sn_3$ coating compared to the $Ti_{45}Cu_{41}Ni_9Zr_5$ coating. The microstructural observation, as shown in Fig. 11d and e, revealed that the $CuNiTi_2$ dendrites formed an amorphous matrix, which effectively increased the hardness and toughness of the metallic coating. The evenly dispersed nano-sized Ni_2SnTi particles in the $CuNiTi_2$ dendrites

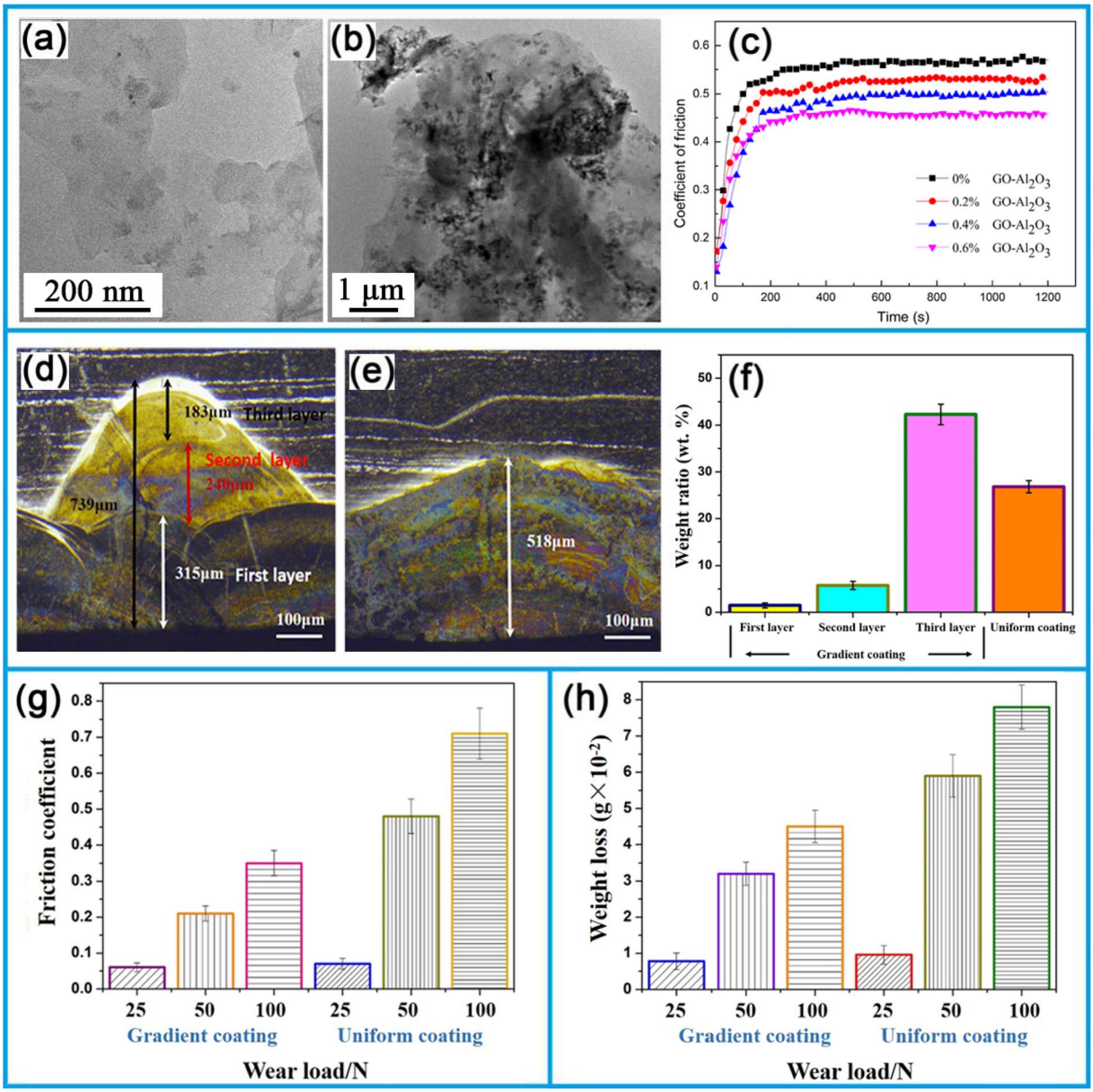

Fig. 12 TEM morphologies of (a) GO and (b) GO-Al_2O_3 hybrids. (c) Friction coefficient of CBCCs-(GO-Al_2O_3). Reproduced from ref. 117 with permission from Elsevier, Copyright 2020. Macrostructures of the gradient (d) and uniform (e) coatings. (f) Weight percentage of Ti in the coating. (g) Friction coefficient and (h) weight loss of the coatings. Reproduced from ref. 60 with permission from Elsevier, Copyright 2020.

contributed to further strengthen the dendrites, as noted in Fig. 11f and g. Hence, improvements in mechanical and tribological performances of $Ti_{45}Cu_{41}Ni_6Zr_5Sn_3$ were obtained. According to the hardness of the metallic coatings in Fig. 11h, the $Ti_{45}Cu_{41}Ni_6Zr_5Sn_3$ coating possessed a hardness of 12.5%, which was higher than that of the $Ti_{45}Cu_{41}Ni_9Zr_5$ coatings. This resulted in the corresponding reduction in friction and wear, as can be detected in Fig. 11i, where the friction coefficient and wear rate decreased by 17.7% and 85.7%, respectively.

In the case of nanofiller-reinforced MBCs, the two critical parameters affecting the friction and wear of metal coatings are the mechanical properties of the composites and the strength of the interfacial bonding.[235] Appropriate surface treatment was demonstrated to be effective in increasing the interfacial bonding strength of nanofillers in conjunction with the coating substrate.[236,237] Nano-Ni-encapsulated submicron WS_2 demonstrated promise for improving the tribological properties of Ni-based coatings.[238] A well-designed Ni/WS_2 nanohybrid aided in preventing the oxidation and vaporization of WS_2 during the fabrication of the coating. This resulted in a noticeable increase in the interfacial compatibility of the composite coating between WS_2 and the Ni matrix. The friction coefficients of the coatings were evaluated using a pin-on-ring friction tester (MMS-1G). The ring with a dimension of Ø 138 mm × 30 mm was hardened ball bearing AISIE52100 steel. The friction coefficient of the cladding layer could be well-evaluated by using a sliding speed of 2 ms^{-1} at a constant normal load of 20 N under dry friction/wear condition. The friction coefficient, μ, was calculated using the following equation:

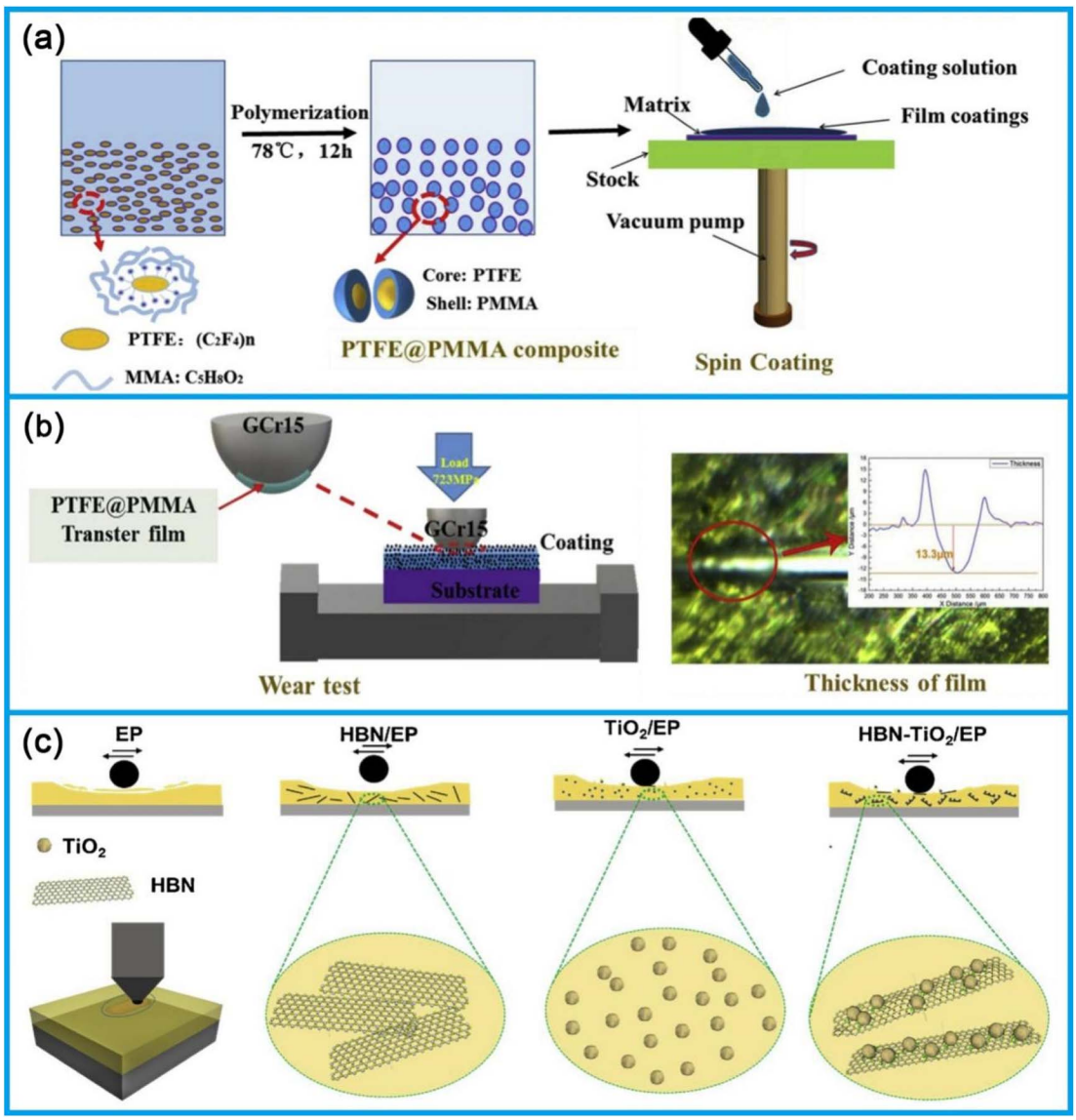

Fig. 13 (a) Schematic of the preparation of PTFE@PMMA coating and (b) wear tests. Reproduced from ref. 248 with permission from Elsevier, Copyright 2019. (c) Schematic of the tribological mechanism of EP-coatings reinforced with HBN, TiO_2 and HBN-TiO_2. Reproduced from ref. 249 with permission from Elsevier, Copyright 2020.

$$\mu = \frac{T}{RP} \quad (13)$$

where T is the friction moment, R the radius of the ring, and P is the normal load acting on the pin specimens.

According to Table 4, the friction coefficient of Ni–Ni/WS_2 was reduced by ~40% compared to bare-Ni, from ~0.60 to 0.36. Meanwhile, the wear resistance of the composites increased by three-fold. The superior friction and wear properties of the Ni–Ni/WS_2 coatings were attributed primarily to the enhanced interfacial strength and lubrication of WS_2.

AA2124/4 wt% B_4C nanocoatings on Ti–6Al–4V alloys were successfully fabricated.[239] A well-proportioned distribution of nano-sized B_4C particles (250 nm) and extremely fine grains appeared in the composite coatings. These fine structures endowed the coatings with prominent interfacial bonding strength between B_4C and the Al-matrix, resulting in the excellent wear-resistance in the nanocoatings. Thereafter, Thakur *et al.*[240] systematically explored the roles of nano-Cr/MWCNTs in the tribological behaviors of WC-CoCr coatings. Specifically 10 wt% Cr additive significantly cooperated with 2 wt%-MWCNTs to enhance the fracture toughness of the nano-WC-CoCr coating. After abrasive wear at a normal load of 30 N and sliding velocity of 0.25 m s^{-1}, the nano-WC-CoCr coating with 10 wt%-Cr + 2 wt%-MWCNTs showed reinforced wear-resistance compared to the pristine coating. The proposed anti-wear enhancement mechanism of the nanocoating was that the high-content of Cr played an important role in improving the adhesion strength of MWCNTs to attach to the substrate, which was responsible for fully exploiting the toughening effect of MWCNTs.

5.2. Ceramic-based coatings

3D-nanofillers are increasingly considered as promising candidates for enhancing the friction and wear performances of ceramic coatings. Similar to MBCs reinforced with 3D-nanofillers, numerous studies demonstrated that the ideal hardening and toughening effects of nanofillers are of great importance for developing the full potential of CBCs in the field of tribology. CrN/AlN superlattice coatings were successfully produced on stainless steel substrates under hot filament plasma currents (I_D).[241] The increase in I_D effectively restricted the growth of the cone-shaped columnar grain and achieved extremely dense microstructures. The refined grain and well-defined nano-layers rendered the superlattice coating with prominent adhesion and crack resistance, along with the maximum hardness of approximately 3800 HV. These excellent mechanical properties endowed the nanocoating with attractive wear-resistance ability under high temperatures. After the wear tests at 900 °C, the CrN/AlN coatings possessed an expected wear-volume of almost 0.043 mm^3 and small friction coefficients ranging from 0.45 to 0.5, as recorded in Table 4.

Liu *et al.*[242] implanted Nb-ions in multilayer TiAlN/CrN nanocoatings to improve their tribological properties. Irradiating the coatings with Nb-ions effectively induced surface amorphization and the formation of multilayer nanostructures. These composite structures played a crucial role in enhancing the wear behavior. The presence of approximately 2×10^{17} ions per cm^2 of Nb-ions reduced the wear rate of the nanocoating to 30% that of the TiAlN/CrN coating without Nb-ions. Additionally, Yan *et al.*[243] focused on the friction and wear properties of Cr+$(Cr,Al)_2O_3$ eutectic nanocoatings and $(Cr,Al)_2O_3$ coatings. A novel 3D nanostructure was observed in the eutectic coating. The incorporation of rod-like nano-Cr in the coatings demonstrated a feasible method for increasing their toughness. The noticeable increase in the toughness enabled the eutectic coating to achieve a higher wear resistance, which was approximately 4.57 times that of the $(Cr,Al)_2O_3$ coatings.

The tribological behavior of a GO-Al_2O_3 hybrid-reinforced ceramic coating was thoroughly investigated.[117] Fig. 12a and b show the TEM morphologies of the GO and GO-Al_2O_3 hybrids, indicating that nano-Al_2O_3 was successfully grafted to the GO surface *via* chemical bonds. These structures contributed to enhancing the bond strength of the GO with the ceramic matrix. After 15 min tests at a speed of 20 mm s^{-1} and load of 20 N, remarkable improvements in the friction and wear behaviors of the composite coatings were well observed. The 0.6 wt% GO-Al_2O_3 ceramic coating exhibited a reduction in friction coefficient and wear rate by ~18.2% and ~61.1%, respectively, compared to the pristine coating (see Fig. 12c). As shown in Table 4, the friction coefficients and wear rates were ~0.45 and ~0.7 $\times$ 10^{-4} mm^3 N m^{-1}, respectively. This marked improvement in the cohesive strength of the composite coating should be responsible for the excellent tribological behaviors.

Subsequently, a graded nano-TiN coating was synthesized above Ti–6Al–4V alloy to realize excellent friction and wear behaviors.[244] The tests were carried out in Hank's solution under the load of 10 N, ensuring that the coefficient of friction (~0.21) and wear rate (~6.2 $\times$ 10^{-7} mm^3 N m^{-1}) of the gradient coatings were smaller than that of the monolayer TiN coating. This excellent tribological performance was mainly attributed to the expected mechanical properties at the substrate/coating interfaces and the strengthening and toughening abilities of the coating nano-crystallites.

Thereafter, further explorations on effect of micro-structure on the tribological behavior of nano-TiC gradient coatings were executed by Wang *et al.*[60] Fig. 12d and e indicate the distinct multilayer microstructures of the gradient coatings. Fig. 12f provides the weight percentage of TiC in the coatings, implying that an increase in the concentration of TiC in the gradient direction resulted in the transformation of nano-TiC particles into the dense TiC-clusters. Consequently, the coating microhardness gradually increased from 612 HV in the bottom to 1088 HV at the top interface. This gradient structure and improved hardness endowed the coatings with an observable enhancement in friction and wear behaviors. Almost 50% reduction in coefficient of friction and about 40% decrease in the wear loss were obtained compared to that of the uniform coating (Fig. 12g and h).

5.3. Polymer-based coatings

Two critical factors in achieving the desired friction and wear behaviors are the dispersibility of the nanofiller and its bonding

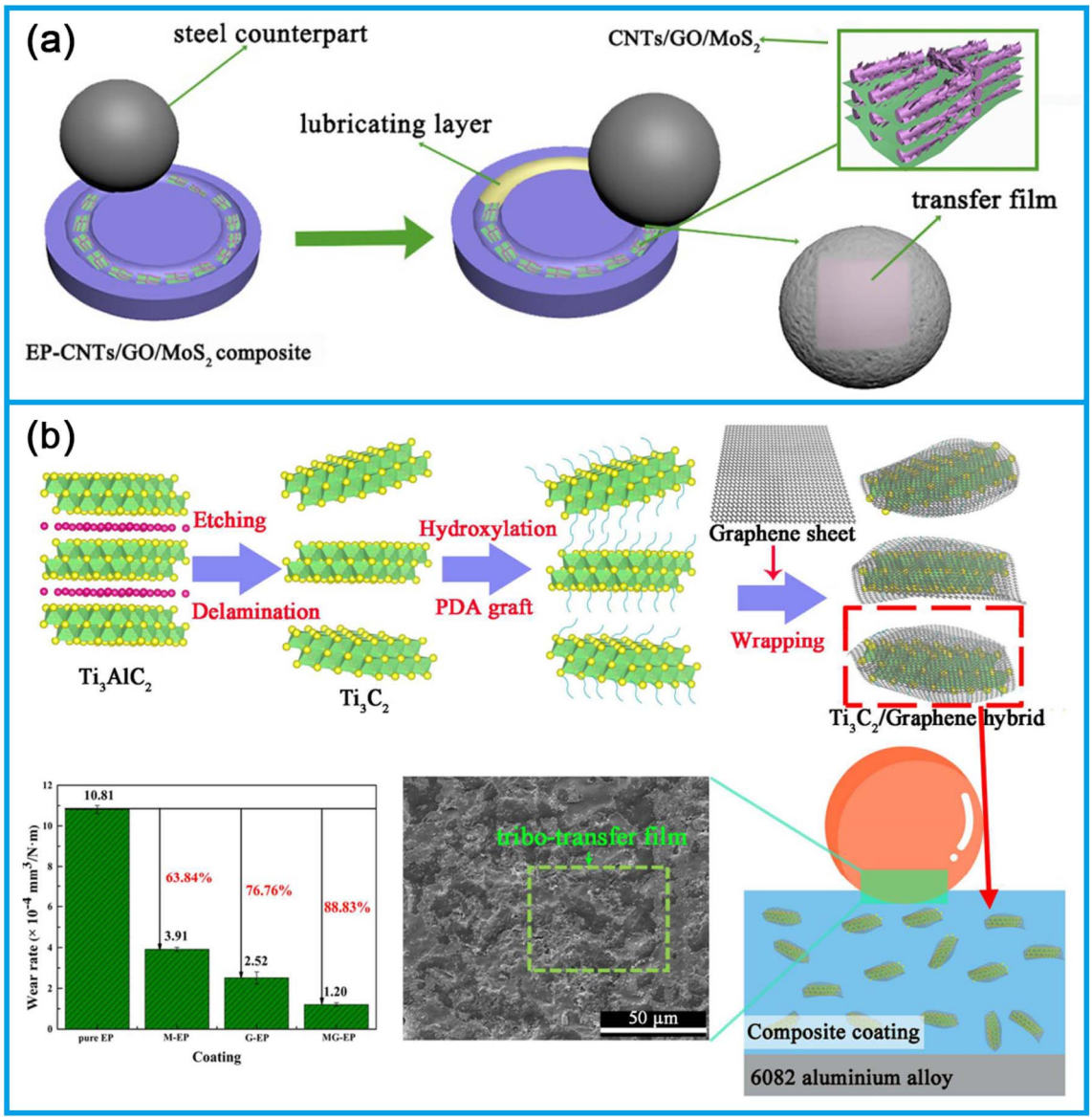

Fig. 14 (a) Tribological mechanisms of EP-CNT/GO/MoS_2 coatings. Reproduced from ref. 251 with permission from Elsevier, Copyright 2018. (b) Schematic of the fabrication of wrapping Ti_3C_2/graphene hybrid and the tribological results. Reproduced from ref. 253 with permission from Elsevier, Copyright 2020.

strength to the corresponding matrix. According to recent reports, the multi-dimensional synergies of 3D-nanomaterials directly contribute to their remarkable improvements in dispersion and interfacial adhesion, resulting in superior tribological performance.[245,246]

To ensure the preceding discussion, a systematic study on the tribological properties of an EP coating reinforced with carbon nanofiber/MoS_2 (CNF/MoS_2) was conducted.[55] Compared to the EP-CNF and EP-MoS_2 coatings, EP-CNF/MoS_2 had superior anti-friction and wear-resistance properties, resulting in a frictional coefficient and wear rate of ~0.075 and ~8.6×10^{-5} mm^3 N^{-1} m^{-1}, respectively. This was primarily due to the excellent synergistic lubrication of CNF and MoS_2, as well as the prominent interfacial adhesion of CNF/MoS_2 in comparison to the EP matrix. Additionally, Li *et al.*[52] produced hybrid CNTs/ZnS to overcome the poor dispersion of CNTs in the polymer. The wear rate and friction coefficient of the EP-CNTs/ZnS coating were reduced with an increase in the content of CNTs/ZnS up to 1.25 wt%. This because of the excellent collaboration of ZnS and CNT, where CNTs provided a nano-rolling effect, while ZnS assumed the stresses applied on the CNTs.

Due to the poor dispersion of the MoS_2 nanosheets, they were prone to agglomerating and resulted in the generation of microcracks in the coating. Therefore, a facile *in situ* hydrothermal method was developed to fabricate a 2D/2D h-BN/MoS_2 hybrid.[247] With respect to the EP-h-BN/MoS_2 system, the presence of hydroxylated h-BN contributed to the homogenous distribution of MoS_2 and enhancement in the interfacial

combination of the hybrids with regard to the EP-matrix. Thus, crucial improvements in the tribological performances were obtained, where the friction coefficient and wear rate of the EP-h-BN/MoS_2 coatings significantly decreased by ~80% and ~88%, respectively, compared to the neat EP coating.

PTFE-encapsulated polytetrafluoroethylene (PTFE@PMMA, core@shell) coatings were well fabricated using a spin coater[248] and the successful procedure for the preparation of this coating is shown in Fig. 13a. Microscopic analysis proved that the nano-scale core@shell structures achieved a homogenous dispersion in the polymer matrix. After the wear tests at a normal load of 3 N with sliding speed of 8.4 mm s^{-1}, a continuous and uniform film of PTFE/PMMA could be well observed on GCr15 steel-balls (Fig. 13b), which resulted in an observable increase in the wear-resistance function of the composite coating. Notably, the wear rate of the PTFE coating reinforced by PTFE@PMMA decreased from 2.32×10^{-4} mm^3 N m^{-1} to 1.04×10^{-6} mm^3 N m^{-1}, and the friction coefficient was reduced by ~15% (approximately 0.069), as indicated in Table 4.

According to the recent research on polymer coatings, insufficient load-bearing capacity remains an impediment to achieving the desired tribological properties.[250] The friction and wear performances of hexagonal boron nitride-titanium dioxide (HBN-TiO_2)-reinforced EP-coatings were explored.[249] The results indicated that the HBN-TiO_2/EP coating exhibited superior wear resistance, where the wear rate was reduced by 65.8% compared to plain EP. The tribological mechanisms of the pure EP and composite coatings are elaborated in Fig. 13c. In the case of the neat EP, its poor mechanical properties were a significant factor in the insufficient anti-wear performance of the material. The addition of hybrid nanofillers enhanced the load-bearing and self-lubricating properties of the EP-coating. Notably, the unique 2D-structures of HBN endowed it with the expected ability to achieve superior friction reduction and wear resistance, and the high-hardness TiO_2 caused a significant increase in load-bearing function. Hence, significant improvements in tribological properties were observed in the HBN-TiO_2-reinforced EP coatings.

Furthermore, according to the report by Chen *et al.*,[251] CNTs/GO/MoS_2 hybrids presented a key approach for improving the friction reduction and anti-wear enhancement of EP coatings. Following the wear tests, it was determined that the EP-CNTs/GO/MoS_2 composite coating had the lowest friction coefficient (~0.042) and the highest wear rate (~3.44×10^{-5} mm^3 N m^{-1}) compared to the composite coatings reinforced with single fillers. Table 4 presents the tribological behaviors in detail. The

Table 5 The latest progress and specific application of nanofillers with different dimensions in the field of tribology

Matrix	Nanofillers	Recent developments	Specific applications
Metal	0D	Ni–B/Al_2O_3 improving wear resistance;[73] Ni–P–1.5TiN reduced wear loss (64.3 wt%).[75]	Petrochemical, automotive, electronics, nuclear, and piston ring-cylinder liners
	1D	Graphite/copper–zinc promoting load-bearing capability;[121] Ni–CeO_2 NRs improving the microhardness (~3 times).[128]	Contact brushes, bearing materials, and automobiles
	2D	WC and WC/Graphene increasing wear resistance (~18%);[179] the hardness increasing (~4.4 times).[190]	Electrical contacts, micro devices, bio-implants and mould materials
	3D	Ni–B–CeO_2 improving the microhardness (~61%);[230] nano TiN particles grafted onto GO solving the dispersion problem.[232]	Oil refinery, shipping, and machinery manufacturing
Ceramic	0D	Silver or copper resulting film structure densification;[87] YSZ ceramic matrix coatings possessing excellent thermal stability.[91]	Sections of low- and high-pressure compressors, and aero-engines
	1D	The fracture toughness and bonding strength increasing (63.18% and 9.9 times);[136] fracture toughness increasing (~38%).[141]	Brakes, high-temperature heat exchangers, and nose cones piston
	2D	Hardness, elastic modulus and fracture toughness increasing (19%, 18% and 300%);[203] the friction coefficient and wear rate decreased (~13% and ~19%).[211]	Power generation, plunger pumps, bearings, and turbine blades
	3D	Thick CrN/AlN coatings exhibiting a maximum micro hardness up to 3800 Hv;[241] the wear resistance increasing (5.57 times).[243]	Valves in oil and gas field, piston ring and cylinder liners
Polymer	0D	The precipitated type of nano-silica replacing the expensive fumed nano-silica;[50] MD simulation to design different types of materials.[101]	Cars manufacturing, industrial production, and astronautics
	1D	SWCNTs enhancing the hardness (~66%) and elastic modulus (~58%);[158] modification with HDI improving the dispersion of TiNTs.[170]	Anticorrosion coating, bearings self-cleaning coatings, and gears
	2D	Transfer film determined polymer tribological performance;[212] PI/3 GP exhibiting low friction (19–29%) and higher wear-resistant (35–78%).[219]	Electrical submersible pumps, air-conditioning, and cable coating
	3D	Wear rate of HBN-TiO_2/EP composite coating decreased (65.8%);[249] the GO-CNTs-PI three-phase structure improving the mechanical properties of the film.[252]	Corrosion protection, ocean, aviation, and microelectronics

results were primarily attributed to the excellent load-bearing capacity of CNTs and GO, attractive lubrication properties of MoS_2, and the formed transfer film (see Fig. 14a). Meanwhile, the GO/CNT nanofillers also played crucial roles in the tribological performances of the PI coatings.[252] The mechanical and tribological properties of the GO/CNT/PI nanocomposite were significantly improved compared to the pure PI coating. According to the proposed mechanism, GO/CNTs played a significant role in improving the load-bearing capacity and lubrication performance of the coating.

The exceptional tribological potential of 3D-nanofillers has been highlighted to accelerate the improvement of their tribological performances, owing to the distinct synergies between their components. Although graphene and Ti_3C_2 MXene sheets have a variety of notable properties and functions, their synergistic effects in organic coatings are rarely discussed. Ti_3C_2/graphene (MG) hybrids with wrapping structures were successfully fabricated for the purpose of evaluating their tribological properties as EP coating additives.[253] Fig. 14b presents the fabrication of the wrapping MG hybrid and the corresponding wear characteristics of the composite coatings in detail. It can be observed that the wear rate of pure EP was almost 10.81×10^{-4} mm^3 N m^{-1}. In comparison, the MG hybrids endowed the coating with an observable reduction in wear-resisting behavior by almost 88.83%. The synergistic effects of the superior load-bearing capacity of the Ti_3C_2 flakes and the commendable self-lubrication properties of graphene enabled not only a reduction in the surface stress but also the formation of a tribo-transfer film, resulting in a remarkable reduction in the friction and wear.

6. Conclusions and outlooks

The energy consumption of mechanical systems caused by friction and wear is directly related to their service life and application accuracy. Accordingly, achieving low friction and wear on moving surfaces has become a focus of attention. Multi-dimensional nanofillers have attracted significant attention because of their proven tribological potential in coatings. Nowadays, nano-coatings containing a large amount of various nanofillers have demonstrated excellent friction and wear behaviors, implying an excellent route to reduce the energy consumption of the ceramic, metal, and polymer-based components.

6.1. Conclusions

The well-distributed dispersibility, ideal nanostructure, and interfacial bonding strength of multi-dimensional nanofillers have been increasingly recognized as crucial factors that determine tribological performances of coatings. Preliminary guidelines were provided for selecting appropriate nanofillers to achieve the expected lubrication behaviors of various coatings. The unique spherical structures and high chemical stability endow 0D-nanofillers with good friction and wear behaviors. The incorporation of 0D-nanofillers has confirmed to be effective for improving the hardness of MBCs and CBCs, which is considered to be the leading factor contributing to the improvement in tribological coatings. Furthermore, hard nanofillers at the frictional interfaces serve as distance holders and ball bearings, thus enhancing the load-bearing capacity and optimizing the anti-wear performance of polymer coatings.

1D-nanofillers with good dispersion improve the fracture toughness of coatings by preventing the propagation and coalescence of short cracks, thus reducing the wear degree of composite coatings. In addition, surface functionalization and chemical structure are two critical characteristics of 1D-nanofillers, which account for their tribological behaviors and wear applications.

According to numerous recent reports, the excellent mechanical strength, thermal stability, and low surface energy of 2D-nanofillers make them suitable for a wide range of applications under friction and wear of interfacial coatings. In the case of polymer coatings, the transfer film plays an important role in the anti-wear enhancement and the friction reduction; therefore, 2D-nanofillers provide a feasible approach to improve the adhesion strength and load-bearing capacity of the transfer film. Furthermore, the application of nanofillers in coatings has accelerated the exploration of transparent conduction coatings with excellent anti-wear behavior, suggesting possible substitutes for the expensive indium tin oxide films in many optoelectronic devices.

3D-nanohybrids inherit the characteristics of their multiple components, which are directly responsible for their excellent tribological performance. Well-designed 3D-nanofillers certify their multidimensional collaboration effects on the friction and wear behaviors of composites, enabling nanohybrids to exhibit superior functions with friction reduction and wear resistance of tribological coatings. In addition, recent attention on 3D-nanofillers has broadened their extensive applications. For example, HIF-MoS_2/RGO and Cu/PDA/MoS_2 have been applied in ionic grease and sunflower oil for the purpose of improving their lubricant performances. Table 5 presents a summary of the recent developments and specific applications of multi-dimensional nanofillers with metal, ceramic, and polymer coatings in the tribological field. It can be seen in Table 5 that metal, ceramic, and polymer coatings have their respective applications. Firstly, in the case of metal-based coatings with nano-additives, the addition of nanofillers significantly increases the microhardness of the coating. Due to their high wear resistance, the application of metal-based coatings is confirmed to be the most extensive among the three types of aforementioned coatings. Furthermore, with an increase in the content of nanofillers, ceramic-based coatings exhibit a clear increase in toughness, and these coatings are mainly suitable for parts operating at high temperature. Finally, the synergistic effect of nanofillers and polymer-based coatings not only results in excellent performances in the fields of friction and wear, but endows polymer-based coatings with potential application in the field of anti-corrosion.

6.2. Challenges and future recommendations

Although the design of new nanofiller coatings provides broads application prospects for controlling friction and wear, there are still many challenges, as follows.

(1) It is a great significance to study new nanofiller coatings under extreme friction conditions. With the rapid development of advanced industrial equipment, the working environments of machinery need to withstand extreme conditions such as high pressure, speed and temperature. Nanofiller coatings can work under some extremely harsh conditions, but their working times are too short to fully exert their anti-wear and friction reducing effects. Therefore, exploring new nanofillers with high tribological properties will be the focus of future basic research and application, especially ideal working hours under extreme conditions. Moreover, the application of nanofillers in composite materials has promoted the exploration of the high wear resistance of thermoelectric coatings, providing a good opportunity for the industrial application of intelligent thermoelectric devices in the future.

(2) The impact of nanofillers on the tribological behavior of coatings is complex, given that the unavoidable defects and contamination of nanofillers reduce the tribological behaviors and reproducibility. Therefore, the complex wear behavior of nanocomposites should be evaluated to eliminate potential hazards related to their tribological applications.

(3) Although well-designed friction and wear coatings have broad application prospects, there are still difficulties in improving the dispersion stability of nanofillers. Physically treated nanoparticles are prone to re-aggregation. Chemical modification may mask the natural characteristics of nanoparticles, but chemical modifiers may degraded easily during wear. Therefore, further research is needed to improve the dispersion method. The self-dispersion method does not require any modifiers and has good dispersion stability, and thus it is a development trend.

(4) Although multi-dimensional hybrid nanofillers have also been produced in the laboratory, their production on an industrial scale is limited due to their complex synthesis procedures. Therefore, further exploration should focus on the production processes, repeatability and practicality of synthesis methods.

(5) Finally, many studies on the coating mechanisms have shown that the formation of high-performance friction coatings largely depends on nanofillers. In this case, carefully designed functional nanofillers make them the best candidate materials for regulating the nanostructure and self-lubricating properties of coatings. Among the numerous nanofiller coating systems, the wear-resistant friction coatings formed using MXene systems possess excellent performance. However, the complex mechanical behavior of MXenes seriously hinders their tribological application. Thus, to achieve efficient friction and wear systems, more fundamental research is necessary to understand the potential friction and wear mechanisms.

The tribology of nano-fillers in coatings has not been fully reviewed. In particular, insight into the critical role of multi-dimensional nanomaterials in different coating substrates has not been reported. Herein, initially, nanofillers were divided into four aspects based on their dimensions, including 0D, 1D, 2D, and 3D. The applications of nanofillers in metal, ceramic, and polymer coatings were described in each case. Furthermore, the tribological mechanism of nanofillers in the coating was expounded. These findings are beneficial in understanding the interface-related tribological behaviors of the coatings, thus widening their applications in various industries. It is expected that the present work will inspire new possibilities for next-generation coating applications, together with superior tribological properties, and stimulate further developments in tribological coating nanotechnology.

Abbreviations

0D	Zero dimensional
1D	One dimensional
2D	Two dimensional
3D	Three dimensional
CNF	Carbon nanofiber
GNPs	Graphene nanoplates
MBCs	Metal-based coatings
CBC	Ceramic-based coatings
YSZ	Yttria-stabilized zirconia
SPPS	Solution precursor plasma spraying
PMMA/SiO_2	Poly-methylmethacrylate/silica
Cu–Sn-PTFE	Cu–Sn–polytetrafluoroethylene
PTFE	Polytetrafluoroethylene
PDA/AgNPs	Polydopamine/Ag-nanoparticles
PS/SiO_2	Polystyrene/nano-SiO_2
EP	Epoxy
TGA	Thermogravimetric analysis
CNTs	Carbon nanotubes
MWCNT	Multi-walled carbon nanotube
SDS	Sodium dodecyl sulfate
HVOF	High velocity oxygen fuel
SiCNW-SiC	SiC nanowire-reinforced SiC
C/C	Carbon/carbon
SiC-Ni coating	SiC coating with added Ni
CVD	Chemical vapor deposition
PBA	[Poly(2-butylaniline)]
THF	Tetrahydrofuran
PAM-CNTs	Polyacrylamide-carbon nanotubes
SWCNTs	Single-walled carbon nanotubes
Decalin/UHMWPE	Decahydronaphthalene/ultra-high molecular weight polyethylene
PU	Polyurethane
TiNTs-HDI	Hexamethylene diisocyanate-modified TiO_2 nanotubes
pDA	Poly-dopamine
BSC	Back-scattered scanning
SEI	Secondary electron image
SAED	Selected area electron diffraction
GO	Graphene oxide
BN	Boron nitride
MD	Molecular dynamics
EDS	Energy dispersive spectrometer
ZrO_2/GNs	Zirconia/graphene nanosheets
GNs/AT-13	Graphene nanosheets/Al_2O_3 + 13 wt% TiO_2
AT-13	Al_2O_3 + 13 wt% TiO_2
$NbSe_2$	Niobium diselenide
g-C_3N_4	Graphitic carbon nitride

PI/FG	Fluorinated graphene-reinforced polyimide
IL-FG	Ionic liquid-modified FG nanosheets
TNTZ	Ti–30Nb–5Ta–7Zr
CNF/MoS_2	Carbon nanofiber/MoS_2
PTFE@PMMA, core@shell	Polytetrafluoroethylene
HBN-TiO_2	Hexagonal boron nitride-titanium dioxide
Ti_3C_2/graphene	MG

Conflicts of interest

There are no conflicts to declare.

Acknowledgements

This an investigation is supported by Henan postdoctoral Foundation (907301210); Postdoctoral Foundation of Anyang Institute of Technology (BHJ2019006); Project for Science and Technology Plan of Henan Province (212102210111, 212102210445); Key Training Project of Young Teacher of Henan province (2021GGJS149). The authors thank the special funding and equipment support of the visiting professor at the school of materials science and engineering (4001-40734).

References

1 J. Luo, M. Liu and L. Ma, Origin of friction and the new frictionless technology—Superlubricity: Advancements and future outlook, *Nano Energy*, 2021, **86**, 106092.
2 S. K. Sahu, N. D. Badgayan and P. R. Sreekanth, Understanding the influence of contact pressure on the wear performance of HDPE/multi-dimensional carbon filler based hybrid polymer nanocomposites, *Wear*, 2019, **438-439**, 102824.
3 D. Berman, A. Erdemir and A. V. Sumant, Graphene: a new emerging lubricant, *Mater. Today*, 2014, **17**(1), 31–42.
4 S. Dabees, V. Tirth, A. Mohamed and B. M. Kamel, Wear performance and mechanical properties of MWCNT/HDPE nanocomposites for gearing applications, *J. Mater. Res. Technol.*, 2021, **12**, 2476–2488.
5 A. G. Olabi, K. Elsaid, E. T. Sayed, M. S. Mahmoud, T. Wilberforce, R. J. Hassiba and M. A. Abdelkareem, Application of nanofluids for enhanced waste heat recovery: A review, *Nano Energy*, 2021, **84**, 105871.
6 H. Tang, J. Sun, J. He and P. Wu, Research Progress of Interface Conditions and Tribological Reactions: A Review, *J. Ind. Eng. Chem.*, 2021, **94**, 105–121.
7 W. Wu, J. Liu, Z. Li, X. Zhao, G. Liu, S. Liu, S. Ma, W. Li and W. Liu, Surface-functionalized nanoMOFs in oil for friction and wear reduction and antioxidation, *Chem. Eng. J.*, 2021, **410**, 128306.
8 D. Berman, K. C. Mutyala, S. Srinivasan, S. K. Sankaranarayanan, A. Erdemir, E. V. Shevchenko and A. V. Sumant, Iron-Nanoparticle Driven Tribochemistry Leading to Superlubric Sliding Interfaces, *Adv. Mater. Interfaces*, 2019, **6**(23), 1901416.
9 D. K. Shukla, B. Mukherjee, A. Islam and A. K. Keshri, Peculiar high temperature tribological behaviour of plasma sprayed graphene nanoplatelets reinforced cerium oxide coatings, *Ceram. Int.*, 2021, **47**(12), 17809–17812.
10 S. Yang, R. Sun and K. Chen, Self-healing performance and corrosion resistance of phytic acid/cerium composite coating on microarc-oxidized magnesium alloy, *Chem. Eng. J.*, 2022, **428**, 131198.
11 W. Song, L. An, Y. Lu, X. Zhang and S. Wang, Friction behavior of TiN–MoS_2/PTFE composite coatings in dry sliding against SiC, *Ceram. Int.*, 2021, **47**(17), 24003–24011.
12 A. R. Govande, A. Chandak, B. R. Sunil and R. Dumpala, Microhardness and frictional characteristics of cryogenically treated carbide coatings, *Mater. Today: Proc.*, 2021, **47**, 3112–3116.
13 A. W. Momber, M. Irmer and T. Marquardt, Effects of polymer hardness on the abrasive wear resistance of thick organic offshore coatings, *Prog. Org. Coat.*, 2020, **146**, 105720.
14 M. Marian, D. Berman, A. Rota, R. L. Jackson and A. Rosenkranz, Layered 2D Nanomaterials to Tailor Friction and Wear in Machine Elements—A Review, *Adv. Mater. Interfaces*, 2022, **9**(3), 2101622.
15 A. Rosenkranz, H. L. Costa, M. Z. Baykara and A. Martini, Synergetic effects of surface texturing and solid lubricants to tailor friction and wear – A review, *Tribol. Int.*, 2021, **155**, 106792.
16 A. Rodriguez, M. S. Jaman, O. Acikgoz, B. Wang, J. Yu, P. G. Grützmacher, A. Rosenkranz and M. Z. Baykara, The potential of Ti_3C_2TX nano-sheets (MXenes) for nanoscale solid lubrication revealed by friction force microscopy, *Appl. Surf. Sci.*, 2021, **535**, 147664.
17 L. Zhang, C. Yuan, C. Dong, Y. Wu and X. Bai, Friction-induced vibration and noise behaviors of a composite material modified by graphene nano-sheets, *Wear*, 2021, **476**, 203719.
18 D. Berman, A. Erdemir and A. V. Sumant, Approaches for achieving superlubricity in two-dimensional materials, *ACS Nano*, 2018, **12**(3), 2122–2137.
19 Y. An, Y. Tian, C. Wei, Y. Tao, B. Xi, S. Xiong, J. Feng and Y. Qian, Dealloying: An effective method for scalable fabrication of 0D, 1D, 2D, 3D materials and its application in energy storage, *Nano Today*, 2021, **37**, 101094.
20 P. Wang, C. Jia, Y. Huang and X. Duan, Van der Waals Heterostructures by Design: From 1D and 2D to 3D, *Matter*, 2021, **4**(2), 552–581.
21 H. Jin, Y. Sun, Z. Sun, M. Yang and R. Gui, Zero-dimensional sulfur nanomaterials: Synthesis, modifications and applications, *Coord. Chem. Rev.*, 2021, **438**, 213913.
22 J. Abraham, R. Arunima, K. C. Nimitha, S. C. George and S. Thomas, One-dimensional (1D) nanomaterials: Nanorods and nanowires; nanoscale processing,

Nanoscale Processing, ed. S. Thomas and P. Balakrishnan, Elsevier, 2021, ch. 3, pp. 71–101.

23 K. Hu, F. Wang, Z. Shen, Y. Yan and H. Liu, Enhancement methods of hydrogen sensing for one-dimensional nanomaterials: A review, *Int. J. Hydrogen Energy*, 2021, **46**(38), 20119–20138.

24 M. Bodik, M. Jergel, E. Majkova and P. Siffalovic, Langmuir films of low-dimensional nanomaterials, *Adv. Colloid Interface Sci.*, 2020, **283**, 102239.

25 A. Alagh, F. E. Annanouch, P. Umek, C. Bittencourt, A. Sierra-Castillo, E. Haye, J. F. Colomer and E. Llobet, CVD growth of self-assembled 2D and 1D WS_2 nanomaterials for the ultrasensitive detection of NO_2, *Sens. Actuators, B*, 2021, **326**, 128813.

26 B. He, M. Feng, X. Chen and J. Sun, Multidimensional (0D-3D) functional nanocarbon: Promising material to strengthen the photocatalytic activity of graphitic carbon nitride, *Green Energy Environ.*, 2021, **6(6)**, 823–845.

27 M. Arumugam, S. J. Lee, T. Begildayeva, S. S. Naik, Y. Yu, H. Lee, J. Theerthagiri and M. Y. Choi, Enhanced photocatalytic activity at multidimensional interface of 1D-Bi_2S_3@2D-GO/3D-BiOI ternary nanocomposites for tetracycline degradation under visible-light, *J. Hazard. Mater.*, 2021, **404**, 123868.

28 A. Ott, S. Rogg, S. Lauterbach, H.-J. Kleebe, C. Hess and G. Mera, Novel 0D-nanocarbon-silica ceramic composites: sol–gel synthesis and high-temperature evolution, *Dalton Trans.*, 2020, **49**(21), 7144–7154.

29 M. Freitas, A. Carvalho, H. P. A. Nouws and C. Delerue-Matos, Tracking Arachis hypogaea Allergen in Pre-Packaged Foodstuff: A Nanodiamond-Based Electrochemical Biosensing Approach, *Biosensors*, 2022, **12**(6), 429.

30 W. Zhai and K. Zhou, Nanomaterials in superlubricity, *Adv. Funct. Mater.*, 2019, **29**(28), 1806395.

31 X. Shi, S. Liu, Y. Sun, J. Liang and Y. Chen, Lowering Internal Friction of 0D–1D–2D Ternary Nanocomposite-Based Strain Sensor by Fullerene to Boost the Sensing Performance, *Adv. Funct. Mater.*, 2018, **28**(22), 1800850.

32 M. Fathi, M. S. Safavi, S. Mahdavi, S. Mirzazadeh, V. Charkhesht, A. Mardanifar and M. Mehdipour, Co–P alloy matrix composite deposits reinforced by nano-MoS_2 solid lubricant: An alternative tribological coating to hard chromium coatings, *Tribol. Int.*, 2021, **159**, 106956.

33 A. S. Kumar, S. Deb and S. Paul, Tribological characteristics and micromilling performance of nanoparticle enhanced water based cutting fluids in minimum quantity lubrication, *J. Manuf. Process.*, 2020, **56**, 766–776.

34 Z. Xi, H. Wan, Y. Ma, Y. Wu, L. Chen, H. Li, H. Zhou, J. Chen and G. Hou, *In situ* synthesis of Cu_2S nanoparticles to consolidate the tribological performance of PAI-PTFE bonded solid lubricating coatings, *Prog. Org. Coat.*, 2021, **154**, 106197.

35 H. Xie, Y. Wei, B. Jiang, C. Tang and C. Nie, Tribological properties of carbon nanotube/SiO_2 combinations as water-based lubricant additives for magnesium alloy, *J. Mater. Res. Technol.*, 2021, **12**, 138–149.

36 I. Ali, A. A. Basheer, A. Kucherova, N. Memetov, T. Pasko, K. Ovchinnikov, V. Pershin, D. Kuznetsov, E. Galunin, V. Grachev and A. Tkachev, Advances in carbon nanomaterials as lubricants modifiers, *J. Mol. Liq.*, 2019, **279**, 251–266.

37 H. Xiao and S. Liu, 2D nanomaterials as lubricant additive: A review, *Mater. Des.*, 2017, **135**, 319–332.

38 K. Yang, H. Ma, W. Zhao, X. Li, H. Lin and Y. Liang, A Synergetic Effect of Silver and Carbon Nanotubes on the Tribological Behavior of TiAl-Based Composites, *J. Mater. Eng. Perform.*, 2019, **28**(9), 5563–5572.

39 C. J. Castilho, D. Li, Y. Xie, H. Gao and R. H. Hurt, Shear failure in supported two-dimensional nanosheet van der Waals thin films, *Carbon*, 2021, **173**, 410–418.

40 B. C. Wyatt, A. Rosenkranz and B. Anasori, 2D MXenes: Tunable Mechanical and Tribological Properties, *Adv. Mater.*, 2021, **33**(17), 2007973.

41 A. Rosenkranz, M. C. Righi, A. V. Sumant, B. Anasori and V. N. Mochalin, Perspectives of 2D MXene Tribology, *Adv. Mater.*, 2023, **35**(5), 2207757.

42 P. Radhika, C. B. Sobhan and S. Chakravorti, Improved tribological behavior of lubricating oil dispersed with hybrid nanoparticles of functionalized carbon spheres and graphene nano platelets, *Appl. Surf. Sci.*, 2021, **540**, 148402.

43 W. Shang, T. Cai, Y. Zhang, D. Liu and S. Liu, Facile one pot pyrolysis synthesis of carbon quantum dots and graphene oxide nanomaterials: All carbon hybrids as eco-environmental lubricants for low friction and remarkable wear-resistance, *Tribol. Int.*, 2018, **118**, 373–380.

44 N. Xiao, Y. Chen, H. Lin, H. liaquat, F. Zhang and K. Yang, Multidimensional nanoadditives in tribology, *Appl. Mater. Today*, 2022, **29**, 101641.

45 C. R. Raghavendra, S. Basavarajappa, I. Sogalad and V. Kallappa Saunshi, Study on surface roughness parameters of nano composite coatings prepared by electrodeposition process, *Mater. Today: Proc.*, 2021, **38**, 3110–3115.

46 S. K. Sahu and P. Rama Sreekanth, Mechanical, thermal and rheological properties of thermoplastic polymer nanocomposite reinforced with nanodiamond, carbon nanotube and graphite nanoplatelets, *Adv. Mater. Process. Technol.*, 2022, **8**(sup4), 2086–2096.

47 S. K. Sahu, N. D. Badgayan and P. R. Sreekanth, Rheological Properties of HDPE based thermoplastic polymeric nanocomposite reinforced with multidimensional carbon-based nanofillers, *Biointerface Res. Appl. Chem.*, 2022, **12**(4), 5709–5715.

48 N. D. Badgayan, S. K. Sahu, S. Samanta and P. R. Sreekanth, An insight into mechanical properties of polymer nanocomposites reinforced with multidimensional filler system: a state of art review, *Mater. Today: Proc.*, 2020, **24**, 422–431.

49 M. U. Azam and M. A. Samad, UHMWPE hybrid nanocomposite coating reinforced with nanoclay and carbon nanotubes for tribological applications under

water with/without abrasives, *Tribol. Int.*, 2018, **124**, 145–155.
50 M. Malaki, Y. Hashemzadeh and A. Fadaei Tehrani, Abrasion resistance of acrylic polyurethane coatings reinforced by nano-silica, *Prog. Org. Coat.*, 2018, **125**, 507–515.
51 F. M. Michael, M. R. Krishnan, W. Li and E. H. Alsharaeh, A review on polymer-nanofiller composites in developing coated sand proppants for hydraulic fracturing, *J. Nat. Gas Sci. Eng.*, 2020, **83**, 103553.
52 X. Li, B. Chen, Y. Jia, X. Li, J. Yang, C. Li and F. Yan, Enhanced tribological properties of epoxy-based lubricating coatings using carbon nanotubes-ZnS hybrid, *Surf. Coat. Technol.*, 2018, **344**, 154–162.
53 D. White, M. Chen, C. Xiao, W. Huang and S. Sundararajan, Microtribological behavior of Mo and W nanoparticle/graphene composites, *Wear*, 2018, **414–415**, 310–316.
54 L. Zhou, Y. Fu, T. Yin, X. Tian and L. Qi, Building the silicon carbide nanowire network on the surface of carbon fibers: Enhanced interfacial adhesion and high-performance wear resistance, *Ceram. Int.*, 2019, **45**(17), 22571–22577.
55 B. Chen, Y. Jia, M. Zhang, H. Liang, X. Li, J. Yang, F. Yan and C. Li, Tribological properties of epoxy lubricating composite coatings reinforced with core-shell structure of CNF/MoS_2 hybrid, *Composites, Part A*, 2019, **122**, 85–95.
56 X. Yin, A. Teng, Z. Zeng, H. Meng and W. Wu, Facile and novel preparation of 2D-MoS_2/carbon nanodots composite with high adsorption efficiency and capacity for dye removal, *Chem. Eng. J.*, 2022, **450**, 138319.
57 X. Si, M. Li, F. Chen, P. Eklund, J. Xue, F. Huang, S. Du and Q. Huang, Effect of carbide interlayers on the microstructure and properties of graphene-nanoplatelet-reinforced copper matrix composites, *Mater. Sci. Eng.: A*, 2017, **708**, 311–318.
58 C. Shang, T. Liu, F. Zhang and F. Chen, Effect of network size on mechanical properties and wear resistance of titanium/nanodiamonds nanocomposites with network architecture, *Compos. Commun.*, 2020, **19**, 74–81.
59 A. Kotia, K. Chowdary, I. Srivastava, S. K. Ghosh and M. K. A. Ali, Carbon nanomaterials as friction modifiers in automotive engines: Recent progress and perspectives, *J. Mol. Liq.*, 2020, **310**, 113200.
60 X. Wang, Z. Zhang, Y. Men, X. Li, Y. Liang and L. Ren, Fabrication of nano-TiC functional gradient wear-resistant composite coating on 40Cr gear steel using laser cladding under starved lubrication conditions, *Opt. Laser Technol.*, 2020, **126**, 106136.
61 M. Hatami, M. Hasanpour and D. Jing, Recent developments of nanoparticles additives to the consumables liquids in internal combustion engines: Part II: Nano-lubricants, *J. Mol. Liq.*, 2020, **319**, 114156.
62 H. Zhao, M. Tian, Z. Li, Y. Zhang, Z. Chen, W. Zhang, S. Zhu, Y. Sun, Z. Zhou and L. Qu, Robust sandwich micro-structure coating layer for wear-resistant conductive polyester fabrics, *Appl. Surf. Sci.*, 2019, **494**, 969–976.
63 S. Seetharaman and M. Gupta, Fundamentals of Metal Matrix Composites, *Reference Module in Materials Science and Materials Engineering*, Elsevier, 2021.
64 M. Shan, C. Zhang, N. Wang, L. Zhang, W. Li and X. Yin, Improvement in wear resistance of laser-clad Fe–Cr–Mo–B–C-(TiC) amorphous-nanocrystalline coating, *Vacuum*, 2023, **207**, 111676.
65 X. Ding, L. Wu, J. Chen, G. Zhang, Z. Xie, D. Sun, B. Jiang, A. Atrens and F. Pan, Enhanced protective nanoparticle-modified MgAl-LDHs coatings on titanium alloy, *Surf. Coat. Technol.*, 2020, **404**, 126449.
66 F. Gustavsson, F. Svahn, U. Bexell and S. Jacobson, Nanoparticle based and sputtered WS_2 low-friction coatings — Differences and similarities with respect to friction mechanisms and tribofilm formation, *Surf. Coat. Technol.*, 2013, **232**, 616–626.
67 M. Tabandeh-Khorshid, K. Ajay, E. Omrani, C. Kim and P. Rohatgi, Synthesis, characterization, and properties of graphene reinforced metal-matrix nanocomposites, *Composites, Part B*, 2020, **183**, 107664.
68 J. Xu, X. Chen, P. Grutzmacher, A. Rosenkranz, J. Li, J. Jin, C. Zhang and J. Luo, Tribochemical Behaviors of Onion-like Carbon Films as High-Performance Solid Lubricants with Variable Interfacial Nanostructures, *ACS Appl. Mater. Interfaces*, 2019, **11**(28), 25535–25546.
69 J. Xu, T. Luo, X. Chen, P. Grützmacher, A. Rosenkranz and J. Luo, Influence of structural evolution on sliding interface for enhancing tribological performance of onion-like carbon films *via* thermal annealing, *Appl. Surf. Sci.*, 2021, **541**, 148441.
70 G. Zhang, R. Sebastian, T. Burkhart and K. Friedrich, Role of monodispersed nanoparticles on the tribological behavior of conventional epoxy composites filled with carbon fibers and graphite lubricants, *Wear*, 2012, **292–293**, 176–187.
71 S. H. Zhang, M. X. Li, J. H. Yoon and T. Y. Cho, Characterization on the coatings of Ni-base alloy with nano- and micron-size Sm_2O_3 addition prepared by laser deposition, *Mater. Chem. Phys.*, 2008, **112**(2), 668–674.
72 M. Alizadeh and H. Safaei, Characterization of Ni-Cu matrix, Al_2O_3 reinforced nano-composite coatings prepared by electrodeposition, *Appl. Surf. Sci.*, 2018, **456**, 195–203.
73 B. Li, X. Li, Y. Huan, W. Xia and W. Zhang, Influence of alumina nanoparticles on microstructure and properties of Ni-B composite coating, *J. Alloys Compd.*, 2018, **762**, 133–142.
74 S. F. Hassan and M. Gupta, Effect of particulate size of Al_2O_3 reinforcement on microstructure and mechanical behavior of solidification processed elemental Mg, *J. Alloys Compd.*, 2006, **419**(1), 84–90.
75 Y. Xu, Q. Zheng, J. Geng, Y. Dong, M. Tian, L. Yao and K. D. Dearn, Synergistic effects of electroless piston ring coatings and nano-additives in oil on the friction and wear of a piston ring/cylinder liner pair, *Wear*, 2019, **422–423**, 201–211.

76 G. N. K. Ramesh Bapu and S. Jayakrishnan, Development and characterization of electro deposited Nickel–Titanium Carbo Nitride (TiCN) metal matrix nanocomposite deposits, *Surf. Coat. Technol.*, 2012, **206**(8), 2330–2336.
77 C. Li, Y. Wang and Z. Pan, Wear resistance enhancement of electroless nanocomposite coatings *via* incorporation of alumina nanoparticles prepared by milling, *Mater. Des.*, 2013, **47**, 443–448.
78 J. S. Moya, S. Lopez-Esteban and C. Pecharromán, The challenge of ceramic/metal microcomposites and nanocomposites, *Prog. Mater. Sci.*, 2007, **52**(7), 1017–1090.
79 J. H. Martin, B. D. Yahata, J. M. Hundley, J. A. Mayer, T. A. Schaedler and T. M. Pollock, 3D printing of high-strength aluminium alloys, *Nature*, 2017, **549**(7672), 365–369.
80 R. Xu, J. Wang, L. He and Z. Guo, Study on the characteristics of Ni–W–P composite coatings containing nano-SiO_2 and nano-CeO_2 particles, *Surf. Coat. Technol.*, 2008, **202**(8), 1574–1579.
81 S. Faraji, A. H. Faraji and S. R. Noori, An investigation on electroless Cu–P composite coatings with micro and nano-SiC particles, *Mater. Des.*, 2014, **54**, 570–575.
82 N. Ghavidel, S. R. Allahkaram, R. Naderi, M. Barzegar and H. Bakhshandeh, Corrosion and wear behavior of an electroless Ni-P/nano-SiC coating on AZ31 Mg alloy obtained through environmentally-friendly conversion coating, *Surf. Coat. Technol.*, 2020, **382**, 125156.
83 T. Ayode Otitoju, P. Ugochukwu Okoye, G. Chen, Y. Li, M. Onyeka Okoye and S. Li, Advanced ceramic components: Materials, fabrication, and applications, *J. Ind. Eng. Chem.*, 2020, **85**, 34–65.
84 S. Calderon Velasco, A. Cavaleiro and S. Carvalho, Functional properties of ceramic-Ag nanocomposite coatings produced by magnetron sputtering, *Prog. Mater. Sci.*, 2016, **84**, 158–191.
85 S. S. Akhtar, A critical review on self-lubricating ceramic-composite cutting tools, *Ceram. Int.*, 2021, **47**(15), 20745–20767.
86 B. R. Golla, A. Mukhopadhyay, B. Basu and S. K. Thimmappa, Review on ultra-high temperature boride ceramics, *Prog. Mater. Sci.*, 2020, **111**, 100651.
87 P. J. Kelly, H. Li, P. S. Benson, K. A. Whitehead, J. Verran, R. D. Arnell and I. Iordanova, Comparison of the tribological and antimicrobial properties of CrN/Ag, ZrN/Ag, TiN/Ag, and TiN/Cu nanocomposite coatings, *Surf. Coat. Technol.*, 2010, **205**(5), 1606–1610.
88 P. J. Kelly, H. Li, K. A. Whitehead, J. Verran, R. D. Arnell and I. Iordanova, A study of the antimicrobial and tribological properties of TiN/Ag nanocomposite coatings, *Surf. Coat. Technol.*, 2009, **204**(6), 1137–1140.
89 C. P. Mulligan and D. Gall, CrN–Ag self-lubricating hard coatings, *Surf. Coat. Technol.*, 2005, **200**(5), 1495–1500.
90 Y. Gu, C. Xia, J. Li, W. Wu and A. Wu, Study of ultra-fine ceramic coatings containing nano-size nickel particles, *Surf. Coat. Technol.*, 2005, **200**(7), 2504–2509.
91 Z. Wang, L. Du, H. Lan, C. Huang and W. Zhang, Preparation and characterization of YSZ abradable sealing coating through mixed solution precursor plasma spraying, *Ceram. Int.*, 2019, **45**(9), 11802–11811.
92 H. Myalska, L. Lusvarghi, G. Bolelli, P. Sassatelli and G. Moskal, Tribological behavior of WC-Co HVAF-sprayed composite coatings modified by nano-sized TiC addition, *Surf. Coat. Technol.*, 2019, **371**, 401–416.
93 X. Li, J. Liang, T. Shi, D. Yang, X. Chen, C. Zhang, Z. Liu, D. Liu and Q. Zhang, Tribological behaviors of vacuum hot-pressed ceramic composites with enhanced cyclic oxidation and corrosion resistance, *Ceram. Int.*, 2020, **46**(9), 12911–12920.
94 R. Ahmed, O. Ali, N. H. Faisal, N. M. Al-Anazi, S. Al-Mutairi, F. L. Toma, L. M. Berger, A. Potthoff and M. F. A. Goosen, Sliding wear investigation of suspension sprayed WC–Co nanocomposite coatings, *Wear*, 2015, **322–323**, 133–150.
95 R. Pileggi, M. Tului, D. Stocchi and S. Lionetti, Tribo-corrosion behaviour of chromium carbide based coatings deposited by HVOF, *Surf. Coat. Technol.*, 2015, **268**, 247–251.
96 A. Förg, G. Konrath, S. Popa, A. Kailer, A. Killinger and R. Gadow, Tribological properties of high velocity suspension flame sprayed (HVSFS) ceramic coatings, *Surf. Coat. Technol.*, 2018, **349**, 901–908.
97 T. Zhang, H. Lan, C. Huang, L. Du and W. Zhang, Formation mechanism of the lubrication film on the plasma sprayed NiCoCrAlY-Cr_2O_3-AgMo coating at high temperatures, *Surf. Coat. Technol.*, 2017, **319**, 47–54.
98 Q. Li, P. Song, X. He, X. Yu, C. Li, T. Huang, K. Lü, Y. Zhou and J. Lu, Plastic metallic-barrier layer for crack propagation within plasma-sprayed Cu/ceramic coatings, *Surf. Coat. Technol.*, 2019, **360**, 259–268.
99 J. Yang, J. Jia, X. Li, C. Lu and X. Feng, Synergistic lubrication of Ag and Ag_2MoO_4 nanoparticles anchored in plasma-sprayed YSZ coatings: Remarkably-durable lubricating performance at 800 °C, *Tribol. Int.*, 2021, **153**, 106670.
100 K. Friedrich, Polymer composites for tribological applications, *Adv. Ind. Eng. Polym. Res.*, 2018, **1**(1), 3–39.
101 Y. Li, Q. Wang and S. Wang, A review on enhancement of mechanical and tribological properties of polymer composites reinforced by carbon nanotubes and graphene sheet: Molecular dynamics simulations, *Composites, Part B*, 2019, **160**, 348–361.
102 J. Pelto, V. Heino, M. Karttunen, I. Rytöluoto and H. Ronkainen, Tribological performance of high density polyethylene (HDPE) composites with low nanofiller loading, *Wear*, 2020, **460–461**, 203451.
103 S. M. Prasanna, K. B. Yogesha, M. Mruthunjaya, B. P. Shivakumar, P. N. Siddappa and B. R. Raju, Mechanical and Tribological Characterization of Hybrid Composites: A Review, *Mater. Today: Proc.*, 2020, **22**, 2351–2358.
104 A. K. Kadiyala, J. Bijwe and P. Kalappa, Investigations on influence of nano and micron sized particles of SiC on performance properties of PEEK coatings, *Surf. Coat. Technol.*, 2018, **334**, 124–133.

105 V. Rodriguez, J. Sukumaran, A. K. Schlarb and P. De Baets, Reciprocating sliding wear behaviour of PEEK-based hybrid composites, *Wear*, 2016, **362–363**, 161–169.

106 L. Chang, Z. Zhang, L. Ye and K. Friedrich, *Synergistic effects of nanoparticles and traditional tribo-fillers on sliding wear of polymeric hybrid composites*, Tribology and Interface Engineering Series, ed. K. Friedrich and A. K. Schlarb, Elsevier, 2008, ch. 3, pp. 35–61.

107 L.-Y. Lin and D.-E. Kim, Tribological properties of polymer/silica composite coatings for microsystems applications, *Tribol. Int.*, 2011, **44**(12), 1926–1931.

108 M. Meng, A. Leech and H. Le, Mechanical properties and tribological behaviour of electroless Ni–P–Cu coatings on corrosion-resistant alloys under ultrahigh contact stress with sprayed nanoparticles, *Tribol. Int.*, 2019, **139**, 59–66.

109 L. X. Ying, K. Wu, D. Y. Li, C. X. Wu and Z. Fu, TiO_2 Sol strengthened Cu-Sn-PTFE composite coatings with high homogeneity and superior resistance to wear, *Wear*, 2019, **426–427**, 258–264.

110 X. Hou, C. X. Shan and K.-L. Choy, Microstructures and tribological properties of PEEK-based nanocomposite coatings incorporating inorganic fullerene-like nanoparticles, *Surf. Coat. Technol.*, 2008, **202**(11), 2287–2291.

111 D. Choudhury, I. I. Niyonshuti, J. Chen, J. A. Goss and M. Zou, Tribological performance of polydopamine + Ag nanoparticles/PTFE thin films, *Tribol. Int.*, 2020, **144**, 106097.

112 S. Bahadur and C. Schwartz, The effect of nanoparticle fillers on transfer film formation and the tribological behavior of polymers, *Tribology of Polymeric Nanocomposites*, ed. K. Friedrich and A. K. Schlarb, Butterworth-Heinemann, Second edition, 2013, ch. 2, pp. 23–48.

113 S. Beckford, Y. A. Wang and M. Zou, Wear-Resistant PTFE/SiO_2 Nanoparticle Composite Films, *Tribol. Trans.*, 2011, **54**(6), 849–858.

114 S. Peng, Y. Guo, G. Xie and J. Luo, Tribological behavior of polytetrafluoroethylene coating reinforced with black phosphorus nanoparticles, *Appl. Surf. Sci.*, 2018, **441**, 670–677.

115 H. Li, S. Li, F. Li, Z. Li and H. Wang, Fabrication of SiO_2 wrapped polystyrene microcapsules by Pickering polymerization for self-lubricating coatings, *J. Colloid Interface Sci.*, 2018, **528**, 92–99.

116 X. Luo, Z. Yao, P. Zhang and D. Gu, Al_2O_3 nanoparticles reinforced Fe-Al laser cladding coatings with enhanced mechanical properties, *J. Alloys Compd.*, 2018, **755**, 41–54.

117 B. Da, G. Yongxin, A. T. Vasu, L. Yaxuan, Z. Yongwu and W. Yongguang, Influence of GO-Al_2O_3 hybrid material on the tribological behavior of chemically bonded ceramic coating, *Ceram. Int.*, 2020, **46**(14), 23027–23034.

118 K. Babaei, A. Fattah-alhosseini and M. Molaei, The effects of carbon-based additives on corrosion and wear properties of Plasma electrolytic oxidation (PEO) coatings applied on Aluminum and its alloys: A review, *Surf. Interfaces*, 2020, **21**, 100677.

119 A. Tyagi, R. S. Walia, Q. Murtaza, S. M. Pandey, P. K. Tyagi and B. Bajaj, A critical review of diamond like carbon coating for wear resistance applications, *Int. J. Refract. Met. Hard Mater.*, 2019, **78**, 107–122.

120 W. Zhai, N. Srikanth, L. B. Kong and K. Zhou, Carbon nanomaterials in tribology, *Carbon*, 2017, **119**, 150–171.

121 H. J. Ling, Y. J. Mai, S. L. Li, L. Y. Zhang, C. S. Liu and X. H. Jie, Microstructure and improved tribological performance of graphite/copper–zinc composite coatings fabricated by low pressure cold spraying, *Surf. Coat. Technol.*, 2019, **364**, 256–264.

122 L. Reinert, S. Suárez and A. Rosenkranz, Tribo-Mechanisms of Carbon Nanotubes: Friction and Wear Behavior of CNT-Reinforced Nickel Matrix Composites and CNT-Coated Bulk Nickel, *Lubricants*, 2016, **4**(2), 11.

123 R. Karslioglu and H. Akbulut, Comparison microstructure and sliding wear properties of nickel–cobalt/CNT composite coatings by DC, PC and PRC current electrodeposition, *Appl. Surf. Sci.*, 2015, **353**, 615–627.

124 C. T. J. Low, J. O. Bello, J. A. Wharton, R. J. K. Wood, K. R. Stokes and F. C. Walsh, Electrodeposition and tribological characterisation of nickel nanocomposite coatings reinforced with nanotubular titanates, *Surf. Coat. Technol.*, 2010, **205**(7), 1856–1863.

125 S. Suárez, A. Rosenkranz, C. Gachot and F. Mücklich, Enhanced tribological properties of MWCNT/Ni bulk composites – Influence of processing on friction and wear behaviour, *Carbon*, 2014, **66**, 164–171.

126 F. Liu and Y. Zhang, *In situ* growth of carbon nanotubes from Ni-based coatings and their wear properties, *Diamond Relat. Mater.*, 2012, **25**, 144–154.

127 I. Ahmad, A. Kennedy and Y. Zhu, Wear resistant properties of multi-walled carbon nanotubes reinforced Al_2O_3 nanocomposites, *Wear*, 2010, **269**(1–2), 71–78.

128 S. Shanmugasamy, K. Balakrishnan, A. Subasri, S. Ramalingam and A. Subramania, Development of CeO_2 nanorods reinforced electrodeposited nickel nanocomposite coating and its tribological and corrosion resistance properties, *J. Rare Earths*, 2018, **36**(12), 1319–1325.

129 C. R. Carpenter, P. H. Shipway and Y. Zhu, Electrodeposition of nickel-carbon nanotube nanocomposite coatings for enhanced wear resistance, *Wear*, 2011, **271**(9), 2100–2105.

130 I. Ahmad, A. Kennedy and Y. Q. Zhu, Wear resistant properties of multi-walled carbon nanotubes reinforced Al_2O_3 nanocomposites, *Wear*, 2010, **269**(1), 71–78.

131 M. Zhou, Y. Mai, H. Ling, F. Chen, W. Lian and X. Jie, Electrodeposition of CNTs/copper composite coatings with enhanced tribological performance from a low concentration CNTs colloidal solution, *Mater. Res. Bull.*, 2018, **97**, 537–543.

132 B. Prasanna Sahoo and D. Das, Tribological behaviour of ceramic and carbon nano-tube reinforced metal matrix composites – a review, *Mater. Today: Proc.*, 2018, **5**(9), 20549–20559.

133 A. V. Radhamani, H. C. Lau and S. Ramakrishna, CNT-reinforced metal and steel nanocomposites: A comprehensive assessment of progress and future directions, *Composites, Part A*, 2018, **114**, 170–187.

134 N. Chronopoulou, E. Siranidi, A. M. Routsi, H. Zhao, J. Bai, A. Karantonis and E. A. Pavlatou, Embedding of hybrid MWCNT-Al_2O_3 particles in Ni matrix: Structural, tribological and corrosion studies, *Surf. Coat. Technol.*, 2018, **350**, 672–685.

135 K. Kang, H. Park, J. Kim and C. Lee, Role of spray processes on microstructural evolution, and physical and mechanical properties of multi-walled carbon nanotube reinforced cu composite coatings, *Appl. Surf. Sci.*, 2015, **356**, 1039–1051.

136 B. Li, B. Mao, X. Wang and T. He, Fabrication and frictional wear property of bamboo-like SiC nanowires reinforced SiC coating, *Surf. Coat. Technol.*, 2020, **389**, 125647.

137 L. Feng, K. Li, Z. Si, H. Li, Q. Song, Y. Shan and S. Wen, Microstructure and thermal shock resistance of SiC/CNT–SiC double-layer coating for carbon/carbon composites, *Ceram. Int.*, 2014, **40**(8), 13683–13689.

138 A. Shi, X. Yang, C. Fang, L. Chen, Y. Weng, H. Liu and Q. Huang, Effect of CNTs addition on microstructure, ablation property and mechanism of ZrC–SiC coating for C/C–ZrC–SiC composites, *Vacuum*, 2020, **172**, 109099.

139 K. Balani, S. P. Harimkar, A. Keshri, Y. Chen, N. B. Dahotre and A. Agarwal, Multiscale wear of plasma-sprayed carbon-nanotube-reinforced aluminum oxide nanocomposite coating, *Acta Mater.*, 2008, **56**(20), 5984–5994.

140 S. Priyadershini, O. S. A. Rahman, K. K. Pandey and A. K. Keshri, Remarkable improvement in tribological behavior of plasma sprayed carbon nanotube and graphene nanoplatelates hybrid reinforced alumina nanocomposite coating, *Ceram. Int.*, 2019, **45**(5), 5768–5778.

141 H. Li, Z. Chen, K. Li, Q. Shen, Y. Chu and Q. Fu, Wear behavior of SiC nanowire-reinforced SiC coating for C/C composites at elevated temperatures, *J. Eur. Ceram. Soc.*, 2013, **33**(15), 2961–2969.

142 R. D. Dukino and M. V. Swain, Comparative Measurement of Indentation Fracture Toughness with Berkovich and Vickers Indenters, *J. Am. Ceram. Soc.*, 1992, **75**(12), 3299–3304.

143 P.-f. He, H.-d. Wang, S.-y. Chen, G.-z. Ma, M. Liu, Z.-g. Xing, Y.-w. Wang, S.-y. Ding, D.-y. He and X. Chen, Interface characterization and scratch resistance of plasma sprayed TiO_2-CNTs nanocomposite coating, *J. Alloys Compd.*, 2020, **819**, 153009.

144 Z. Y. Pan, Y. Wang, X. W. Li, C. H. Wang and Z. W. Zou, Effect of Submicron and Nano SiC Particles on Erosion Wear and Scratch Behavior of Plasma-Sprayed Al_2O_3/8YSZ Coatings, *J. Therm. Spray Technol.*, 2012, **21**(5), 995–1010.

145 S. Hazra and P. P. Bandyopadhyay, Scratch induced failure of plasma sprayed alumina based coatings, *Mater. Des.*, 2012, **35**, 243–250.

146 C. Zishan, L. Hejun and F. Qiangang, SiC wear resistance coating with added Ni, for carbon/carbon composites, *Surf. Coat. Technol.*, 2012, **213**, 207–215.

147 P. Nash, *Phase diagrams of binary nickel alloys*, ASM International, USA, 1991, vol. 394.

148 K. Sang and Z. Jin, Unlubricated friction of reaction-sintered silicon carbide and its composite with nickel, *Wear*, 2000, **246**(1), 34–39.

149 Y. Huang, J. Li, L. Wan, X. Meng and Y. Xie, Strengthening and toughening mechanisms of CNTs/Mg-6Zn composites *via* friction stir processing, *Mater. Sci. Eng.: A*, 2018, **732**, 205–211.

150 A. J. López, A. Ureña and J. Rams, Fabrication of novel sol–gel silica coatings reinforced with multi-walled carbon nanotubes, *Mater. Lett.*, 2010, **64**(8), 924–927.

151 F. Zivic, N. Palic, Z. Jovanovic and N. Grujovic, Processing Routes for Ceramic Matrix Composites (CMCs), *Reference Module in Materials Science and Materials Engineering*, Elsevier, 2021.

152 K. Balani and A. Agarwal, Process map for plasma sprayed aluminum oxide–carbon nanotube nanocomposite coatings, *Surf. Coat. Technol.*, 2008, **202**(17), 4270–4277.

153 A. K. Keshri, J. Huang, V. Singh, W. Choi, S. Seal and A. Agarwal, Synthesis of aluminum oxide coating with carbon nanotube reinforcement produced by chemical vapor deposition for improved fracture and wear resistance, *Carbon*, 2010, **48**(2), 431–442.

154 A. J. López, A. Ureña and J. Rams, Wear resistant coatings: Silica sol–gel reinforced with carbon nanotubes, *Thin Solid Films*, 2011, **519**(22), 7904–7910.

155 D. Chaira, Powder Metallurgy Routes for Composite Materials Production, *Reference Module in Materials Science and Materials Engineering*, Elsevier, 2021.

156 L. He, Y.-f. Tan, H. Tan, C.-h. Zhou and L. Gao, Tribological properties of nanostructured Al_2O_3-40%TiO_2 multiphase ceramic particles reinforced Ni-based alloy composite coatings, *Trans. Nonferrous Met. Soc. China*, 2013, **23**(9), 2618–2627.

157 S. C. Jambagi, Scratch adhesion strength of plasma sprayed carbon nanotube reinforced ceramic coatings, *J. Alloys Compd.*, 2017, **728**, 126–137.

158 M. A. Samad and S. K. Sinha, Mechanical, thermal and tribological characterization of a UHMWPE film reinforced with carbon nanotubes coated on steel, *Tribol. Int.*, 2011, **44**(12), 1932–1941.

159 M. Pöllänen, S. Pirinen, M. Suvanto and T. T. Pakkanen, Influence of carbon nanotube–polymeric compatibilizer masterbatches on morphological, thermal, mechanical, and tribological properties of polyethylene, *Compos. Sci. Technol.*, 2011, **71**(10), 1353–1360.

160 W. Gao, D. Cao, Y. Jin, X. Zhou, G. Cheng and Y. Wang, Microstructure and properties of Cu–Sn–Zn–TiO_2 nano-composite coatings on mild steel, *Surf. Coat. Technol.*, 2018, **350**, 801–806.

161 H.-J. Song and Z.-Z. Zhang, Study on the tribological behaviors of the phenolic composite coating filled with modified nano-TiO_2, *Tribol. Int.*, 2008, **41**(5), 396–403.

162 Y. Wang, D. Cao, W. Gao, Y. Qiao, Y. Jin, G. Cheng, W. Gao and Z. Zhi, Microstructure and properties of sol-enhanced

Co-P-TiO_2 nano-composite coatings, *J. Alloys Compd.*, 2019, **792**, 617–625.

163 M. Cui, S. Ren, S. Qiu, H. Zhao, L. Wang and Q. Xue, Non-covalent functionalized multi-wall carbon nanotubes filled epoxy composites: Effect on corrosion protection and tribological performance, *Surf. Coat. Technol.*, 2018, **340**, 74–85.

164 R. Jeyakumar, R. Ramamoorthi and K. Balasubramanian, Mechanical and wear characteristics of glass fiber reinforced modified epoxy nano composites – A review, *Mater. Today: Proc.*, 2020, **37**, 901–907.

165 W. Österle, A. I. Dmitriev, B. Wetzel, G. Zhang, I. Häusler and B. C. Jim, The role of carbon fibers and silica nanoparticles on friction and wear reduction of an advanced polymer matrix composite, *Mater. Des.*, 2016, **93**, 474–484.

166 C. R. Vandenabeele and S. Lucas, Technological challenges and progress in nanomaterials plasma surface modification – A review, *Mater. Sci. Eng., R*, 2020, **139**, 100521.

167 X. Li, W. Guan, H. Yan and L. Huang, Fabrication and atomic force microscopy/friction force microscopy (AFM/FFM) studies of polyacrylamide–carbon nanotubes (PAM–CNTs) copolymer thin films, *Mater. Chem. Phys.*, 2004, **88**(1), 53–58.

168 A. S. Mohammed and M. I. Fareed, Improving the friction and wear of poly-ether-etherketone (PEEK) by using thin nano-composite coatings, *Wear*, 2016, **364–365**, 154–162.

169 H.-J. Song, Z.-Z. Zhang and X.-H. Men, Surface-modified carbon nanotubes and the effect of their addition on the tribological behavior of a polyurethane coating, *Eur. Polym. J.*, 2007, **43**(10), 4092–4102.

170 H.-J. Song, Z.-Z. Zhang and X.-H. Men, Tribological behavior of polyurethane-based composite coating reinforced with TiO_2 nanotubes, *Eur. Polym. J.*, 2008, **44**(4), 1012–1022.

171 J. C. Spear, B. W. Ewers and J. D. Batteas, 2D-nanomaterials for controlling friction and wear at interfaces, *Nano Today*, 2015, **10**(3), 301–314.

172 S. Zhang, T. Ma, A. Erdemir and Q. Li, Tribology of two-dimensional materials: From mechanisms to modulating strategies, *Mater. Today*, 2019, **26**, 67–86.

173 D. Berman, A. Erdemir and A. V. Sumant, Reduced wear and friction enabled by graphene layers on sliding steel surfaces in dry nitrogen, *Carbon*, 2013, **59**, 167–175.

174 D. Berman, A. Erdemir and A. V. Sumant, Few layer graphene to reduce wear and friction on sliding steel surfaces, *Carbon*, 2013, **54**, 454–459.

175 D. Berman, A. Erdemir, A. V. Zinovev and A. V. Sumant, Nanoscale friction properties of graphene and graphene oxide, *Diamond Relat. Mater.*, 2015, **54**, 91–96.

176 C. Lee, X. Wei, J. W. Kysar and J. Hone, Measurement of the Elastic Properties and Intrinsic Strength of Monolayer Graphene, *Science*, 2008, **321**(5887), 385–388.

177 P. Zhang, L. Ma, F. Fan, Z. Zeng, C. Peng, P. E. Loya, Z. Liu, Y. Gong, J. Zhang, X. Zhang, P. M. Ajayan, T. Zhu and J. Lou, Fracture toughness of graphene, *Nat. Commun.*, 2014, **5**(1), 3782.

178 L. Xiang, Q. Shen, Y. Zhang, W. Bai and C. Nie, One-step electrodeposited Ni-graphene composite coating with excellent tribological properties, *Surf. Coat. Technol.*, 2019, **373**, 38–46.

179 M. Uysal, H. Akbulut, M. Tokur, H. Algül and T. Çetinkaya, Structural and sliding wear properties of Ag/Graphene/WC hybrid nanocomposites produced by electroless co-deposition, *J. Alloys Compd.*, 2016, **654**, 185–195.

180 S. C. Tjong, Recent progress in the development and properties of novel metal matrix nanocomposites reinforced with carbon nanotubes and graphene nanosheets, *Mater. Sci. Eng., R*, 2013, **74**(10), 281–350.

181 J. Chen, J. Zhang, M. Hu, Z. Zheng, K. Wang and X. Li, Preparation of Ni/graphene hydrophobic composite coating with micro-nano binary structure by poly-dopamine modification, *Surf. Coat. Technol.*, 2018, **353**, 1–7.

182 D. Zhang, X. Cui, G. Jin, X. Feng, B. Lu, Q. Song and C. Yuan, Effect of *in situ* synthesis of multilayer graphene on the microstructure and tribological performance of laser cladded Ni-based coatings, *Appl. Surf. Sci.*, 2019, **495**, 143581.

183 M. Marian, G. C. Song, B. Wang, V. M. Fuenzalida, S. Krauß, B. Merle, S. Tremmel, S. Wartzack, J. Yu and A. Rosenkranz, Effective usage of 2D MXene nanosheets as solid lubricant – Influence of contact pressure and relative humidity, *Appl. Surf. Sci.*, 2020, **531**, 147311.

184 Q. Huang, X. Shi, Y. Xue, K. Zhang and C. Wu, Recent progress on surface texturing and solid lubricants in tribology: Designs, properties, and mechanisms, *Mater. Today Commun.*, 2023, **35**, 105854.

185 F. Zhang, K. Yang, G. Liu, Y. Chen, M. Wang, S. Li and R. Li, Recent advances on graphene: Synthesis, properties and applications, *Composites, Part A*, 2022, **160**, 107051.

186 K. Yang, H. Ma, L. Wang, Z. Cao and C. Zhang, Analysis of self-regulating tribological functions of the MgAl microchannels prepared in the Ti alloys, *Tribol. Int.*, 2021, **154**, 106717.

187 A. Chouhan, H. P. Mungse and O. P. Khatri, Surface chemistry of graphene and graphene oxide: A versatile route for their dispersion and tribological applications, *Adv. Colloid Interface Sci.*, 2020, **283**, 102215.

188 S. Singh, S. Samanta, A. K. Das and R. R. Sahoo, Tribological investigation of Ni-graphene oxide composite coating produced by pulsed electrodeposition, *Surf. Interfaces*, 2018, **12**, 61–70.

189 C. Liu, F. Su and J. Liang, Producing cobalt–graphene composite coating by pulse electrodeposition with excellent wear and corrosion resistance, *Appl. Surf. Sci.*, 2015, **351**, 889–896.

190 H. Zhang, N. Zhang and F. Fang, Fabrication of high-performance nickel/graphene oxide composite coatings using ultrasonic-assisted electrodeposition, *Ultrason. Sonochem.*, 2020, **62**, 104858.

191 Y. Wang, K. Brogan and S. C. Tung, Wear and scuffing characteristics of composite polymer and nickel/ceramic composite coated piston skirts against aluminum and cast iron cylinder bores, *Wear*, 2001, **250**(1), 706–717.

192 Y. J. Mai, Y. G. Li, S. L. Li, L. Y. Zhang, C. S. Liu and X. H. Jie, Self-lubricating Ti_3C_2 nanosheets/copper composite coatings, *J. Alloys Compd.*, 2019, **770**, 1–5.

193 X. Li, C. H. Zhang, S. Zhang, C. L. Wu, Y. Liu, J. B. Zhang and M. Babar Shahzad, Manufacturing of Ti_3SiC_2 lubricated Co-based alloy coatings using laser cladding technology, *Opt. Laser Technol.*, 2019, **114**, 209–215.

194 M. B. Maros and A. K. Németh, Wear maps of HIP sintered Si_3N_4/MLG nanocomposites for unlike paired tribosystems under ball-on-disc dry sliding conditions, *J. Eur. Ceram. Soc.*, 2017, **37**(14), 4357–4369.

195 T. Cygan, M. Petrus, J. Wozniak, S. Cygan, D. Teklińska, M. Kostecki, L. Jaworska and A. Olszyna, Mechanical properties and tribological performance of alumina matrix composites reinforced with graphene-family materials, *Ceram. Int.*, 2020, **46**(6), 7170–7177.

196 M. Gaier, Z. N. Farhat and K. P. Plucknett, The effects of graphene nano-platelet additions on the sliding wear of TiC-Ni_3Al cermets, *Tribol. Int.*, 2019, **130**, 119–132.

197 T. Bai, Y. Fang and J. Wang, Preparation and tribological properties of graphene/TiO2 ceramic films, *Ceram. Int.*, 2017, **43**(16), 13299–13307.

198 W. Liu, C. Blawert, M. L. Zheludkevich, Y. Lin, M. Talha, Y. Shi and L. Chen, Effects of graphene nanosheets on the ceramic coatings formed on Ti6Al4V alloy drill pipe by plasma electrolytic oxidation, *J. Alloys Compd.*, 2019, **789**, 996–1007.

199 Y. Zhao, T. Yu, C. Guan, J. Sun and X. Tan, Microstructure and friction coefficient of ceramic (TiC, TiN and B_4C) reinforced Ni-based coating by laser cladding, *Ceram. Int.*, 2019, **45**(16), 20824–20836.

200 A. Amudha, H. S. Nagaraja and H. D. Shashikala, Plasma-sprayed graphene oxide reinforced alumina composite coatings on low carbon steel with improved fracture toughness, brittleness index, and microhardness, *Mater. Today: Proc.*, 2021, **39**, 1503–1508.

201 Q. Li, X. Yuan, H. Xu, P. Song, Q. Li, K. Lü, T. Huang, C. Li and J. Lu, Microstructure and fracture toughness of *in situ* nanocomposite coating by thermal spraying of Ti_3AlC_2/Cu powder, *Ceram. Int.*, 2019, **45**(10), 13119–13126.

202 A. Nieto, J. M. Zhao, Y.-H. Han, K. H. Hwang and J. M. Schoenung, Microscale tribological behavior and *in vitro* biocompatibility of graphene nanoplatelet reinforced alumina, *J. Mech. Behav. Biomed. Mater.*, 2016, **61**, 122–134.

203 S. Ranjan, B. Mukherjee, A. Islam, K. K. Pandey, R. Gupta and A. K. Keshri, Microstructure, mechanical and high temperature tribological behaviour of graphene nanoplatelets reinforced plasma sprayed titanium nitride coating, *J. Eur. Ceram. Soc.*, 2020, **40**(3), 660–671.

204 J. W. Murray, G. A. Rance, F. Xu and T. Hussain, Alumina-graphene nanocomposite coatings fabricated by suspension high velocity oxy-fuel thermal spraying for ultra-low-wear, *J. Eur. Ceram. Soc.*, 2018, **38**(4), 1819–1828.

205 Y. Wang, Y. Zhu, Z. He and H. Wu, Multiscale investigations into the fracture toughness of SiC/graphene composites: Atomistic simulations and crack-bridging model, *Ceram. Int.*, 2020, **46**(18), 29101–29110.

206 J. Zhang, Z. Chen, H. Wu, J. Zhao and Z. Jiang, Effect of graphene on the tribolayer of aluminum matrix composite during dry sliding wear, *Surf. Coat. Technol.*, 2019, **358**, 907–912.

207 Z.-y. Li, Z.-b. Cai, Y. Ding, X.-J. Cui, Z.-b. Yang and M.-h. Zhu, Characterization of graphene oxide/ZrO_2 composite coatings deposited on zirconium alloy by micro-arc oxidation, *Appl. Surf. Sci.*, 2020, **506**, 144928.

208 K. Yang, X. Shi and W. Zhai, Effects of MoS_2 and Multiwalled Carbon Nanotubes on Tribological Behavior of TiAl Matrix Composite, *J. Mater. Eng. Perform.*, 2016, **25**(3), 1094–1102.

209 D. Bian, T. V. Aradhyula, Y. Guo and Y. Zhao, Improving tribological performance of chemically bonded phosphate ceramic coatings reinforced by graphene nano-platelets, *Ceram. Int.*, 2017, **43**(15), 12466–12471.

210 H. Li, Y. Xie, K. Li, L. Huang, S. Huang, B. Zhao and X. Zheng, Microstructure and wear behavior of graphene nanosheets-reinforced zirconia coating, *Ceram. Int.*, 2014, **40**(8), 12821–12829.

211 Y. Feng, J. Fang, J. Wu, K. Gu and P. Liu, Mechanical and tribological properties of plasma sprayed graphene nanosheets/Al_2O_3 + 13 wt%TiO_2 composite coating, *Tribol. Int.*, 2020, **146**, 106233.

212 E. E. Nunez, R. Gheisari and A. A. Polycarpou, Tribology review of blended bulk polymers and their coatings for high-load bearing applications, *Tribol. Int.*, 2019, **129**, 92–111.

213 J. Chen, J. Yang, B. Chen, S. Liu, J. Dong and C. Li, Large-scale synthesis of $NbSe_2$ nanosheets and their use as nanofillers for improving the tribological properties of epoxy coatings, *Surf. Coat. Technol.*, 2016, **305**, 23–28.

214 L. Wu, Z. Zhang, M. Yang, J. Yuan, P. Li, F. Guo and X. Men, One-step synthesis of g-C_3N_4 nanosheets to improve tribological properties of phenolic coating, *Tribol. Int.*, 2019, **132**, 221–227.

215 X. Ye, X. Liu, Z. Yang, Z. Wang, H. Wang, J. Wang and S. Yang, Tribological properties of fluorinated graphene reinforced polyimide composite coatings under different lubricated conditions, *Composites, Part A*, 2016, **81**, 282–288.

216 S. Zhou, W. Li, W. Zhao, C. Liu, Z. Fang and X. Gao, Tribological behaviors of polyimide composite films enhanced with fluorographene, *Colloids Surf., A*, 2019, **580**, 123707.

217 X. Yin, J. Jin, X. Chen, A. Rosenkranz and J. Luo, Ultra-wear-resistant MXene-based composite coating *via in situ* formed nanostructured tribofilm, *ACS Appl. Mater. Interfaces*, 2019, **11**(35), 32569–32576.

218 H. Yan, M. Cai, W. Li, X. Fan and M. Zhu, Amino-functionalized $Ti_3C_2T_x$ with anti-corrosive/wear function for waterborne epoxy coating, *J. Mater. Sci. Technol.*, 2020, **54**, 144–159.

219 A. Roy, L. Mu and Y. Shi, Tribological properties of polyimide-graphene composite coatings at elevated temperatures, *Prog. Org. Coat.*, 2020, **142**, 105602.
220 W. Li, W. Zhao, L. Mao, S. Zhou, C. Liu, Z. Fang and X. Gao, Investigating the fluorination degree of FG nanosheets on the tribological properties of FG/PI composite coatings, *Prog. Org. Coat.*, 2020, **139**, 105481.
221 A. Toosinezhad, M. Alinezhadfar and S. Mahdavi, Tribological behavior of cobalt/graphene composite coatings, *Ceram. Int.*, 2020, **46**(10), 16886–16894.
222 Y. Liu, X. Chen, J. Li and J. Luo, Enhancement of friction performance enabled by a synergetic effect between graphene oxide and molybdenum disulfide, *Carbon*, 2019, **154**, 266–276.
223 B. Da, X. Rongli, G. Yongxin, L. Yaxuan, T. V. Aradhyula, Z. Yongwu and W. Yongguang, Tribological behavior of graphene reinforced chemically bonded ceramic coatings, *Ceram. Int.*, 2020, **46**(4), 4526–4531.
224 P. Miranzo, M. Belmonte and M. I. Osendi, From bulk to cellular structures: A review on ceramic/graphene filler composites, *J. Eur. Ceram. Soc.*, 2017, **37**(12), 3649–3672.
225 C. Wang, B. Wang, R. Qiao, F. Zhang, Z. Wang and L. Chen, Effect of sintering temperature on microstructures and tribological characteristics of dense α-Si_3N_4-based ceramic coating on porous Si_3N_4 ceramics, *J. Alloys Compd.*, 2019, **776**, 927–933.
226 X. L. Xu, G. X. Bo, X. He, X. K. Tian and Y. J. Yan, Structural effects of dimensional nano-fillers on the properties of Sapium sebiferum oil-based polyurethane matrix: Experiments and molecular dynamics simulation, *Polymer*, 2020, **202**, 122709.
227 J. F. Archard, Contact and Rubbing of Flat Surfaces, *J. Appl. Phys.*, 1953, **24**(8), 981–988.
228 N. Cinca, R. Drehmann, D. Dietrich, F. Gärtner, T. Klassen, T. Lampke and J. M. Guilemany, Mechanically induced grain refinement, recovery and recrystallization of cold-sprayed iron aluminide coatings, *Surf. Coat. Technol.*, 2019, **380**, 125069.
229 Y. Liu, F. Zheng, Y. Wu, C. C. Koch, P. Han, C. Zhang, Y. Liu and Y. Zhang, Grain refinement induced friction reduction and anti-wear performances of electrodeposited graphene/Ni composites with low content reduced graphene oxide, *J. Alloys Compd.*, 2020, **826**, 154080.
230 J. K. Pancrecious, J. P. Deepa, V. Jayan, U. S. Bill, T. P. D. Rajan and B. C. Pai, Nanoceria induced grain refinement in electroless Ni-B-CeO_2 composite coating for enhanced wear and corrosion resistance of Aluminium alloy, *Surf. Coat. Technol.*, 2018, **356**, 29–37.
231 I. Makarova, I. Dobryden, D. Kharitonov, A. Kasach, J. Ryl, E. Repo and E. Vuorinen, Nickel-nanodiamond coatings electrodeposited from tartrate electrolyte at ambient temperature, *Surf. Coat. Technol.*, 2019, **380**, 125063.
232 C. Yan, K. Namachivayam, H. Li, Y. Kang and D. Xiong, The nickel based composite coating fabricated by pulse electroplating through graft between nano-TiN and graphene oxide, *Ceram. Int.*, 2020, **46**(10), 15714–15718.
233 S. M. Lari Baghal, M. Heydarzadeh Sohi and A. Amadeh, A functionally gradient nano-Ni–Co/SiC composite coating on aluminum and its tribological properties, *Surf. Coat. Technol.*, 2012, **206**, 4032–4039.
234 X. Lan, H. Wu, Y. Liu, W. Zhang, R. Li, S. Chen, X. Zai and T. Hu, Microstructures and tribological properties of laser cladded Ti-based metallic glass composite coatings, *Mater. Charact.*, 2016, **120**, 82–89.
235 V. Sivamaran, D. V. Balasubramanian, D. M. Gopalakrishnan, D. V. Viswabaskaran, D. A. G. Rao and D. G. Sivakumar, Mechanical and tribological properties of Self-Lubricating Al 6061 hybrid nano metal matrix composites reinforced by nSiC and MWCNTs, *Surf. Interfaces*, 2020, **21**, 100781.
236 V. Adibnia, M. Mirbagheri, J. Faivre, J. Robert, J. Lee, K. Matyjaszewski, D. W. Lee and X. Banquy, Bioinspired polymers for lubrication and wear resistance, *Prog. Polym. Sci.*, 2020, **110**, 101298.
237 P.-H. Gao, B.-Y. Chen, W. Wang, H. Jia, J.-P. Li, Z. Yang and Y.-C. Guo, Simultaneous increase of friction coefficient and wear resistance through HVOF sprayed WC-(nano WC-Co), *Surf. Coat. Technol.*, 2019, **363**, 379–389.
238 A. H. Wang, X. L. Zhang, X. F. Zhang, X. Y. Qiao, H. G. Xu and C. S. Xie, Ni-based alloy/submicron WS2 self-lubricating composite coating synthesized by Nd:YAG laser cladding, *Mater. Sci. Eng., A*, 2008, **475**(1–2), 312–318.
239 I. Esther, I. Dinaharan and N. Murugan, Microstructure and wear characterization of AA2124/4 wt% B_4C nano-composite coating on Ti6Al4V alloy using friction surfacing, *Trans. Nonferrous Met. Soc. China*, 2019, **29**(6), 1263–1274.
240 L. Thakur and N. Arora, An investigation on the development and wear performance of chromium-MWCNTs transformed HVOF sprayed nano-WC-CoCr coatings, *Surf. Coat. Technol.*, 2020, **388**, 125610.
241 J. Lin, X. Zhang, F. Ge and F. Huang, Thick CrN/AlN superlattice coatings deposited by hot filament assisted HiPIMS for solid particle erosion and high temperature wear resistance, *Surf. Coat. Technol.*, 2019, **377**, 124922.
242 B. Liu, B. Deng and Y. Tao, Influence of niobium ion implantation on the microstructure, mechanical and tribological properties of TiAlN/CrN nano-multilayer coatings, *Surf. Coat. Technol.*, 2014, **240**, 405–412.
243 D.-r. Yan, X.-r. Dai, Y. Yang, Y.-c. Dong, X.-g. Chen, Z.-h. Chu and J.-x. Zhang, Microstructure and properties of *in situ* ceramic matrix eutectic nanocomposite coating prepared by plasma spraying Al-Cr_2O_3-Al_2O_3 powder, *J. Alloys Compd.*, 2018, **748**, 230–235.
244 W.-f. Cui, F.-j. Niu, Y.-l. Tan and G.-w. Qin, Microstructure and tribocorrosion performance of nanocrystalline TiN graded coating on biomedical titanium alloy, *Trans. Nonferrous Met. Soc. China*, 2019, **29**(5), 1026–1035.
245 J.-Y. Lee, D.-P. Lim and D.-S. Lim, Tribological behavior of PTFE nanocomposite films reinforced with carbon nanoparticles, *Composites, Part B*, 2007, **38**(7), 810–816.
246 J. Yu, W. Zhao, Y. Wu, D. Wang and R. Feng, Tribological properties of epoxy composite coatings reinforced with

functionalized C-BN and H-BN nanofillers, *Appl. Surf. Sci.*, 2018, **434**, 1311–1320.

247 B. Chen, M. Zhang, X. Li, Z. Dong, Y. Jia and C. Li, Tribological properties of epoxy-based self-lubricating composite coating enhanced by 2D/2D h-BN/MoS_2 hybrid, *Prog. Org. Coat.*, 2020, **147**, 105767.

248 S. Peng, L. Zhang, G. Xie, Y. Guo, L. Si and J. Luo, Friction and wear behavior of PTFE coatings modified with poly(methyl methacrylate), *Composites, Part B*, 2019, **172**, 316–322.

249 Z. Huang and W. Zhao, Coupling hybrid of HBN nanosheets and TiO2 to enhance the mechanical and tribological properties of composite coatings, *Prog. Org. Coat.*, 2020, **148**, 105881.

250 L. Wang, S. Xing, H. Liu, C. Jiang and V. Ji, Improved wear properties of NiTi nanocomposite coating with tailored spatial microstructures by extra adding CeO_2 nanoparticles, *Surf. Coat. Technol.*, 2020, **399**, 126119.

251 B. Chen, X. Li, Y. Jia, L. Xu, H. Liang, X. Li, J. Yang, C. Li and F. Yan, Fabrication of ternary hybrid of carbon nanotubes/graphene oxide/MoS2 and its enhancement on the tribological properties of epoxy composite coatings, *Composites, Part A*, 2018, **115**, 157–165.

252 C. Min, D. Liu, C. Shen, Q. Zhang, H. Song, S. Li, X. Shen, M. Zhu and K. Zhang, Unique synergistic effects of graphene oxide and carbon nanotube hybrids on the tribological properties of polyimide nanocomposites, *Tribol. Int.*, 2018, **117**, 217–224.

253 H. Yan, L. Zhang, H. Li, X. Fan and M. Zhu, Towards high-performance additive of Ti_3C_2/graphene hybrid with a novel wrapping structure in epoxy coating, *Carbon*, 2020, **157**, 217–233.